A-1388

AD

RESEARCH AND DEVELOPMENT TECHNICAL REPORT
ECOM-0087-F

PRECISION SINGLE SIDEBAND CRYSTAL UNITS

FINAL REPORT

By

R. K. Hart and W. H. Hicklin

MAY 1973

DISTRIBUTION STATEMENT

Approved for public release;
distribution unlimited.

ECOM

UNITED STATES ARMY ELECTRONICS COMMAND • FORT MONMOUTH, N.J.
CONTRACT DAAB07-71-C-0087
Engineering Experiment Station
GEORGIA INSTITUTE OF TECHNOLOGY
Atlanta, Georgia

NOTICES

Disclaimers

The findings in this report are not to be construed as an official Department of the Army position, unless so designated by other authorized documents.

The citation of trade names and names of manufacturers in this report is not to be construed as official Government indorsement or approval of commercial products or services referenced herein.

Disposition

Destroy this report when it is no longer needed. Do not return it to the originator.

TECHNICAL REPORT ECOM-0087-F
MAY 1973

REPORTS CONTROL SYMBOL
OSD-1366

PRECISION SINGLE SIDEBAND CRYSTAL UNITS

Final Report

December 15, 1971 to January 31, 1973

CONTRACT NO. DAAB07-72-C-0087

DA PROJECT NO. DAAB07-72-Q-0060
TASK-04

DISTRIBUTION STATEMENT

Approved for public release; distribution unlimited.

Prepared by:

R. K. Hart and W. H. Hicklin
Engineering Experiment Station
Georgia Institute of Technology
Atlanta, Georgia 30332

for

U. S. Army Electronics Command
Fort Monmouth, New Jersey

ABSTRACT

The purpose of this work was to develop single sideband (SSB) quartz crystal units which exhibit long-term aging of $< \pm 2 \times 10^{-10}$/week when measured at the upper turning point (UTP) of 62°C, and after a stabilization period of four weeks. In addition to the low aging requirement, the frequency hysteresis that often occurs under conditions of varying temperatures was investigated.

Two concurrent work programs were employed to a) fabricate resonators under precisely controlled conditions and b) investigate their characteristics. All wafers used in resonator construction were preterminated by electrobonding in HC-6 holders, plated with copper electrodes, and then hermetically sealed in containers by the cold-weld process. The plating and sealing operations were carried out in an ultrahigh vacuum chamber without venting to air between operations.

Both the cleaned surfaces of quartz wafers and of deposited electrode material were chemically and physically characterized by Auger electron spectroscopy, electron microscopy and electron diffraction. The results of these investigations were related to the various processes used in resonator preparation.

The lowest drift rates of a few parts per 10^{10} per week were from wafers a) etched 1 min, b) alkylchlorosilane coated before electrode deposition, and c) final fabrication of mounted wafers in same low pressure environment. The frequency deviation requirement of $< \pm 1 \times 10^{-8}$ during temperature cycling (-55 to +90°C) was met in 84% of cases tested.

The results of this work indicate that the performance of quartz resonators can be improved by fabricating them in systems and from materials that enable precise control of variables to be exercised. Monitoring of these variables by suitably sensitive instrumentation is essential.

TABLE OF CONTENTS

		Page
I.	INTRODUCTION	1
	A. Statement of the Problem	1
	B. Approach to the Problem	1
II.	EXPERIMENTAL WORK	3
	A. Quartz Resonator Assembly and Measurement	3
	1. Introduction	3
	2. Apparatus and Procedures	3
	3. Experimental Data	9
	B. Studies of Quartz Surfaces	12
	1. Introduction	12
	2. Apparatus and Procedures	12
	3. Results of Surface Characterizations	14
	4. Morphology of Quartz Surfaces	15
	C. Studies on Copper Surfaces	17
	1. Introduction	17
	2. Apparatus and Procedures	18
	3. Results with Evaporated Electrodes	19
	4. Surface Characterization of Copper Foils	21
III.	DISCUSSION	23
IV.	CONCLUSIONS AND RECOMMENDATIONS	25
V.	ACKNOWLEDGEMENTS	25
VI.	REFERENCES	26
VII.	TABLES AND FIGURES	27
	DISTRIBUTION LIST	71
	DOCUMENT CONTROL DATA	

LIST OF TABLES

Page

1. Electrical Parameters of Resonators Used to Obtain Long-Term Aging Data at 62°C. 27

2. Analysis of Selected Area Diffraction Pattern (SAD) from Hi-Q Cultured Quartz, Sample No. Hi-Q, 3-E 29

3. Comparison between AES Data from Freshly Prepared Resonator Electrode Surface and from a Similar Unit after Aging for 30 Days at 85°C. 30

LIST OF FIGURES

1. Placement of the Cr+Au bonding sites, the tab clips, and the Ni electroplate on the quartz wafers. 31

2. Vacuum equipment for quartz resonator plating, vacuum baking, and sealing. 32

3. Vacuum bakeout and cold-weld sealing system. 33

4. Electrode evaporation system shown in the plating position. Note that the upper section of the cold-weld die and the latching plate for the retractable mask are removed for clarity 34

5. Electrode evaporation system shown in the sealing position. Note that the electrode mask is retracted from the plating position so as to allow the die to be closed 35

6. System for measuring the long-term aging of quartz resonators stored at the upper turning point temperature. 36

7. Circuit diagram of the crystal bridge shown in the block diagram of Fig. 6. The crystal unit impedance is balanced at F_s by the forward biased diode D_1. 37

8. System for measuring the series resonant frequency (F_s) and series resistance (R_s) over the temperature range -55°C to +90°C. 38

9. Frequency measuring system used during plating to frequency by vacuum evaporation 39

10. Long-term aging data for natural quartz unit No. 18. Bakeout for 16 hours at 200°C. 40

11. Long-term aging data for natural quartz unit No. 21 with polysiloxane coated quartz. Bakeout for 16 hours at 200°C 41

LIST OF FIGURES (CONTINUED)

Page

12. Long-term aging data for Hi-Q cultured quartz unit No. 51, with solid getter in holder. Bakeout for 16 hours at 200°C. . . 42

13. Long-term aging data for Hi-Q cultured quartz unit No. 56, with polysiloxane coating. Bakeout for 16 hours at 200°C . . . 43

14. Long-term aging data for ECOM-furnished-quartz unit "H", with polysiloxane coating. Bakeout for 16 hours at 200°C. . . . 44

15. Long-term aging data for ECOM-furnished-quartz unit "J", with solid getter in holder. Bakeout for 16 hours at 200°C. . . 45

16. Thermal frequency deviation for various resonators. Temperature was cycled from -55°C to +90°C at about one week intervals. 46

17. Frequency and resistance vs temperature data for natural quartz unit No. 9. 47

18. Frequency and resistance vs temperature data for natural quartz unit No. 5. 48

19. Frequency and resistance vs temperature data for Hi-Q quartz unit No. 50. 49

20. Frequency and resistance vs temperature data for ECOM-furnished-quartz unit "F". 50

21. Auger electron spectrum from the surface of a quartz wafer in the as-received condition. 51

22. Kikuchi-line diffraction pattern obtained from a freshly cleaned Hi-Q cultured quartz wafer. The cleaning agent was chrome-sulfuric acid 52

23. Surface replica of an as-received Hi-Q cultured quartz wafer . . 53

24. Surface replica of an as-received natural quartz wafer, prepared by ECOM 54

25. Platinum preshadowed carbon extraction replica of a cleaned Hi-Q cultured quartz surface showing extracted particles 55

26. Scanning electron micrograph of a natural quartz wafer surface which had been etch-polished for 40 min. 56

27. Scanning electron micrograph of a natural quartz wafer surface which had been etched 10 min in saturated $NH_4F.HF$. 57

LIST OF FIGURES (CONTINUED)

Page

28. Scanning electron micrograph of an etched (15 min) Hi-Q cultured quartz wafer, showing aligned surface features. 58

29. Scanning electron micrograph of an etched (15 min) natural quartz wafer which had been prepared by ECOM 59

30. Auger electron spectrum from a copper electrode surface immediately following 25°C deposition at 10^{-9} torr 60

31. Auger electron spectrum from a copper electrode surface 25°C deposition and a 20 hr bakeout in vacuum at 200°C 61

32. Auger electron spectrum from a copper-plated quartz wafer after it was vapor degreased with trichloroethylene. 62

33. Auger electron spectrum from a copper-plated specimen after cleaning it with MICRO® and then rinsing in distilled water . . 63

34. Auger electron spectrum from a copper-plated quartz wafer after it was rinsed in methanol. 64

35. Aging data for quartz resonators initially heated in vacuum to 200°C with copper electrodes deposited a) at 25°C followed by a 200°C bakeout, b) 200°C followed by a 200°C bakeout, and c) 25°C followed by a 300°C bakeout. 65

36. The 85°C aging data for a copper-plated quartz resonator which was finally cleaned with MICRO® rather than by vapor degreasing in trichloroethylene. The subsequent bakeout in vacuum was 20 hr at 200°C, followed by cold-weld sealing at low pressure. Note negative aging. 66

37. Auger electron spectrum from a copper foil specimen after it was given a light etch in nitric acid and rinsed in tap water. . 67

38. Auger electron spectrum from the same specimen used to obtain the data of Fig. 37, after heating for 2 min at 600°C in the spectrometer vacuum. 68

39. Auger electron spectrum from the copper foil specimen after cycling the AES system to atmosphere of air and then reevacuating to about 10^{-10} torr. 69

40. Auger electron spectrum from the copper foil specimen after heating 1 min at 300°C in the AES system following exposure to one atmosphere of air and reevacuating. 70

I. INTRODUCTION

A. Statement of the Problem

The purpose of this research was to develop single sideband (SSB) quartz resonators capable of meeting stringent aging, reliability, and thermal repeatability requirements. The units are intended to be used in temperature compensated crystal oscillators (TCXO), and operate in the ambient temperature range of -55°C to +90°C.

Quartz resonators achieve their optimum aging performance when stored continuously at a constant temperature. Also important, but to a lesser degree, is the continuous operation of the resonator at a low, regulated drive level in an electronic oscillator. The above operating conditions are not presently realized in conventional TCXO operation. However, TCXO operation which approaches the performance requirements of oven-controlled crystal oscillators (OCXO) is urgently needed.

The aging rate presently desired for TCXO resonators is $\pm 2 \times 10^{-10}$/week after four weeks at the nominal upper turning point (UTP) of 62°C. Such low aging is not routinely obtained with fundamental 5 MHz resonators but can be obtained with 5th overtone units. However, these overtone units cannot be used in TCXO's because their high inductance ("stiffness") precludes the use of frequency "pulling" by means of a reactive element in series with the crystal.

A maximum frequency deviation of $\pm 1 \times 10^{-8}$ is also desired for TCXO units when measured at the upper and lower turning points after temperature excursions from -55°C to +85°C.

B. Approach to the Problem

Our plan has been to follow two basic approaches to the problem stated above. The first approach was the usual one taken during studies of the long-term aging and thermal repeatability. Resonators were assembled with planned variables inserted into the fabrication process. The effects of such variables were then evaluated by measurements of aging and retrace. This approach has been used for years during which time quartz resonators have improved due to the evolution of fabrication recipes. The "recipe" method of research was due mostly to the inability to measure other parameters with the same degree of precision that we can measure frequency.

In recent years, however, analytical instrumentation has become available that enables us to measure other parameters of quartz resonators with sufficient resolution for direct comparison with frequency measurements. One of the most promising techniques is Auger electron spectroscopy (AES). Other instrumentation suitable for investigating aging studies includes scanning electron microscopy (SEM), high energy electron diffraction (HEED), photoelectron spectroscopy (ESCA) and x-ray fluorescence. All of the above equipment except ESCA is available at the Engineering Experiment Station. Neutron activation analysis (NAA) facilities are also available in the Georgia Tech Research Reactor.

The second approach to the problem was then to use the various types of analytical equipment, as dictated by experiment, to measure resonator parameters other than frequency, and then apply the results to improve the existing methods of resonator processing.

These two approaches to the problem should lead to a better understanding of the aging-retrace phenomenon, and the application of this knowledge can lead to improved resonator fabrication processes, materials, and methods.

II. EXPERIMENTAL WORK

A. Quartz Resonator Assembly and Measurement

1. Introduction

The purpose of this research was to improve the overall performance of quartz resonators when operated as the frequency controlling elements in temperature-compensated crystal oscillators (TCXO). Aging rates of $\pm 2 \times 10^{-10}$/week and thermal frequency repeatability of not greater than $\pm 1 \times 10^{-8}$ variation, after exposing the resonators to temperatures ranging from -55°C to +85°C, are the most stringent requirements to achieve. This section describes the assembly and measurement of quartz resonators. Other experiments which relate to the problem will be considered in subsequent sections.

2. Apparatus and Procedures

a. Quartz Cleaning. The quartz plates used during this work had the following specifications:*

(1) Frequency - 5.030 kHz ± 5 kHz

(2) Mode - fundamental

(3) Diameter - 0.528" + 0.0000 - 0.0002"

(4) Shape - plano-convex, 2.5 diopter

(5) Orientation angle - 35° 13.5' ± 0.5'

(6) Surface finish - optical polish, no etch

(7) Special - 0.015" flat perpendicular to the X axis.

Wafers of natural and premium grade Hi-Q cultured quartz made to these specifications were purchased from the Electronics Division, Bulova Watch Co.

All of the wafers received at Georgia Tech had been cleaned in some manner prior to shipment. We were concerned only with final cleaning before plating and encapsulation.

Many processes to clean glass and quartz are described in the literature. Wasshausen[1] described a seven-step procedure for cleaning quartz wafers; the final cleaning agent being hot, 30% hydrogen peroxide. A recent change** was to use a platinum catalyst to decompose the H_2O_2 rather than NaOH which was previously used. White[2] used a dichromate-sulfuric acid solution for cleaning glass specimens. Krieger[3] discussed the use of oxidation reactions for removing organic contaminants; however, the use of the so-called "chromic acid", i.e., the potassium dichromate-sulfuric acid formula, was discouraged because of the possibility of leaving insoluble salts on the surface of the cleaned part. The Tube Laboratory Manual prepared by the Research Laboratory of Electronics, M.I.T.(1951), recommends that "chromic acid" be made of chromium trioxide (CrO_3) and concentrated sulfuric acid (H_2SO_4)

*10 each 5 MHz wafers having somewhat different specifications were obtained from ECOM late in the program.

**Private communication with Dr. J. R. Vig.

to avoid the presence of insoluble salts remaining on cleaned surfaces.

We have used the last named cleaning solution for several years and continued to do so during this program. Our cleaning solution was made by placing about 270 gm of reagent grade CrO_3 in a one-liter bottle and then filling the bottle with reagent grade H_2SO_4. The solution was then stirred by ultrasonic agitation. Some of the CrO_3 dissolved in the H_2SO_4 to produce a saturated solution; undissolved CrO_3 settled to the bottom. When more solution was needed, we merely added more acid and repeated the process.

The solution was used in two ways. The first, when cleaning batches of wafers a mixture of 2 parts solution to 1 part distilled water in a 100 ml beaker was suspended in an ultrasonic tank filled with 75°C water. After cleaning, the wafers in the beaker were then ultrasonically rinsed several times in boiling distilled water, then 25°C methanol, and dried with warm air. The second method of using this solution, and the one currently preferred since the wafers to be plated are already mounted and bonded, was to flow the concentrated CrO_3-H_2SO_4 solution over the wafer using a "medicine" dropper. The solution was then rinsed off with flowing, distilled water at ambient temperature, followed by an alcohol rinse, and drying with warm air. This latter method was especially useful because the holder as well as the wafer could be cleaned at the same time to produce a hydrophylic surface just before placing in the plating and sealing system. The presence of chromium was not detected by AES on any specimen of quartz or metal cleaned by this second method. Also, the cleaning time was very short and thus can be repeated several times; however, the parts being cleaned must be thoroughly dried before each application of the cleaning solution, otherwise the metal parts will tarnish.

The cleaning of quartz wafers before Cr + Au bonding-site plating was a batch operation. Before loading wafers into the mask cleaning was usually by the first CrO_3 + H_2SO_4 method described above. However, the cleaning solution is used at 25°C rather than at 75°C.

We assembled a few resonators using etched quartz wafers. The etchant was an aqueous solution of $NH_4F.HF$, saturated at 25°C. Each etch period was limited to 1 min during which time between 150 and 200 Å of quartz was removed from each side of the wafer. Etching preceded any plating operation, including the bonding-zone plating.

As the last step before placing in the vacuum chamber, a number of mounted and bonded wafers were coated with polysiloxane, by dipping them into a solution of alkychlorosilanes dissolved in CCL_4*. When applied to a wet-cleaned surface Naiditch and Wreede[4] have shown that the resulting surface is relatively free of residual contamination. Kahn[5] demonstrated that the surface energy of the wafer was lowered by the use of the polysiloxane coating. During some in-house research on the penetration of the quartz by the metal film electrodes we found that the coating effectively "sealed" the quartz surface thereby minimizing the penetration of metal into the quartz.

b. Lead Bonding. We had been making the electrical connection

---

*Obtained as DESICOTE, a product of Beckman Instruments, Inc., Fullerton, California.

from the resonator electrodes to the support posts using ultrasonically bonded (USB) aluminum foil; this method of bonding was excellent from an electrical standpoint. The noise level of these resonators, readily detected by our method of measuring frequency, was very low. Also, the stress introduced into the quartz was the lowest of all bonding methods, as indicated by the source image distortion (SID) x-ray technique. However, with respect to shock and vibration resistance, USB is a poor technique and there seems to be little hope of improving the strength of the bond while also preserving the desirable features mentioned above. Since the crystals fabricated during this research project were expected to pass military shock and vibration standards as described in MIL-STD-202, we elected to use the relatively new nickel electrobonding technique described by Stanley[6].

The wafers were first cleaned, etched when required, and then loaded into a 10-position mask for the Cr(500 Å) + Au(1500 Å) bonding site plating. Both sides of each wafer were plated during one operation in an oil-free system at pressures below 10^{-7} torr. The wafers were then mounted in Ni strike-plated tab clips leaving a 0.0625" clearance between the flat on the quartz and the HC-6 holder. All of the Cr + Au film was then coated with photoresist* except for a small area near the clip. When the resist was dry the assembly was electroplated in a sulfamate Ni plating solution, heated to about 55°C, at 5 mA for 45 to 60 min. This produced a nickel film between 0.0005" and 0.00075" thick. The final mounting configuration is shown in Fig. 1.

As reported in Monthly Status Report No. 3, studies of the strain pattern associated with the sulfamate Ni film using the SID technique revealed the presence of stress in the quartz in the immediate area of the Ni. Also, an electron microprobe analysis of the Ni indicated the presence of 0.4 o/o Co, 0.03 o/o Cr, and O_2. An AES analysis failed to identify Co on the surface, but did detect the presence of Cu.

c. Electrode Plating. An important requirement of the present program was that resonators be plated and sealed by coldwelding in the same vacuum. The sealing portion of the system was completed during the first half of the project and was used to bake out and seal the resonators fabricated during the first half of this project. By the time the new wafers were received for this project, the plating portion of the fabricating unit had been completed. All the frequency data in section II-A of this report were obtained from resonators which were plated and sealed in the same vacuum.

Figure 2 shows a general view of the vacuum equipment used during this project. Figure 3 is a close-up of the combination plating and sealing chamber before the addition of the electrode plating equipment.

Figure 4 shows the subassembly which was added to the system as shown in Fig. 3 for the plating by evaporation of the resonator electrodes. The same parts are shown in Fig. 5, except in this view the plating mask has been retracted and the die closed for sealing. A recent modification was the addition of a shutter to the magnetically positioned electrode mask so the evaporation sources, 1/4" O.D. Ta tubes with a 1/8" side hole,**

---

*Shipley No. AZ-111 positive resist.

**R. D. Mathis Model S17A-005 Ta.

could be brought up to plating temperature before exposing the quartz plate to the evaporant.

The coldweld die in which the mounted wafer was placed for plating, as well as for baking and sealing, was modified by spark milling the holder pin holes to a larger diameter. This modification was necessary so that polyimide inserts could be used to prevent the pins from shorting to the die. Electrical leads were spotwelded to the base pins.

The following sequence of operations was used during reloading the system, plating, baking, and sealing (assume the wafer has been electrobonded to the HC-6 base mounts).

1) Reload the Ta sources with 1 to 2 ft lengths of 0.010" Cu* wire cut into 1 in lengths for easy feeding through the side hole in Ta tubes. Before sectioning, the copper wire is vapor degreased in trichloroethylene, electrocleaned in a Na_3PO_4 solution** (20 gm/liter of distilled water), and then ultrasonically cleaned in MICRO® *** (10.0 cc/liter of distilled water). It is rinsed with tap water, followed with distilled water and methanol, then dried with warm air.

2) Place the polyimide inserts on the holder pins.

3) Spotweld the 0.010" Teflon insulated Ni leads to the pins.

4) Final clean the wafer and holder by flowing on CrO_3-H_2SO_4 solution and follow with rinses of flowing distilled water, methanol, and then dry in warm air.

5) Mount the wafer and holder in the base portion of the coldweld die.

6) Clean the HC-6 cap as described for 4 above and insert in upper portion of die. If a solid getter**** is used it is spotwelded to the inside of the cap immediately before the cap is placed in the die.

7) Assemble the die and load it into the plating-sealing system.

8) Rough pump to about 10^{-3} torr and start ion pumps. The system

---

*The Cu wire is Materials Research Corporation "MARZ" Grade. A typical analysis of the vacuum melted Cu shows < 32 ppm total impurities; major impurities are Al and Zn (< 10 ppm of each) and Mo (< 5 ppm).

**The solution is contained in a stainless-steel vessel. The parts to be cleaned are made 6V negative with respect to the vessel.

***International Products, Inc., Trenton, N. J.

****CERALLOY 400 Continuous Getters, Ronson Metals Corporation, Newark, N. J.

should then be pumped for approximately 5 to 6 hours, at which time the pressure would be in the low 10^{-9} torr range. Titanium sublimation pumping is used in addition to ion pumping to achieve the low pressure.

9) The vapor sources are then preset to the proper current (100 to 110 A) and the electrode mask moved from the shutter to plate position.

10) The frequency is monitored aurally and visually as the resonator approaches a preset reference frequency.

The natural quartz wafers obtained from the commercial vendor were much too high in frequency to plate to 5000 kHz with Cu; these were plated to a nominal frequency of 5030 kHz measured with a 30 pF load capacitance. The specifications for the premium High Q wafers were changed to provide a lower wafer frequency, but these were still too high to obtain 5000 kHz and were plated to between 5010 and 5015 kHz. The frequency range of the wafers from ECOM was said to be between 5025 and 5030 kHz; these wafers were easily and consistently plated to the desired frequency. The plate back for all wafers was about 30 kHz ± 5kHz.

d. Resonator Vacuum Bakeout and Sealing. Our usual procedure during operations in the plating-sealing system was to plate to frequency, bake out, then seal. This sequence was questioned during a recent project conference, as ECOM representatives stated they preferred to use the sequence bakeout, plate, and seal. There is merit in either method. However, our system was designed to start with the die in the plating position and subsequently lowered to the bakeout position and then to the sealing position. Our sequence was based on the requirement that the crystal units be adjusted to 5.000 MHz ± 5 ppm at 27°C ± 1°C.

The procedure followed after plating the resonator to frequency, described in section II-A-2-C, was the following:

1) After the proper frequency has been obtained, the mask is magnetically retracted and the die lowered to the bakeout position. This latter position allows some space for the gases released during bakeout to escape from the resonator holder and to be pumped away.

2) Apply power to the heater which is attached to the side of the die. The die reaches 200°C fairly quickly but the quartz wafer temperature continues to rise for hours, but apparently never reaches the die temperature, as judged by frequency measurements made during bakeout.

3) The bakeout is normally started at 1600 hr and continued overnight until 0800 hr the following day.

4) The coldweld seal is then made with 8 tons of force while the resonator is at the bakeout temperature and in a residual gas pressure of about 1 to 2 X 10^{-9} torr.

5) After sealing, the system is brought up to atmospheric pressure by admitting dry nitrogen and the unit retrieved from the hot die as quickly as possible. The solid getters are most effective

during this period and will "soak up" desorbed gas. However, the temperature should be lowered as quickly as possible to prolong the useful life of the getter.

6) The resonators after processing are placed in the 62°C upper turning point oven by 0900 hr and the first measurement made at 1300 hr.

The bakeout temperature for all experiments during the second half of the project was 200°C, since higher temperature bakeouts did not yield resonators of superior aging properties. However, a comprehensive analysis of the effect of bakeout temperature was not undertaken during this program.

The planned experiments with helium backfilled units were given a low priority due to the late delivery of quartz wafers.

e. Frequency Measurements.

1. Long-term frequency aging measurements were made at the nominal upper turning point (UTP) temperature of 62°C for these wafers (orientation angle, Θ, = 35° 13.5' ± 0.5'). Measurements on the units made with ECOM wafers (Θ = 35° 16.5') were also carried out at 62°C, although their UTP was at a much higher temperature.

Long-term aging measurements were made with equipment developed and used at Georgia Tech during similar studies over the past several years. The block diagram shown in Fig. 6 illustrates the basic system. All of the equipment shown in Fig. 6 is commercial equipment except the crystal impedance bridge. The circuit diagram for this impedance bridge is shown in Fig. 7.

The crystal resonators were stored in the 62°C oven and their frequency measured periodically by making them the passive element in the bridge. This method of measurement yields information (F_s and R_s) about the unit under test; no correction factors are needed to compensate for oscillator aging, etc. The aging rate is apparently unaffected by the on-off nature of the measurement, so long as the unit is driven at a low power level (a few microwatts) and remains at an essentially constant temperature. The measurement accuracy of ± 0.001 Hz is equivalent to $\pm 2 \times 10^{-10}$.

2. The thermal frequency repeatability variation measurements were made in the 62°C oven and with the same system used for the long-term aging measurements. The resonator frequencies were first measured at 62°C, then the units were soaked for 30 min at -55°C (acetone and dry ice mixture), and the frequencies then remeasured after 30 min at 62°C. The units were then soaked for 30 min in 90°C silicone oil and returned to the 62°C oven for reaging measurements, the first of which was taken after 30 min. This technique departs considerably from the one outlined in the Technical Guidelines for three reasons: 1) the specified temperature cycles required about 15 hr, 2) we were unable to obtain the required temperature stability to make measurements of $\pm 1 \times 10^{-8}$ or better at the lower turning point (-11°C), and 3) we consider several shorter temperature cycles interspersed with reaging measurements to be technically more significant.

3. The frequency (F_s) vs temperature and resistance (R_s) vs temperature measurements were made with the system shown in block form in

Fig. 8. The frequency was measured by logging the counter readings at 5°C intervals. The resonator resistance was measured by recording the variation of the crystal impedance (CI) meter grid current on the Y-axis of an X-Y recorder; the X-axis was calibrated to monitor the temperature of the oil bath using a thermistor probe as the sensing element. The low temperature (-55°C) was obtained by adding "dry ice" to the stirred silicone oil bath; power was then applied to an immersion heater to increase the temperature at a rate of about 2.5°C/min to the maximum temperature of 90°C. The frequency measurements were precise to about $\pm 1 \times 10^{-7}$, the temperature measurements accurate to about ± 1% and the resistance measurements accurate to about 1 Ω in the 0 to 15 Ω range. A small tracking error exists between quartz temperature and oil bath temperature but apparently does not affect the quality of the data.

4. The frequency measurements during plating were made with the equipment shown in block form in Fig. 9. The frequency measurements, made at the series resonant frequency were precise to about $\pm 1 \times 10^{-6}$, since the temperature uncertainty during plating degrades the overall system performance. The counter was used for the coarse measurement of frequency. As the reference frequency, supplied by the synthesizer, was approached the beat between the reference and oscillator frequencies was displayed on the oscilloscope and this was then used to visually monitor the frequency, while the vapor source was manually controlled to obtain zero beat. The digital-to-analog converter output was plotted on an X-Y recorder to provide a permanent record of the plate back and plating rate.

3. Experimental Data

a. Long-term Aging. The resonators used for long-term aging rate evaluation were assembled during the last four months of the project. Seven of the first twelve units assembled failed or gave anomalous behavior due to poor electrobonding techniques; the entire Cu + Au bonding zone had been Ni plated and the continuity of the over-plated copper-film electrodes was poor. The problem was eliminated when the process was changed to the one described in section II-A-2-b. Later, another problem was encountered with the installation of the solid getters. We found that unless great care was used when spotwelding the getters to the inside of the HC-6 cap a leak to the atmosphere developed at the weld. The units were subsequently assembled with unwelded, spring-loaded getters in the cap. Such action, while poor from a military shock and vibration consideration, was adequate for aging studies.

A certain amount of time was needed to learn to use the plating and sealing system efficiently. Minor modifications were made as the need became apparent. For example, a shutter was added to the retractable plating mask so the evaporation sources could be outgassed and then brought up to the desired temperature, determined by an optical pyrometer before exposure of the mounted quartz wafer. A real problem resulted from changes in the evaporation source performance which was due to the residual copper

in the tantalum sources.* The sources were recently modified by flattening an additional 1/2 inch of their length at each end. This action resulted in a more uniform heating of the cavity containing the evaporant and gave more predictable and uniform (with time) evaporation rates.

The average aging rate of resonators assembled with commercially obtained natural quartz wafers was similar to that shown for unit No. 18 in Fig. 10. This unit was baked for 16 hr at 200°C in vacuum after plating, and before the coldweld seal was made with the system at the bakeout temperature and the pressure 3×10^{-9} torr. A few similar units were not baked in vacuum after plating and these units were found to age at about twice the rate of unit No. 18.

The application of an alkylchlorosilane coating on the natural quartz before plating appears to have a beneficial effect on aging. An excellent example of the improvement that can be made in aging rate by this process is shown in Fig. 11. The aging rate was less than 10^{-9}/week after the first few measurements.

Premium Hi-Q quartz wafers were not received until late in the program and thus aging data for this material were limited. All the Hi-Q wafers used for resonator fabrication were etched for 1 min in a saturated solution of $NH_4F.HF$ before the bonding-sites were evaporated onto their surfaces.

Typical aging data for a unit assembled with Hi-Q quartz and with a solid getter is shown in Fig. 12. The beneficial effect of solid getters was not so evident during the second half of the project when the aging oven temperature was reduced from the previous values of 85°C to 62°C. Some of the polysiloxane coated Hi-Q quartz wafers showed excellent aging characteristics. Aging data from unit No. 56, see Fig. 13, show a very low rate in spite of the three thermal repeatability cycles.

Ten natural quartz wafers were supplied by ECOM for comparison with similar (but not identical) commercially prepared wafers. The aging rates which were recorded from the seven complete resonators we made from these wafers were quite poor. Part of the problem was the fact that the aging oven in the screen room was at 62°C and the UTP for the ECOM wafers in the range of 70 to 75°C. Unit "H", a polysiloxane-coated wafer, aged as shown in Fig. 14. Note that the thermal repeatability cycles caused frequency deviation but no dramatic change in aging rate. Unit "J" with an enclosed solid getter performed as illustrated in Fig. 15.

Table I gives the electrical parameters of the units measured for aging at 62°C. The average Q value was well above the specified minimum of 5×10^5; specific averages were 9.0×10^5 for natural-quartz resonators, 8.9×10^5 for Hi-Q quartz resonators (units Nos. 53 and 54 not included) and 7.6×10^5 for the ECOM-wafer units. The pin-to-pin capacity was about 3.7 pf and the capacitance ratio (C_o/C_1) was about 340 ± 10%; both values indicated that a minor adjustment in the electrode size was in order. The final aging rate which was determined during the last month of the project, is also shown, when possible, along with the dominant variables introduced during assembly. Starting with unit No. 16 an overnight (~ 16 hr) bakeout at 200°C was routinely carried out. All units starting from "E" and below in Table I were plated using the combination shutter and plating mask.

---

*R. D. Mathis No. S-17 A-.005Ta.

Shock and vibration data are lacking. Some of the early rejected units were vibrated but their poor performance was considered due to the electro-bonding method used during assembly rather than the vibration.

b. Thermal Frequency Repeatability. Eight selected resonators were temperature cycled, as previously described, at about seven-day intervals. Reaging measurements were made at 62°C between cycles. The resonator fabrication variables were 1) the source and type of quartz, 2) the effect of solid getters in the holders, and 3) the effect of polysiloxane coatings on the quartz.

The deviations obtained for all resonators except unit No. 50 are shown by Fig. 16. Unit No. 50, Hi-Q quartz in a gettered holder, was given a temperature cycle of -55°C to 90°C, which caused a frequency shift of $+ 1.3 \times 10^{-7}$ during a resistance vs temperature test, before starting with the thermal frequency repeatability measurements; subsequent repeatability cycles gave anomalous behavior and most of the data points were off scale.

The best units with respect to thermal frequency repeatability were Nos. 55 and 56, both using Hi-Q quartz wafers. Perhaps a more significant variable was the fact that each wafer was etched 1 min before plating Unfortunately, the thermal frequency repeatability of resonators made from other types of etched quartz was not measured.

Excluding unit No. 50, then, 84% of the thermal frequency repeatability measurements fell within the permitted variation of $\pm 1 \times 10^{-8}$.

The reaging rates were also important factors in the repeatability measurements. We rarely obtained the classical reaging curve which is a repeat of the accrued aging preceding the thermal interruption. In most cases thermal cycling produced offsets in the aging data but produced very little change in aging rates. A typical example of such behavior is shown in Fig. 14 for unit "H". Resonator No. 56 (see Fig. 13) also gave excellent performance with respect to both the thermal frequency deviation and reaging.

c. Frequency and Resistance vs Temperature. The resonator parameters checked during these tests were: 1) the operating temperature range, 2) resistance vs temperature, and 3) frequency deviation vs temperature. The test method was described in section II-A-2-e-3.

All the tested resonators were operable over the temperature range of -55 to +90°C. Most of the units were relatively free of activity dips and met the maximum permissible resistance variation requirement of 1 Ω/3°C R_s variation. An example of an unacceptable resistance variation is shown in Fig. 17 for unit No. 9 fabricated from a commercially obtained natural quartz wafer. However, a similar unit gave the acceptable results shown in Fig. 18 for unit No. 5. One of the best units, No. 50, was fabricated of Premium Hi-Q quartz and the data are shown in Fig. 19. The units assembled using ECOM wafers had acceptable resistance vs temperature behavior but were generally not as "clean" as the best resonators assembled with commercial wafers. An example of the results obtained with an ECOM quartz wafer (unit No. F) are shown in Fig. 20.

None of the units tested passed the frequency deviation requirement of ± 3 ppm maximum frequency difference at -45°C and the UTP of 62°C.* Frequency

*The ECOM wafers were not designed to meet this requirement.

measurements, in addition to those shown by the previous figures of this section, were made at the fixed temperatures of -45°C and +62°C and revealed the frequency at -45°C to be consistently about 23 ppm lower. It appears that the actual angle of the purchased wafers was 3 to 4 min lower than specified.

The frequency deviation requirement can be met by selecting the optimum angle and then holding the angle tolerance to about ± 30 sec maximum deviation on the finished wafer.

B. Studies of Quartz Surfaces

1. Introduction

During the course of this work various chemical and physical aspects of quartz surfaces have been investigated, especially those on which aging of quartz resonators is thought to depend. The identification of elemental material and chemical compounds on the immediate quartz surface has been the subject of Auger electron spectroscopy (AES) and high energy electron diffraction (HEED) investigations. The spatial distribution of these surface deposits as well as the morphology of quartz surfaces have been the subjects of examinations by scanning electron microscopy (SEM) and transmission electron microscopy (TEM) of surface replicas.

2. Apparatus and Procedures

a. The Quartz Surface. Both polished and polished then etched surfaces were examined by the analytical techniques mentioned above. The commercial supplier of both the natural quartz and the Hi-Q cultured quartz wafers that we used in this project would not divulge the lapping and polishing processes which were used to prepare our samples. A small number (10) of polished natural quartz wafers were also obtained from ECOM for comparative evaluation. These wafers were prepared as described by Wasshausen[1], the polishing process being carried out with cerium oxide abrasive.

Four of the purchased natural quartz wafers were given additional polishes, using an etch-polish technique [7]. The method consisted of polishing individual wafers, each waxed to the base of a plastic mount, in a slurry of gamma alumina; the liquid medium was saturated ammonium bifluoride ($NH_4F.HF$). Individual wafers were polished on one side for either 20 min or 40 min.

All samples referred to in the text that follows as being polished were given a final cleaning in chrome-sulfuric acid, rinsed with distilled water then alcohol, and dried in a current of warm air.

The chrome-sulfuric acid cleaning step was unnecessary with freshly etched samples, thus these samples were only rinsed with water, then alcohol, and air dried before examination.

b. Auger Electron Spectroscopy. The spectrometer used to analyze the quartz specimens was a three-grid, retarding-potential type with an energy resolution of about 30. It was located in a large stainless steel ultrahigh vacuum chamber which operates in the 10^{-10} torr pressure range and

can be brought down to operating pressure in about 8 hr. The pumping system was of sufficient capacity and type that it was not necessary to bake out during each pumping cycle.

Two electron guns were provided in this chamber to generate the primary electron beams. One of these guns was situated normal to the specimen surface and behind the spectrometer grids. The electron beam passed through a drift tube in the grid system. The second gun was located so that its electron beam contacted the specimen surface at a glancing angle of 15°.

Polished quartz samples were mounted on stainless steel backing plates by two stainless steel clips. Up to five samples were mounted at one time on a windmill-type sample holder. The potential of each sample while under observation could be raised to as much as 200 volts above ground. This is an important feature when dealing with insulating materials, since by suitable adjustment of the sample potential during electron irradiation charging can be eliminated. Judicial use of the two electron guns at once also helps to reduce charge buildup on the quartz surface.

c. High Energy Electron Diffraction. Samples that had either been subjected to AES or had freshly prepared surfaces were examined by the HEED glancing angle technique, using an electron beam of 100 keV energy. The apparatus was an RCA-EMU-3F electron microscope with a high resolution diffraction attachment. Incident angles of about 2° were used, and the electron beam was focussed down to about 10 microns at the photographic plate.

Again, it was necessary to charge neutralize the quartz surfaces during observation by use of an auxiliary electron gun which operated in the vicinity of 1 keV. However, the combined actions of the high energy and low energy beams rapidly contaminated the surface. This high rate of contamination made it imperative to record diffraction patterns in as short time as possible. These samples were not used for any other purposes since it was feared that even after subsequent cleaning in chrome-sulfuric acid all the contaminating layer would not be removed.

d. Scanning Electron Microscopy. Quartz surfaces in both polished and etched states were observed in a Cambridge Stereoscan II microscope. The wafers, after mounting onto specimen stubs, were coated with a metal alloy consisting of 60% gold and 40% palladium to a thickness of a few hundred angstroms. This was done to prevent charging of the quartz surface while being observed in the electron microscope.

e. Transmission Electron Microscopy. The surfaces of a number of quartz wafers were replicated for examination by TEM, this technique allowed details down to a few angstroms resolution to be observed. Two replication processes were employed. The first was the conventional two stage process, which entails laying down a plastic film from a 1 w/o solution of collodion in amyl acetate, stripping, shadowing with gold palladium at $\tan^{-1/3}$ and then depositing a thin (~ 300 Å) carbon film on the metalized plastic surface. After mounting the composite replica on a microscope grid the plastic film was dissolved away before the metal shadowed carbon replica was observed in the electron microscope.

The second process employed was that of extraction replication with

platinum preshadowed carbon substrates. The substrates were evaporated directly onto the wafer surfaces by the method described by Cook[8]. After scoring the continuous film into squares of approximately 2 mm per side, the underlying quartz was attacked with saturated ammonium bifluoride solution. In about five minutes the replicas floated off the wafer surface. Individual squares were mounted on microscope grids, washed in distilled water, dried, and examined in the electron microscope.

A Philips 200 electron microscope was used to examine all the replica specimens. When particulate matter was observed adhering to the replica surface, a selected area diffraction (SAD) pattern was recorded. These diffraction patterns enabled us to identify various materials which were extracted from the quartz surface.

3. Results of Surface Characterizations

a. Elemental Composition of Quartz Surfaces. The AES data obtained from quartz wafer surfaces, which were investigated in the as-received condition, were similar to that shown in Fig. 21. Besides the expected spectrum lines from chemically bound as well as physically bound silicon and oxygen, there were spectrum lines which corresponded to the strongest lines of sulfur (149 eV), chlorine (181 eV) and carbon (257 eV).

Carbon was a very prevalent contaminant, and was found in varying amounts on practically all surfaces which were investigated in the as-received condition. This is not withstanding the fact that samples were analyzed in very clean systems. Usually, the surface carbon can be reduced to a very low level, if not entirely removed, by argon ion bombardment or sometimes by heating the sample to a high temperature. Of course, heating quartz to about 500 to 600°C will ruin it as a resonator, leaving ion bombardment as the only practical method of thoroughly cleaning quartz wafers which are to be used in resonators.

Another difficulty which resulted from the presence of carbon on a quartz surface was that it reacted with the quartz to form silicon carbide under the fairly intense electron irradiation to which it was subjected during AES analysis. Silicon carbide is an extremely stable compound and not readily removed by any of the customary surface cleaning techniques.

Sulfur and chlorine appeared in much smaller percentages than carbon, and their relative ratios changed from sample to sample. Initially, the presence of chlorine was attributed to sodium chloride, which can almost be considered, like carbon, as a universal contaminant. However, AES investigations of copper electrodes on quartz wafers (details given elsewhere in this report) that had been cleaned in chlorinated hydrocarbons, e.g., trichloroethylene, showed that appreciable amounts of chlorine were retained by these surfaces. As the complete history of the commercial wafers is unknown, it is not possible to say whether or not the presence of chlorine on an as-received wafer is due to cleaning solvents.

The origin of small amounts of sulfur on polished quartz is unknown. It is logical to assume that it was in the quartz as an impurity, since residual gas analyses taken in the spectrometer from time to time have never revealed the presence of any sulfur bearing compound.

b. Structural Composition of Quartz Surfaces. Samples of polished natural quartz and cultured quartz wafers, as well as natural quartz further processed by etch-polishing up to 40 min, were examined by reflection electron diffraction at 100 keV. This technique was chosen over x-ray methods since it is a very sensitive method for detecting the structure of material in the immediate surface. Furthermore, all the diffraction information is generated from a depth below the free surface of no greater than about 200 Å. Thus, deep seated defect structures are eliminated and we only observe the region of direct interest to our particular problem of resonator aging.

All samples that were investigated revealed a very high degree of perfection in the quartz structure at the wafer surface. This is clearly in evidence by observing the sharpness of the Kikuchi lines in the diffraction patterns, as shown in Fig. 22. There was only a minimum of diffuse scatter adjacent to the primary beam spot, which indicates the lack of measurable amounts of "amorphous"[9] film on these wafers.

Several other features were observed in these diffraction patterns. The vertical spotty line seen extending from the primary beam spot in Fig. 22 is due to diffractions from a carbonaceous deposit which built up during observation. The particular instrument used in this work had quite a high contamination rate, and thus it was necessary to record diffraction patterns as soon as a new area of the surface was exposed to the primary beam.

Faint ring diffraction patterns were also observed, concentric to the primary beam spot, on some of the recorded diffraction patterns.

These ring patterns, although very faint and usually displaying only the strongest lines, were found to fit reasonably well with diffraction maxima in either y-alumina or cerium oxide, depending on which of these two compounds was used to polish a particular wafer. Positive identification of these compounds in the wafer surfaces was made by using selected area diffraction (SAD) on extraction replicas.

4. Morphology of Quartz Surfaces

a. As-Received Wafer Surfaces. Except for a very small amount of macroscopic waviness, which could be observed by eye when light was reflected off the surface at an appropriate angle, all wafers exhibited a high quality surface finish. However, microscopic examinations revealed a number of features which degraded the overall perfection of each surface.

Examination of wafer surfaces in the as-received state was carried out with the aid of surface replicas. By and large these surfaces were smooth over large areas and contained so few features on which to focus the microscope that TEM and to a much greater degree SEM investigations were difficult to accomplish. The most prominent feature observed on polished quartz was the sparse occurrence of roughly hemispherical particulate matter. Figure 23 (two stage shadowed carbon replica) shows a few such particles scattered over the surface of a Hi-Q cultured quartz wafer. These particles varied in size from about 0.1 μ to about 0.5 μ in diameter. Because of the lack of any other defining features, we were unable to identify these particles, although it is plausible to assume that they are partially embedded particles of polishing compound which have survived the final

cleaning processes.

An occasional scratch was also observed, as shown towards the left of Fig. 23. However, on the whole the surfaces we observed were remarkably free from scratches.

Several quartz wafers prepared in the ECOM laboratories, Fort Monmouth, were also replicated for TEM analysis. Micrographs, as shown in Fig. 24, showed these surfaces to be very smooth and almost featureless. There was the extremely isolated occurrence of particulate matter, an example of which is also shown in this figure.

From platinum preshadowed carbon extraction replicas we were able to remove particulate matter from the quartz surface and obtain selected area diffraction patterns of sufficient clarity to make accurate identification. An example of extracted particles of about 0.1 μ average diameter is shown in Fig. 25. These particles were positioned within two quite large depressions in the surface. The larger of the two depressions was about 5 μ long by 1.5 μ wide and appeared to be about 0.5 μ deep. These depressions probably resulted from scarring of the surface by extraneous coarse abrasive during some stage of the polishing process.

Selected area diffraction patterns from these areas showed good correspondence with cerium oxide, CeO_2, X-ray Powder Diffraction File, Card No. 4-0593, Joint Committee on Powder Diffraction Standards, Swarthmore, Pennsylvania. The measured diffractions are listed in Table II, which show a good correspondence with the materials CeO_2 and platinum; the latter being placed on the surface as a shadowing agent. It is most likely that cerium oxide was carried over from the final polishing operation and being sheltered in depressions was able to resist dislodgement during the final cleaning process.

b. Etch-Polished Wafer Surfaces. This surface finishing process led to a degrading of surfaces, when compared with as-received surfaces. Surfaces which had either been etch-polished for 20 min or for 40 min contained shallow depressions similar to those shown in Fig. 25. They are also visible in the scanning micrograph, shown in Fig. 26, of a 40 min etch-polished surface. The particulate material in this instance was identified as γ-Al_2O_3 (X-Ray Powder Diffraction File, Card No. 10-425) from reflection electron diffraction patterns. Non-dispersive x-ray analysis of these surfaces in the scanning electron microscope also revealed the presence of aluminum.

Ultrasonic agitation in a dilute MICRO® solution (10 cc /liter of distilled water), followed by chrome-sulfuric acid treatment did not remove these particles. Thus, it appears that a small amount of final polishing abrasive was sufficiently firmly imbedded in the quartz surface as to resist removal by severely physical processes.

Leftover polishing media was, however, removed by etching the quartz in ammonium bifluoride for a short period of time, usually about 10 min.

Since the morphology of polished quartz wafers was not improved by our application of the etch-polishing technique, only a few crystals were prepar ed and then this line of investigation was discontinued.

c. Etched Wafer Surfaces. Wafer surfaces which had been etched in ammonium bifluoride for 10 min or longer, e.g., 15 min, displayed features which were not observed on either the as-received or etch-polished surfaces.

The nature of these etch features, as can be seen in Fig. 27, was slightly curved lines and averaging about 5 μ in length. In some areas on the surface they appeared to be essentially randomly oriented with respect to each other. However, there were areas on the surfaces of wafers that did show these features aligned with respect to each other, as shown in Fig. 28; at the magnification of Fig. 28 it can readily be seen that each line represents the top of an etch pit wall and that a contoured trough leads from the wafer surface to a lower region of the pit wall.

Similar features were also observed in the etched surfaces of ECOM wafers, although the frequency of their occurrence was very much less than we observed with commercial quartz wafers. The result of a 15 min etch on an ECOM wafer is shown in Fig. 29. Notice that the features are less prominent as well as occurring less frequently.

Although the cause of these etch features is not known with absolute certainty, a logical explanation follows. During the successive stages of lapping and polishing a surface, not all the deeper scratches, caused by preceding coarser abrasives are always removed. In the final lapping or polishing operation the immediate surface is caused to "flow", creating what is commonly referred to as a Bielby Layer[10,11]. This material, naturally, will fill the depressed areas in the surface, creating a surface with a highly polished appearance.

The whole polished surface retains a certain amount of strain from the polishing process with high strain points probably existing beneath the remains of scratch lines. It is at these locations that the most severe deformation (high point loading) has occurred in the as-polished surface. On commencing to etch such a surface, the etchant will first attack the highest energy crystallographic planes or highly strained artifacts. This is the basic mechanism for etch pit formation. The remainder of the surface will dissolve at a somewhat slower rate and show little, or no, faceting.

If our interpretation of these micrographs is correct, and there is every reason to believe that it is, then the frequency of occurrence of these features is an indication of how well successively finer abrasives have removed previous surface damage. Should each step in polishing a surface be of such duration as to remove all the features left by the previous step, then the observed etch pattern should not appear.

C. Studies on Copper Surfaces

1. Introduction

All indications to date point to quartz resonator aging as principally an interfacial problem. Specifically, we are dealing with the surface of the deposited electrode, its interaction with the ambient atmosphere, the quartz-electrode interface, and the polished surfaces of the

quartz wafer.

Several investigations[12,13] appear to indicate the predominance of adsorption or desorption, depending on the sign of the aging vector. Hafner and Blewer[14], on the other hand, used experimental methods that probably eliminated most of the aging due to mass transfer. In these resonators the aging process was most probably due to the relaxation of mechanical strain in the quartz-electrode interface. Copper electrodes were found to yield the lowest aging rate.

Kolkolm and Berry[15] have reported that stress associated with evaporated metal films is low for Cu and Ag, but for most other metals, including Al and Au, it is high.

X-ray studies[16] of the strain, impurity levels, defect structures and modes of motion of quartz have been made during the course of previous research programs. The strain in quartz resonators resulting from epitaxial misfit may also be an important factor in aging, which is given too little consideration. Relief of this strain by suitable selection of materials and annealing procedure is essential if an improvement in aging is to be realized.

Specific contaminants on the electrode surface or in the interfacial zone influence to various degrees the aging and retrace characteristics of quartz resonators. During this program we have employed the very sensitive AES technique to determine the composition of the free surfaces of evaporated copper electrodes.

2. Apparatus and Procedures

a. Evaporated Copper Electrodes. In this particular set of experiments, the copper electrodes were evaporated onto quartz wafers in batches of ten. This insured a sufficient number of similar samples to carry out both the surface analysis and to make resonators for aging studies.

All the crystals were plated with copper to about 1500 Å thickness by evaporating from a stranded tantalum filament. The copper was in the form of 0.010" wire for which a typical analysis is given in section II-A-2-c of this report.

One group of crystals, designated "A" type, were prepared by evaporating the copper electrodes onto the quartz surfaces while they were held at room temperature (about 25°C), after they were first heated to 200°C for 30 min in vacuum. The operating pressure in the oil-free ultrahigh vacuum system during each evaporation was in the 10^{-9} torr range. This system was used for all evaporations described in this section of the report.

Another group of crystals, designated "B" type, had the copper electrodes evaporated onto their surfaces while they were held at 200°C.

After the electrodes were evaporated onto each batch of crystals, the batch was allowed to cool to room temperature before removal from the vacuum system. Most of the plated crystals were bonded to the tab clip

mounts on type HC-6 bases, using the ultrasonic bonding technique.

Each mounted crystal was subjected to a final cleaning before it was placed into the vacuum system for a final bakeout at 200°C for 20 hr, and sealing into a holder. In the first instance, the final cleaning of crystals was by vapor degreasing in trichloroethylene. As the results will show, chlorine was detected on the surface of these crystals, so other methods of final cleaning were sought. One of these alternate cleaning processes was to gently scrub the mounted crystals in a MICRO® cleaning solution, as previously described in this report. Crystals were rinsed with distilled water, then with methanol, and finally dried in a stream of warm air. The other cleaning process was simply to wash the mounted crystals in methanol and air dry.

After aging data had been collected for 30 days from both A and B types of crystal units, several units of each type were broken open and the electrode surfaces analyzed by AES.

b. Studies Using Copper Foil. For comparison purposes, as well as to conserve quartz wafers which were in short supply, a few experiments were carried out on polycrystalline copper foil. This material was of the same purity as the copper wire used for evaporation.

Samples of the as-received copper foil were prepared for AES examination by lightly etching them in dilute nitric acid and then rinsing in tap water. After an initial AES examination, samples were heated in the ultrahigh spectrometer vacuum at various temperatures and for various periods of time. One sample was cycled to air and then reevaluated by AES.

c. Auger Electron Spectroscopy. All the copper surface characterizations were carried out in the Auger electron spectrometer that has already been described. When working at conducting surfaces one is not plagued with the problem of surface charging. As a result, the AES data is likely to be somewhat more definitive of the surface composition.

3. Results with Evaporated Copper Electrodes

a. Surface Composition of Evaporated Copper. AES data, similar to that shown in Fig. 30, were obtained from the free surfaces of copper electrodes, which were evaporated onto quartz at 25°C, after it was preheated at 200°C. The quartz wafers were vapor degreased in trichloroethylene before loading into the evaporator. This spectrum has one prominent peak from carbon and a number of small peaks from copper, sulfur, chlorine, nitrogen and oxygen. Analyses from all as-received samples showed the prominence of carbon on "clean" surfaces, which partially obscured other lines in the spectrum.

The presence of copper, nitrogen, and oxygen were naturally expected, but not so sulfur and chlorine. The most probable sources of these two elements were the evaporant, copper, which contains sulfur as an impurity, and the trichloroethylene in which the wafers were degreased.

Samples prepared by evaporating the copper onto the quartz surface held at 200°C and then transferred to the spectrometer at ambient temperature yielded similar AES data to that recorded in Fig. 30.

The copper surface of an "A" type crystal unit, after a 20 hr bakeout at 200°C yielded an Auger electron spectrum similar to that shown in Fig. 31. On viewing this spectrum it is immediately apparent that the carbon peak is appreciably smaller than that shown in Fig. 30, while the copper, nitrogen and oxygen peaks are enhanced. However, note the strong response from chlorine and a slightly increased response from sulfur. This bakeout treatment has obviously removed part of the persistent carbon contamination and allowed the less prevalent, though very important, minor impurities to be more distinctly portrayed.

After baking plated crystals in vacuum for 20 hr at 300°C instead of 200°C the spectrum lines from chlorine and sulfur were found to have decreased in magnitude and to have reversed their relative intensities. The higher temperature almost completely eliminated chlorine from the surface, while the increased amount of sulfur can best be explained by the diffusion of sulfur from the bulk of the copper electrode to the surface.

Additional heating of baked out (300°C) samples in the spectrometer for a few minutes at 300°C failed to significantly change the surface composition. This indicates that the composition of the copper surface had stabilized by the end of a 20 hr bakeout at 300°C.

b. Wet Cleaning of Evaporated Copper on Quartz. Three quartz samples which were plated with copper at 200°C were retrieved from the plating chamber, placed in a clean, covered, petri dish and stored in a vacuum dessicator for about two weeks. They were then used in the following experiments.

Sample No. 1 was vapor degreased with trichloroethylene (B.P. ~ 85°C) as was the custom in the early part of this project. The AES spectrum from the copper surface of this sample is shown in Fig. 32. The relative intensities of the spectrum lines in Fig. 32 are similar to those shown in Fig. 31 from a type "A" crystal which had been given a 200°C bakeout for 20 hr.

Sample No. 2 was treated in a MICRO® solution, rinsed with distilled water, then methanol and air dried before subjecting it to AES analysis. The resulting spectrum, shown in Fig. 33, still shows carbon as the most prevalent surface element. However, notice the sizable reduction in chlorine content, which is to be expected, since no chlorine-bearing substance was purposely brought in contact with this surface.

Figure 34 is the Auger electron spectrum yielded by sample No. 3, which had only been washed with electronic grade methanol after film deposition and storage. The carbon peak has remained about the same height as shown in Figs. 32 and 33, but the chlorine peak is almost as prominent as shown in the spectrum from the trichloroethylene washed sample. It can only be assumed that the chlorine came from the methanol, since this was the only substance to touch the copper surface.

c. Surface Composition after Aging for 30 Days. The AES analysis of a copper-plated quartz wafer which had been baked in vacuum for 20 hr at 200°C and then analyzed shortly thereafter is presented in Fig. 31. This quartz wafer was called specimen 200-1. More germane to this project is the AES analysis from a copper-plated quartz wafer after a 30 day storage period

at the 85°C aging temperature. During this period of time most of the aging of resonators usually occurs. Thus, specimen "B" was prepared by baking a copper-plated wafer at 200°C in vacuum, sealing it in an evacuated coldweld holder, and storing it for 30 days at 85°C. The holder was then opened and the quartz wafer immediately transferred to the spectrometer.

The AES spectrum from specimen 200-2 was compared to the AES spectrum from specimen 200-1, in the following way: the response lengths of all spectrum lines in a given spectrum were summed and then the ratio of each element's response length to the total gave an approximate value for the percentage of this element in the surface. Scale factors must of course be observed. It must be realized that at best this approach can only be described as semi-quantitative, but at least it gave us some figures to work with. The results for the 200°C bakeout case are given in Table III.

Only the major responses were included. The data in this table indicate that chlorine was lost during the 30 day period at 85°C. The concentrations of carbon and oxygen agree within the range of experimental variation. The apparent increase in copper is the result of the loss of surface material masking the copper from the incident electrons. A similar analysis was made for two specimens baked at 300°C. In this case the chlorine response had apparently increased after 30 days at 85°C. Such action agrees with the negative aging obtained after a 300°C bakeout. However, a mechanism whereby chlorine is adsorbed by the resonator is lacking.

d. Aging Data for Resonators. The aging curves shown in Fig. 35 are for resonator units in which the quartz wafers were bonded ultrasonically to the clip mounts. Curve a, which was obtained from 200-1 type crystal units, indicates a larger aging rate than was anticipated. However, our previous experience with metal films deposited at room temperature has been that such films have a lower-than-theoretical density and are subject to thermally induced structural changes which could cause resonator aging. Curve b for crystal units of 200-2 type shows that only marginal improvement can be expected over 200-1 type units. On increasing the bakeout temperature to 300°C a change in aging direction was noted, as shown in curve c, as well as a small reduction in aging rate.

Since we have demonstrated by AES that chlorine is present on resonators given a final VDG cleaning in trichloroethylene, a logical experiment would be to investigate a resonator which had been fabricated without using the VDG cleaning step. Thus, several units were given a final mechanical cleaning with a solution of MICRO® instead of VDG. Figure 36 shows the aging curve for one such unit. The difference between this crystal's aging performance and that of a VDG crystal is obvious when one compares the results, i.e., Figs. 35 and 36.

4. Surface Characterization of Copper Foils

The AES spectrum from a copper foil surface, which had been lightly etched in dilute nitric acid and then rinsed in tap water, is shown in Fig. 37. The carbon response was relatively small. However, the chlorine was high, and probably resulted from the use of tap water to dilute the acid and then to rinse the specimen. The use of tap water was unknown to us until after the experiment had been performed. The sulfur

was probably in the copper as an impurity.

Next, the foil was heated for 2 min at about 600°C in the spectrometer vacuum and the exceptionally clean spectrum shown in Fig. 38 was then obtained. Note that this spectrum was recorded with a high instrumental sensitivity. Although the surface possesses a high degree of cleanliness, additional elements such as Ca, N and Ar were detected. The source of calcium, which has a vapor pressure of 10^{-2} torr at 600°C, is unknown. At ambient temperature the vapor pressure of calcium is lower than the residual vacuum pressure, so it is not likely to readily evaporate, except by electron impact desorption during AES analysis.

After the spectrum shown in Fig. 38 was recorded, the system was brought up to atmospheric pressure by admitting air, and then repumped to 10^{-9} torr. The spectrum shown in Fig. 39 was then recorded. An important change in the spectrum was the increase in the oxygen response. The apparent reduction in the copper response was most probably the result of the masking effect of the adsorbed oxygen on the surface. Finally, the foil was heated for 1 min at 300°C and the analysis shown in Fig. 40 was obtained. In this spectrum the oxygen has returned to about the level obtained before exposure to air and the copper appears to have increased but this action is due to the loss of the oxygen cover.

Other elements have changed in concentration or disappeared entirely. Although the same copper foil was used for this series of experiments, the exact area covered by the incident beam of electrons varied. Thus, small changes in trace element concentration are not unusual.

III. DISCUSSION

The development of high-precision SSB quartz resonators, exhibiting maximum frequency aging in the order of $\pm 2 \times 10^{-10}$/week, rests in our ability to determine which are the insidious fabrication variables and how we can best remove them from the system, or at least make them ineffective.

Analytical techniques have shown that even after the most rigorous cleaning methods have been applied to quartz surfaces, they still retain traces of impurities which are usually relatable to their past history.

During the latter part of this program we have consistently made resonators from quartz wafers which have been cleaned with chrome-sulfuric acid. None of the uniquely identifiable elements forming the compounds used in this cleaning process, e.g., chromium, sulfur, have been detected on the cleaned quartz in quantities above the background level. This was not the case when chlorinated hydrocarbons were used, since with them we detected an increased level of chlorine on the surface.

In the as-received state all cleaned quartz surfaces yielded spectrum lines of considerable magnitude which were attributable to carbon. This contaminant is found, in varying amounts, in all electron-optical systems, no matter how low the residual gas pressure. Its occurrence in AES spectra does not necessarily mean that it was residue from the cleaning process, unless inordinate amounts are identified. In ultrahigh vacuum system, carbon is believed to come from the residual carbon monoxide gas, which is easily converted to nascent carbon by the impinging electron beam. Carbon contamination can be removed by either ion bombardment or by heating the material, while under observation, to a few hundreds of degrees centigrade.

The role of carbon in resonator aging is an undefined factor; the solution does not appear to be an increased bakeout temperature before sealing, because such action does not necessarily produce a superior crystal unit. The answer is not forthcoming at present, however, we believe that with the aging rates now being required, carbon contamination can no longer be completely ignored in resonator fabrication.

The phenomenon of frequency deviation due to thermal interruption (retrace) is well documented. However, the reason for this type of performance is still not completely understood. We observed thermal retrace in all the resonators made during this project, and fortunately the measured amounts were usually within the $\pm 1 \times 10^{-8}$ tolerance limit.

Noteworthy is the fact that our lowest and most consistent frequency deviation due to temperature cycling was with Hi-Q cultured quartz wafers that had been etched for 1 min in saturated $NH_4F.HF$. Such a short etch can only be responsible for removing about 150 to 200 angstroms of material. This may well be enough material removed to reduce most of the immediate surface strain to a low, stable, level. It is certainly not a long enough etch to reveal, and certainly not to remove, the defect structures which are observed.

Hopefully, light etches will loosen partially embedded polishing abrasive so that they can either be washed away or physically shaken (ultrasonically) from the surface. These are aspects of the interface problem which need to be thoroughly investigated.

The selection of copper for the electrode material was apparently a good one. Although not as chemically inert as gold, it does withstand some corrosive environments. More importantly, the available data indicate that it produces less stress in the quartz during its overgrowth from the vapor than most other suitable electrode metals.

It has been found to be an excellent practice to carry out the plating, baking, and sealing operations in the fabrication of resonators in one environmentally controlled chamber. This chamber should be compatible with ultrahigh vacuum technology and be essentially free from contaminants which are most likely to influence the aging properties of resonators. This procedure also eliminates a number of additional handling and cleaning steps which could only degenerate the quality of the completed units.

Using a bond of electroplated nickel between the tab clips and bonding pads on the quartz appears to be an excellent procedure for meeting the military shock and vibration specifications. It is not as evident that it is superior to other bonding methods for producing resonators with very low aging rates. This is a question that has yet to be answered. The use of diametrically opposed lab clip wafer supports is also questionable on the grounds that they can be easily misaligned and in such a situation can surely stress the quartz wafer.

Alternative methods to mount wafers, such as the one-point wafer support, may not be sufficiently robust for military requirements. However, it does appear that the time is rapidly approaching when it will be imperative to come up with resonator mounts that will meet the more stringent performance requirements.

The use of a molecular layer of polysiloxane between the quartz surface and the metal electrodes appears to improve aging of resonators. The resulting configuration apparently has a lower free energy than that produced by evaporating metal directly onto clean quartz. One explanation of this observation is that the polysiloxane film accommodates the thermal mismatch between the quartz and metal, yet still maintains close coupling between the two resonator components.

Such layers have also been shown to prevent evaporated metal from penetrating into the quartz lattice. It is not known at this time what the relative contributions of these effects are on resonator aging.

IV. CONCLUSIONS AND RECOMMENDATIONS

The target long-term aging requirement of not greater than $\pm 2 \times 10^{-10}$/week measured at the 62°C upper turning point has not been achieved. However, the results obtained indicate that resonators having the desired aging may be consistently assembled by the process of continuously updating critical fabrication variables. The evaluation of these variables was, and should continue to be, made by studies of the physical and chemical composition of the various surfaces as well as by making aging studies of assembled crystal units. The most important features of a low-aging crystal unit are: a) a very low level of contamination in the sealed holder, and b) low stress in the quartz plate due either to the mounting method or the deposited electrodes. The requirement needed to meet the first of these two features is to use proven wet-cleaning methods followed by plating and sealing in an oil-free vacuum system without venting between operations. The latter feature is difficult to achieve; the presently-used mounting system in the HC-6 coldweld holder has great potential for causing stress in the quartz. Copper electrodes have been reported to cause minimum stress in the wafer and appear to be an excellent choice for the electrode metal.

The maximum frequency deviation requirement after temperature cycling from -55°C to +90°C may prove to be easier to achieve than the low-aging requirement. The maximum acceptable deviation of $\pm 1 \times 10^{-8}$ after temperature cycling from -55°C to +90°C was achieved for 84% of the tests made. The measured deviation is apparently not due to an exchange of mass between the resonator and interior of the holder since the behavior varies on successive cycles; we are left with the conclusion that temperature induced frequency deviation is the result of stress changes in the quartz. A low-stress mounting structure should be devised and compared during both frequency aging and deviation measurements with the one presently used.

A thorough understanding of quartz resonator aging and related phenomena by simply fabricating and measuring units is not a likely occurrence. Rather, a quantitative analysis of surface structure, cleanliness, etc., by AES, HEED and SEM is an important part of a comprehensive resonator study program. We recommend that such a program be continued.

V. ACKNOWLEDGEMENTS

The authors wish to express their appreciation to Mr. L. H. Glassman for his assistance in performing the electron optical investigations, to Mr. J. House for operating the Auger electron spectrometer, and to Mr. L. A. Phillips for the way he handled the tedious job of collecting frequency data.

VI. REFERENCES

1. H. Wasshausen, "Processing Techniques for Shock Resistant Precision Quartz Crystal Units," Research and Development Technical Report ECOM-3524 (December 1971).

2. M. L. White, "The Detection and Control of Organic Contaminants on Surfaces," Published as part of "Clean Surfaces: Their Preparation and Characterization for Interfacial Studies," Edited by George Goldfinger, Marcel Dekker, Inc., New York (1970).

3. G. L. Krieger, "The Physical Chemistry of Cleaning," Report SC-TM-66-428, Sandia Laboratory (September 1966).

4. S. Naiditch and S. E. Wreede, "Cleanness of Glass Surfaces Measured by Evolution of Hydrogen from Sodium-Ammonia Solutions," The Journal of Vacuum Science and Technology, Vol. 5, No. 2 (1968).

5. G. M. Khan, "The Adsorption of Alkylchlorosilanes on Quartz Crystal Surfaces," Canadian Journal of Chemistry, Vol. 50 (1972).

6. J. M. Stanley, "Nickel Electrobonded Quartz Blanks," Research and Development Technical Report ECOM-3452 (August 1971).

7. L. E. Samuels, "Metallographic Polishing by Mechanical Methods," Pitman and Sons, London, 2nd Edition, p. 145 (1971).

8. C. F. Cook, Jr., Rev. Sci. Instrum., 33, 359 (1962).

9. L. E. Samuels and J. V. Sanders, J. Inst. Metals, 89, 129 (1958-59).

10. Sir George Beibly, "Aggression and Flow of Solids," Macmillan, London (1921).

11. F. P. Bowden and T. P. Hughes, Proc. Roy. Soc., 160A, 575 (1937).

12. A. W. Warner, D. B. Fraser and C. D. Stockbridge, IEEE Transactions of Sonics and Ultrasonics, SU-12, 52 (1965).

13. R. J. Byrne and J. L. Hokanson, IEEE Transactions on Instrumentation and Measurements, IM-17, No. 1, 76 (1968).

14. E. Hafner and R. S. Blewer, Proc. IEEE (letters), 56, 366 (1968).

15. E. Kolkolm and B. S. Berry, J. Electrochem. Soc., 115, 823 (1968).

16. R. A. Young and C. E. Wagner, J. Appl. Phys., 37, 4070 (1966).

TABLE I

ELECTRICAL PARAMETERS OF RESONATORS USED TO OBTAIN LONG-TERM AGING DATA AT 62°C.

Unit No.	R_s (Ω)	F_s-F_{30}** (Hz)	Q ($\times 10^{-6}$)	C_1 (ρF)	C_0 (ρF)	L (mH)	C_0/C_1	F.A.R.*** $\Delta F/F \times 10^{-8}$ per week	Dominant variables
1	3	743	1.06	.0100	3.7	104	370	+0.55	fast evapn. no bakeout
5	4	729	0.81	.0098	3.7	105	377	+0.22	slow evapn. no bakeout
8	5	737	0.64	.0099	3.7	104	373	+0.33	thick plating 200°C bakeout
9	6	707	0.56	.0095	3.7	109	389	+1.30	activity dip
10	6	746	0.53	.0101	3.7	103	366	+0.29	solid getter 200°C bakeout
13	3	779	1.01	.0105	3.7	99	352	-0.31	impd. bonding no bakeout
14	2.5	757	1.25	.0102	3.7	102	363	+0.38	no bakeout
16	3	794	0.99	.0107	3.7	97	346	+0.15	200°C bakeout
17	3	781	1.01	.0105	3.7	98	352	+0.08	200°C bakeout
18	5	755	0.63	.0102	3.7	102	363	+0.18	200°C bakeout
19	2.5	815	1.16	.0109	3.7	94	339	NOTE 2	solid getter 200°C bakeout
21	4	797	0.74	.0107	3.7	97	346	-0.04	silicone coat 200°C bakeout
22	3	815	0.97	.0110	3.7	94	339	NOTE 2	silicone coat 200°C bakeout
E	3	732	1.08	.0099	3.7	105	373	NOTE 2	solid getter 200°C bakeout
F	4	801	0.74	.0108	3.7	96	342	---	solid getter 200°C bakeout
50*	4	812	0.73	.0109	3.7	95	339	NOTE 2	solid getter 200°C bakeout
G	3	798	0.99	.0107	3.7	96	346	---	solid getter silicone coat
H	5	780	0.61	.0105	3.7	99	352	NOTE 2	200°C bakeout
51*	4	788	0.75	.0106	3.7	98	349	-0.09	solid getter 200°C bakeout
52*	4	780	0.76	.0105	3.7	99	352	-0.15	solid getter 200°C bakeout
53*	10	817	0.29	.0110	3.7	94	336	---	poor unit
54*	12	722	0.27	.0097	3.7	107	381	---	poor unit
55*	2.5	799	1.1	.0108	3.9	96	361	NOTE 2	200°C bakeout
56*	3	778	1.0	.0105	∿3.7	99	352	NOTE 2	silicone coat 200°C bakeout
57*	3	747	1.05	.0101	3.7	103	334	+0.09	silicone,getter 200°C bakeout
I*	6	777	0.51	.0105	3.7	99	321	---	silicone coat 200°C bakeout
J*	5	791	0.60	.0107	3.7	97	315	---	solid getter 200°C bakeout
L*	4	763	0.77	.0103	3.7	101	327	Hi NEG	200°C bakeout
25*	3	800	0.98	.0108	3.7	96	312	-0.13	silicone coat 200°C bakeout
26*	3	821	0.96	.0111	3.7	94	304	-0.52	silicone coat 200°C bakeout

more/.

TABLE I - (continued)

Unit No.	R_s (Ω)	F_s-F_{30}** (Hz)	Q ($x10^{-6}$)	C_1 (ρF)	C_0 (ρF)	L (mH)	C_0/C_1	F.A.R.*** $\Delta F/Fx10^{-8}$ per week	Dominant variables
27*	4	786	0.75	.0106	3.7	98	318	-0.06	solid getter 200°C bakeout
28*	3	805	0.98	.0109	3.7	96	309	-0.65	solid getter 200°C bakeout
29*	2.5	814	1.16	.0110	3.7	95	306	-0.40	200°C bakeout
31*	3	814	0.96	.0111	3.7	95	304	---	very long plating time

NOTES: 1) Units are listed in order of fabrication. All number-series units below 50 were assembled with natural quartz wafers; all units numbered 50 and above were assembled with Hi-Q cultured quartz wafers. The letter-series resonators were assembled with ECOM wafers.

2) Aging data interrupted by other experiments.

* Wafer etched one minute in saturated solution of $NH_4F.HF$ in distilled water.

** F_{30} measured with a 30ρF load capacity.

*** Final aging rate.

Table II

ANALYSIS OF SELECTED AREA DIFFRACTION PATTERN (SAD)
FROM HI-Q CULTURED QUARTZ, SAMPLE NO. HI-Q,3-E

Radius (cm)	Intensity	d-Spacing (Å)	hkl (CeO_2)	hkl (Pt)
0.45	Spot	3.15	(111)	
0.53	Spot	2.69	(200)	
0.59	Spot	2.42	--	--
0.63	VS(R)	2.26		(111)
0.73	M(R)	1.95		(200)
0.74	Spot	1.92	(220)	
0.88	Spot	1.62	(311)	
0.90	Spot	1.58	(222)	
1.00	Spot	1.43	--	--
1.06	W(R) + Spot	1.35	(400)	(220)
		1.24	(331)	
1.18	Spot	1.21	(420)	
		1.18	(311)	
1.23	diff(R)	1.16		(222)
1.30	Spot	1.10	(422)	
		1.04	(511)	
1.43	W(R)	0.997		(400)
		0.956	(440)	
		0.915	(531)	
1.58	Spot	0.902	(600)	(331)

VS(R) = very strong ring; M(R) = medium ring; W(R) = weak ring; diff(R) = diffuse ring; -- = unidentified diffraction; $d = \lambda L/R$ where camera constant $\lambda L = 1.426$ Å cm.

TABLE III

COMPARISON BETWEEN AES DATA FROM FRESHLY PREPARED RESONATOR ELECTRODE SURFACE AND FROM A SIMILAR UNIT AFTER AGING FOR 30 DAYS AT 85°C

Response Length (cm)				
Element	Specimen 200-1	(%)	Specimen 200-2	(%)
C	16.5	(48.2)	4.2	(44.2)
Cl	8.1	(23.6)	1.5	(15.8)
O	4.5	(13.1)	1.5	(15.8)
Cu	5.2	(15.1)	2.3	(24.2)
Total	34.3		9.5	

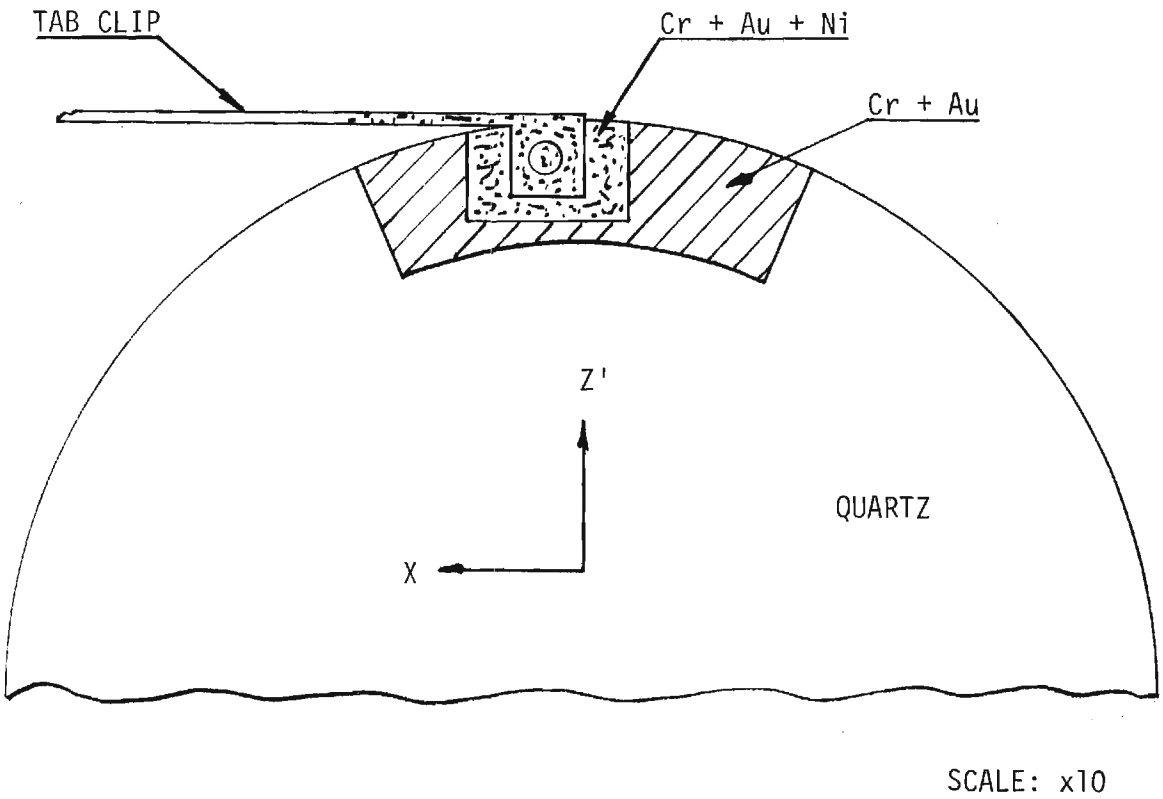

Fig. 1. Placement of the Cr + Au bonding sites, the tab clips, and the Ni electroplate on the quartz wafers.

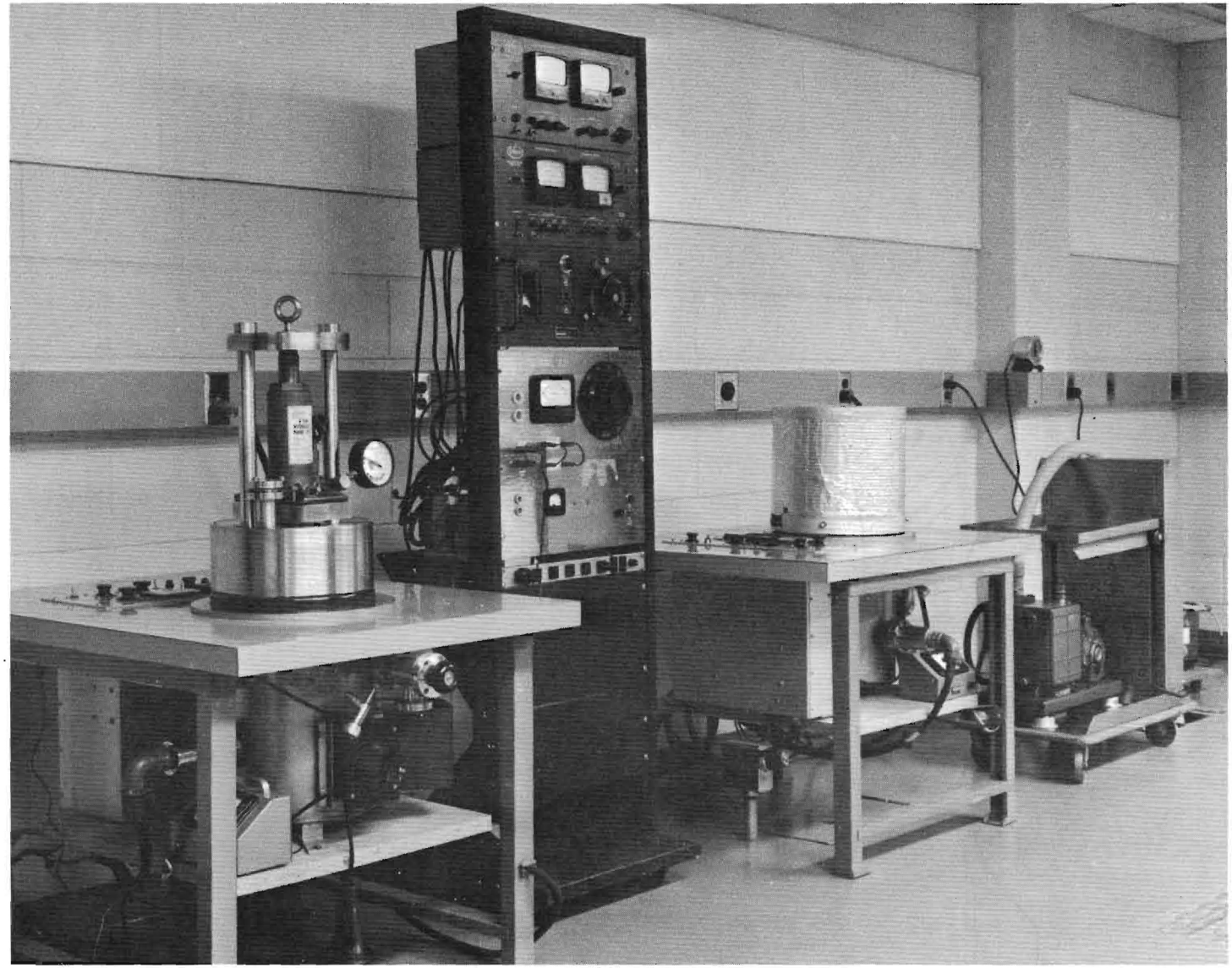

Fig. 2. Vacuum equipment for quartz resonator plating, vacuum baking, and sealing.

Fig. 3. Vacuum bakeout and cold-weld sealing system.

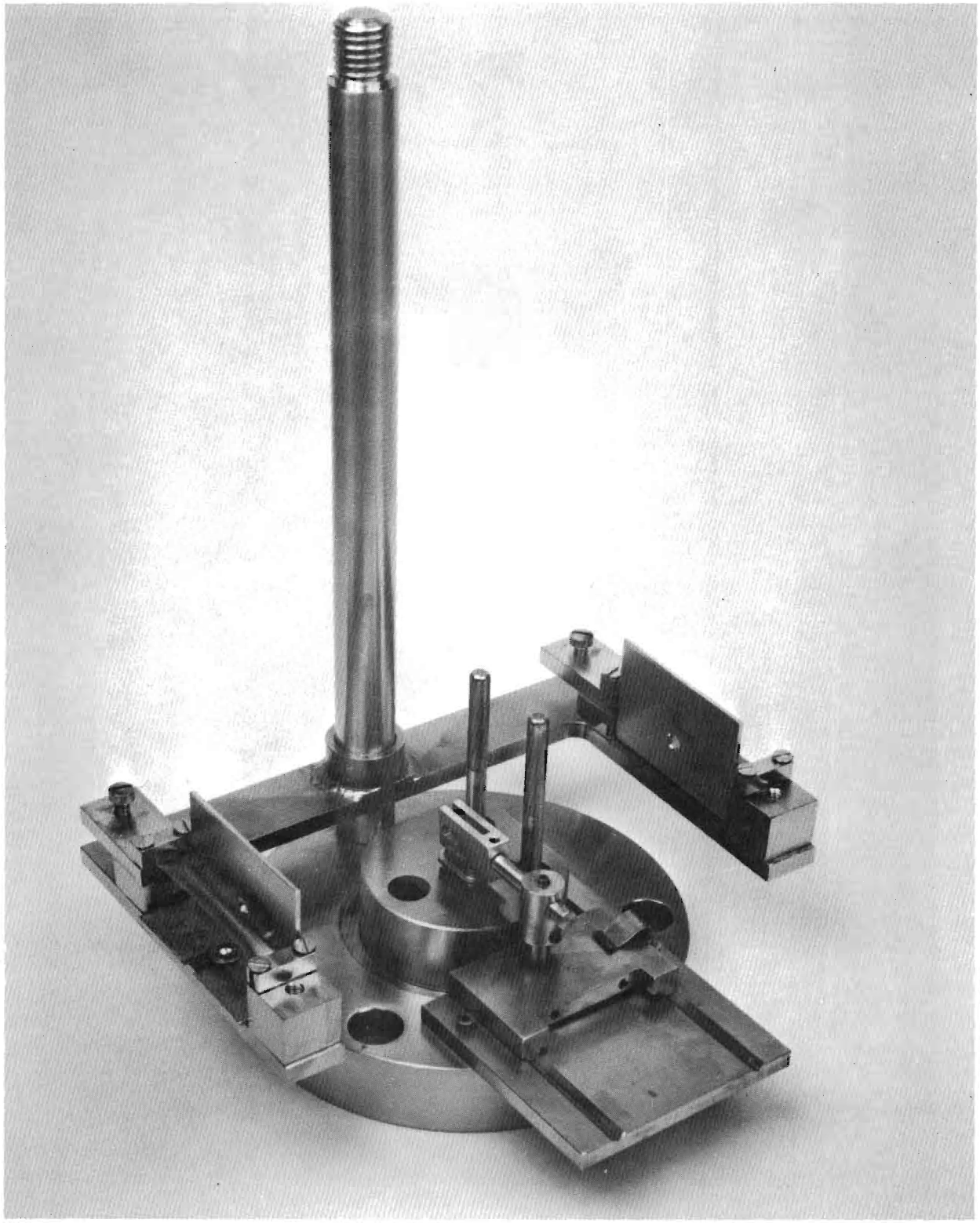

Fig. 4. Electrode evaporation system shown in the plating position. Note that the upper section of the coldweld die and the latching plate for the retractable mask are removed for clarity.

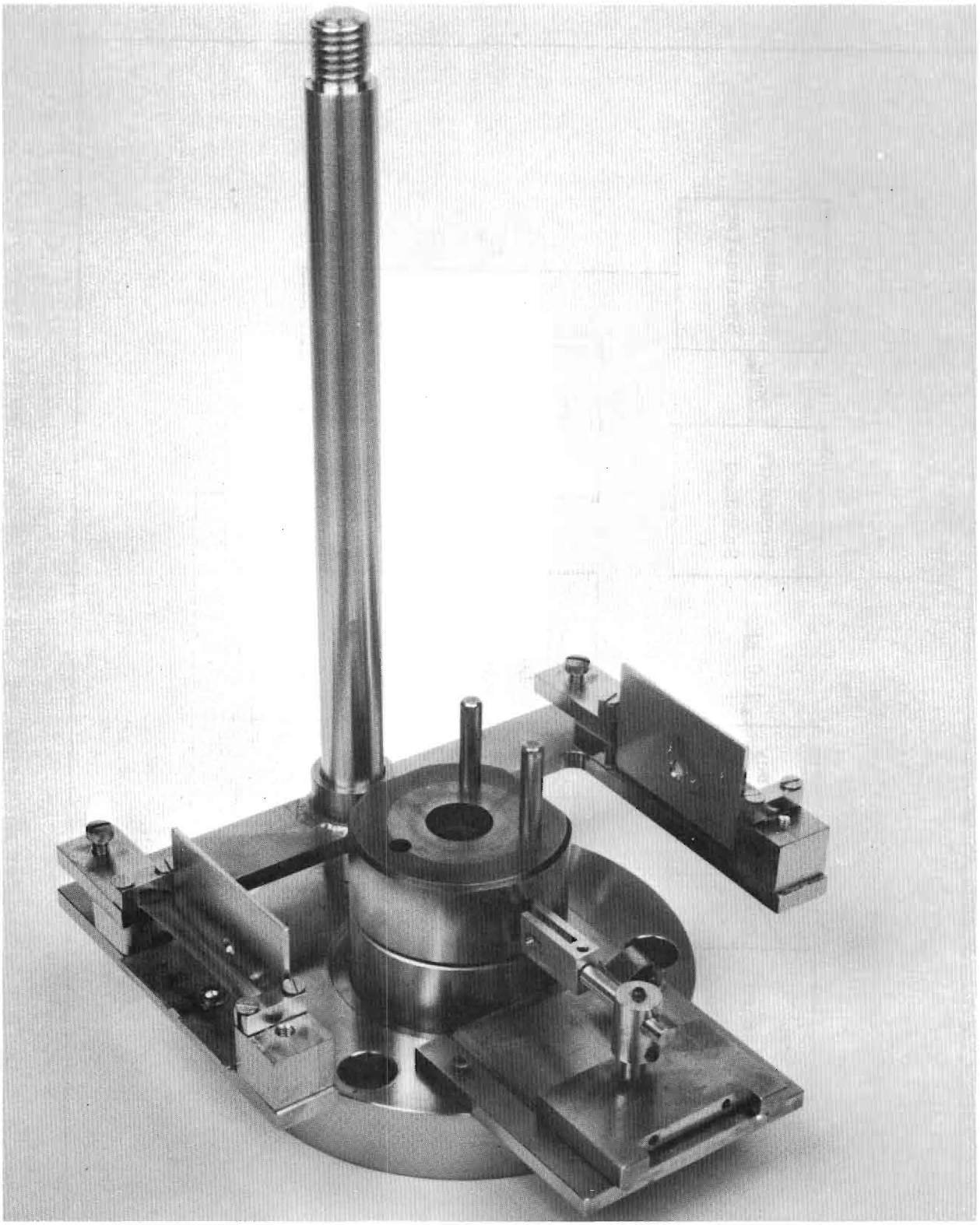

Fig. 5. Electrode evaporation system shown in the sealing position. Note that the electrode mask is retracted from the plating position so as to allow the die to be closed.

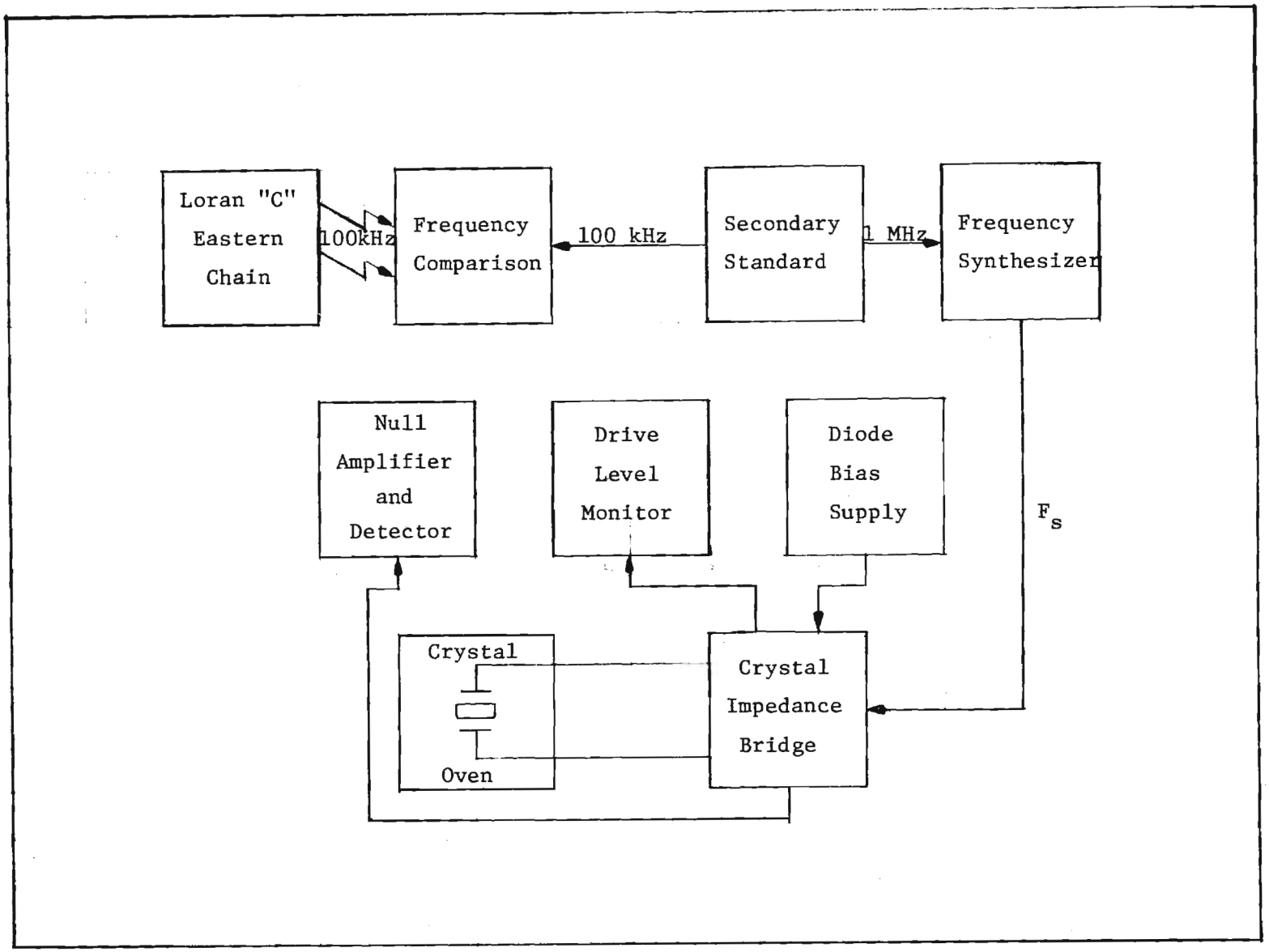

Fig. 6. System for measuring the long-term aging of quartz resonators stored at the upper turning point temperature.

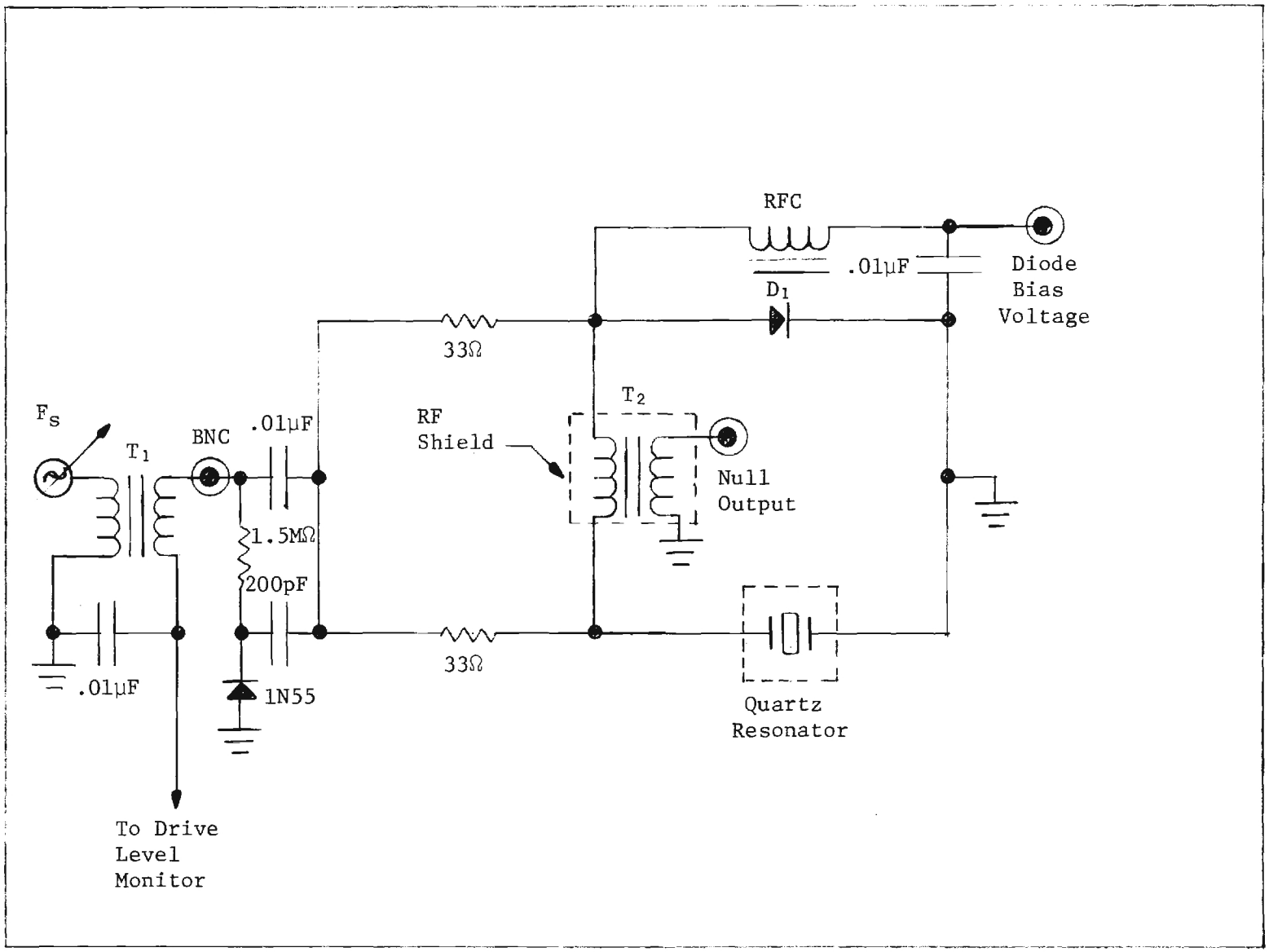

Fig. 7. Circuit diagram of the crystal bridge shown in the block diagram of Fig. 6. The crystal unit impedance is balanced at F_s by the forward biased diode D_1.

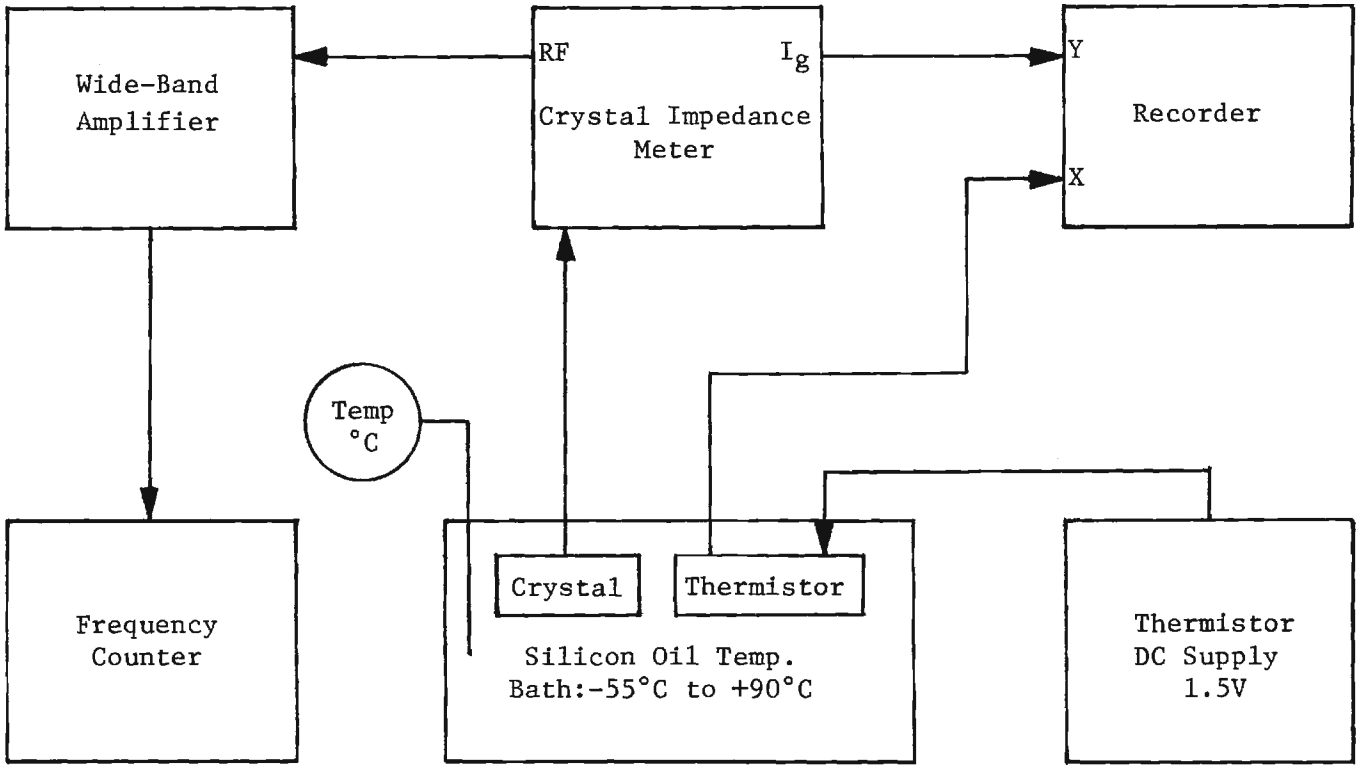

Fig. 8. System for measuring the series resonant frequency (F_s) and series resistance (R_s) over the temperature range -55°C to +90°C.

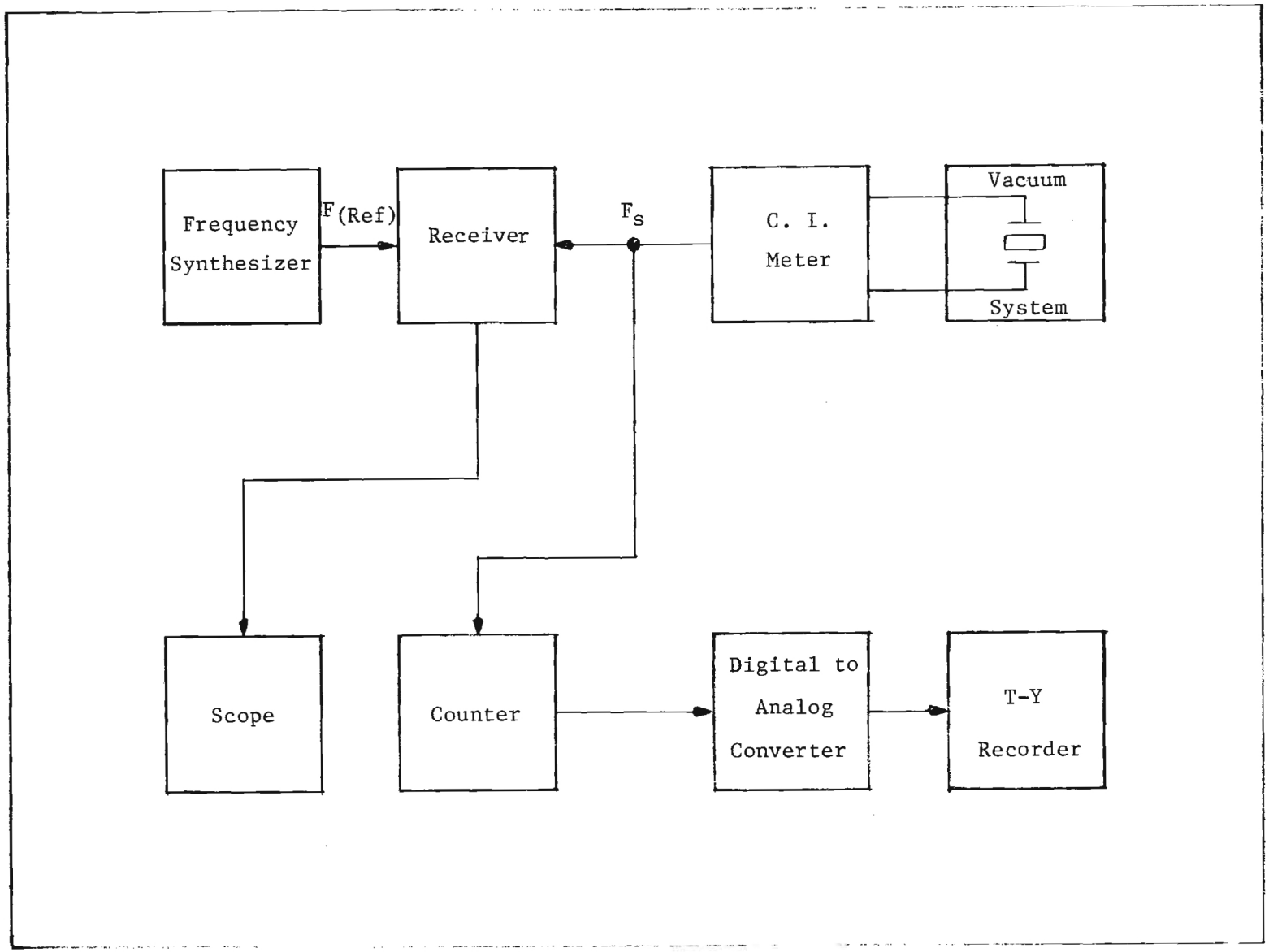

Fig. 9. Frequency Measuring System used during plating to frequency by vacuum evaporation.

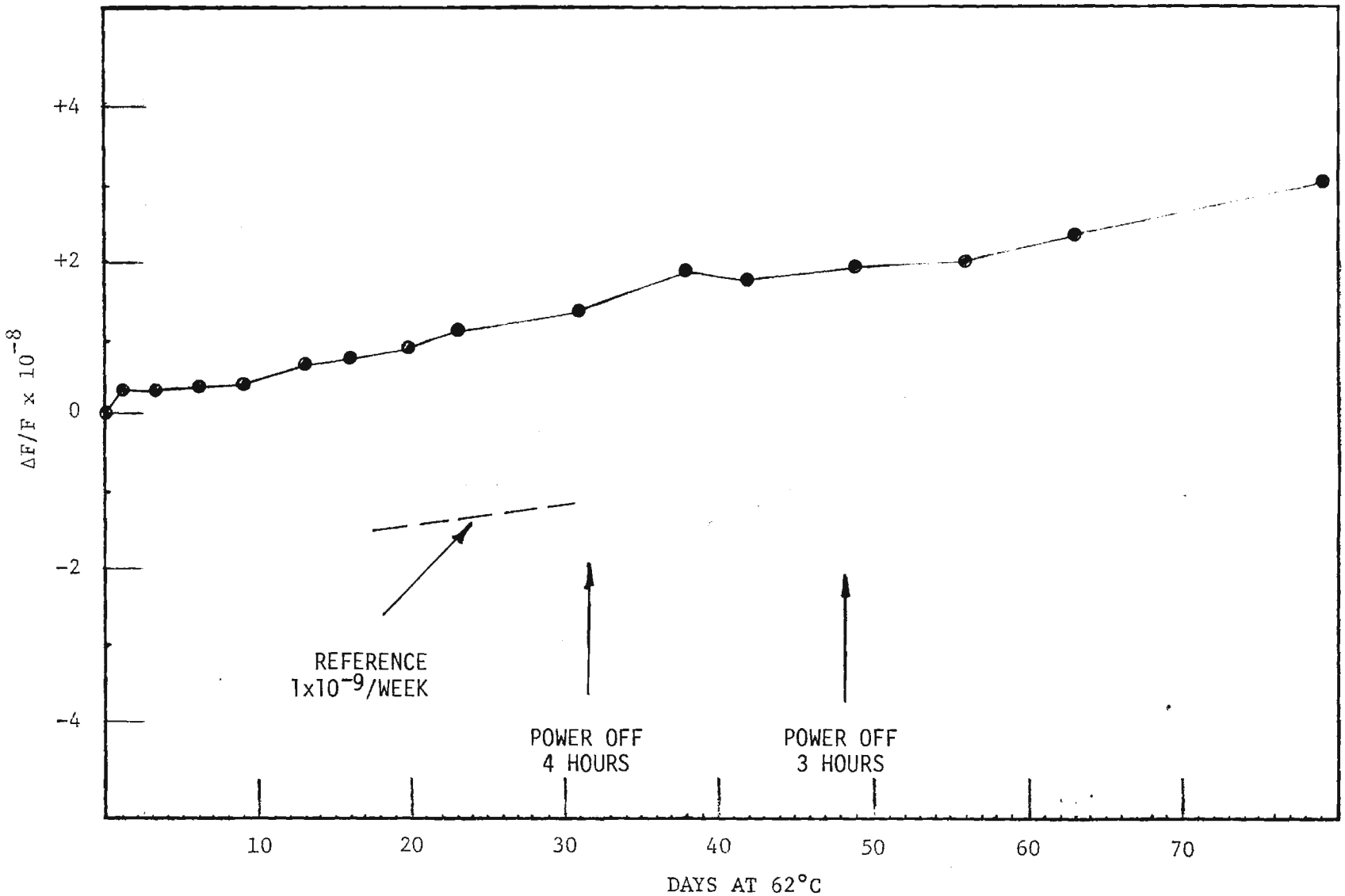

Fig. 10. Long-term aging data for natural quartz unit No. 18. Bakeout for 16 hours at 200°C.

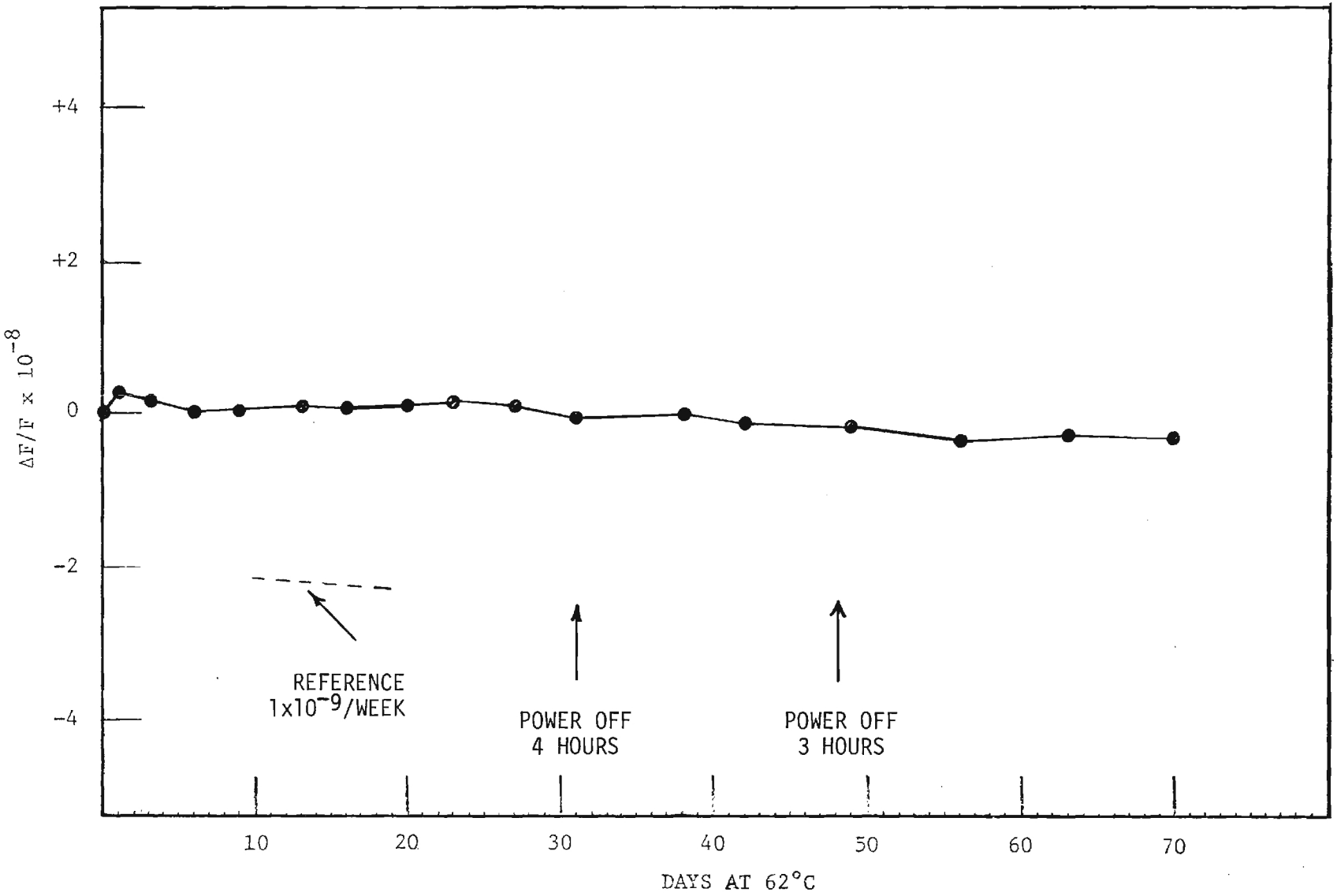

Fig. 11. Long-term aging data for natural quartz unit No.21 with polysiloxane coated quartz. Bakeout for 16 hours at 200°C.

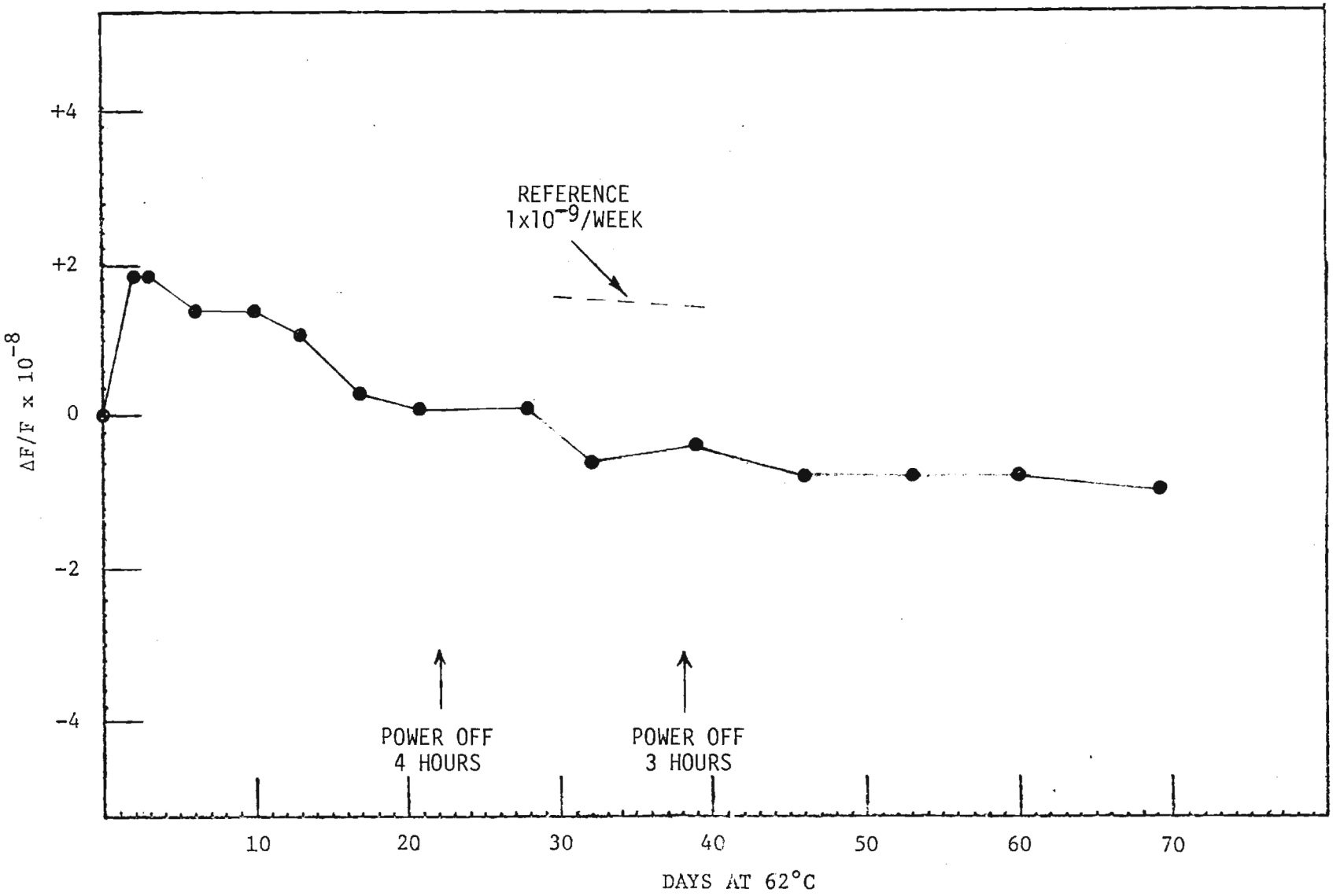

Fig. 12. Long-term aging data for Hi-Q cultured quartz unit No.51, with solid getter in holder. Bakeout for 16 hours at 200°C.

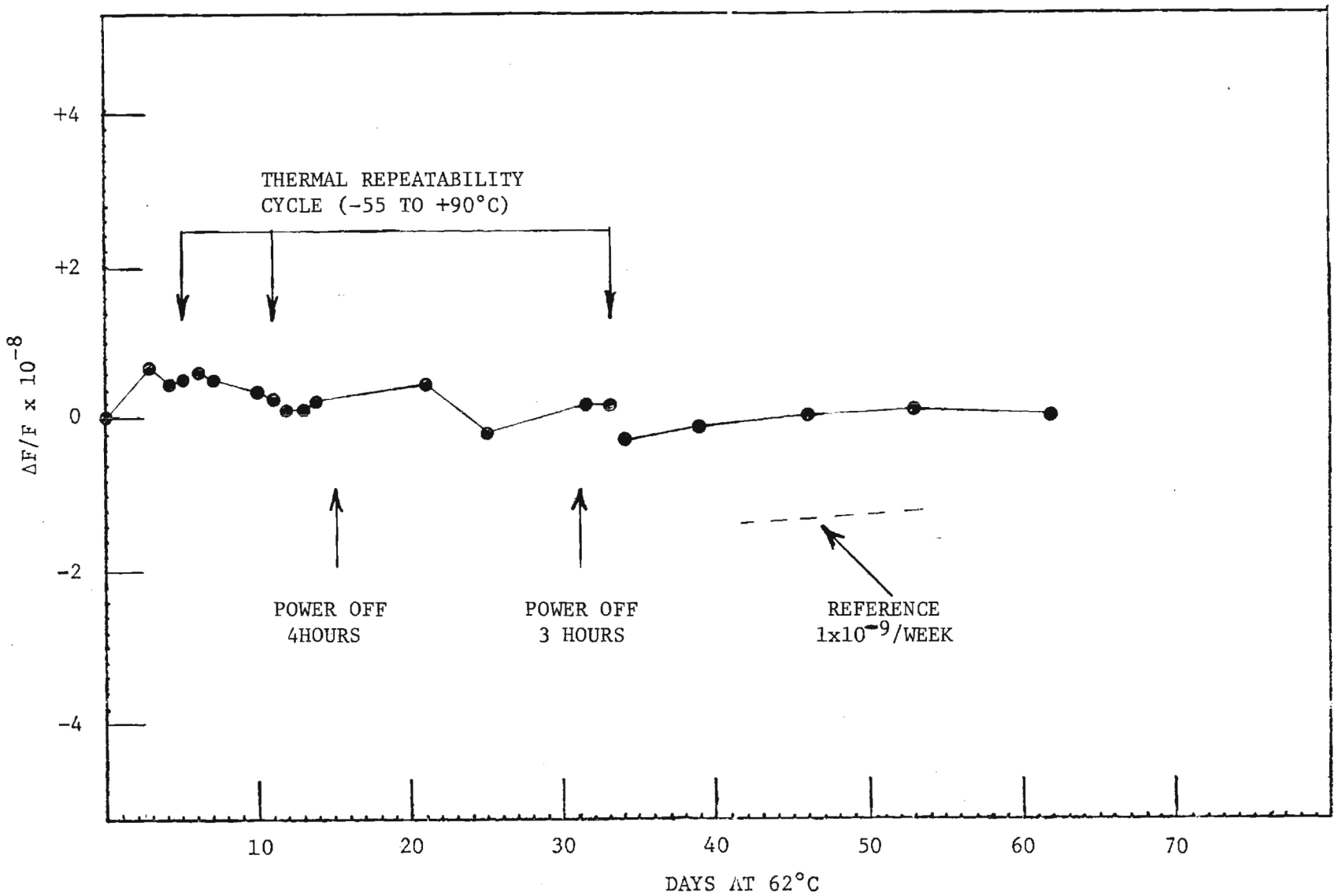

Fig. 13. Long-term aging data for Hi-Q cultured quartz unit No.56, with polysiloxane coating. Bakeout for 16 hours at 200°C.

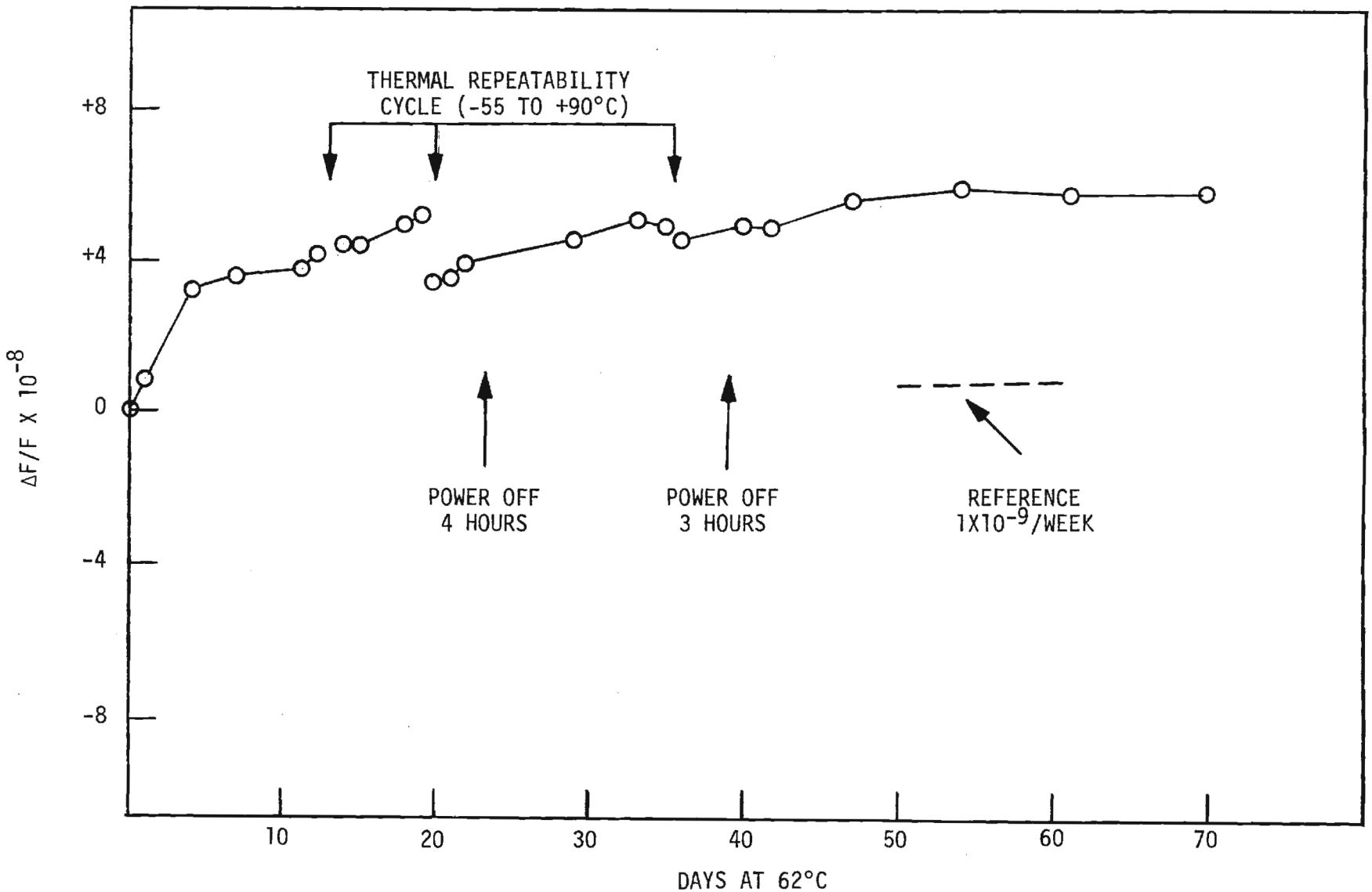

Fig. 14. Long-term aging data for ECOM-furnished-quartz unit "H", with polysiloxane coating. Bakeout for 16 hours at 200°C.

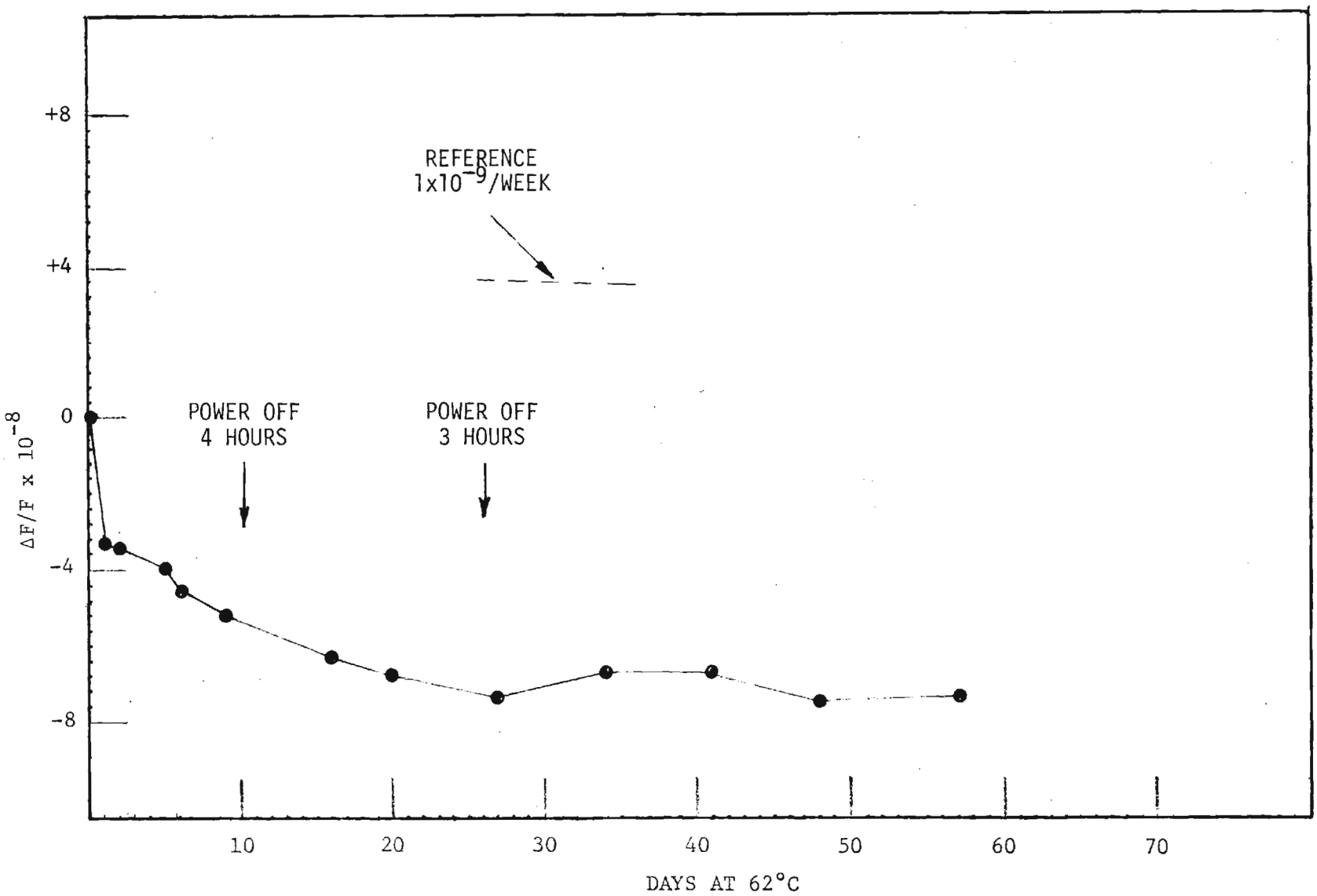

Fig. 15. Long-term aging data for ECOM-furnished-quartz unit"J", with solid getter in holder. Bakeout for 16 hours at 200°C.

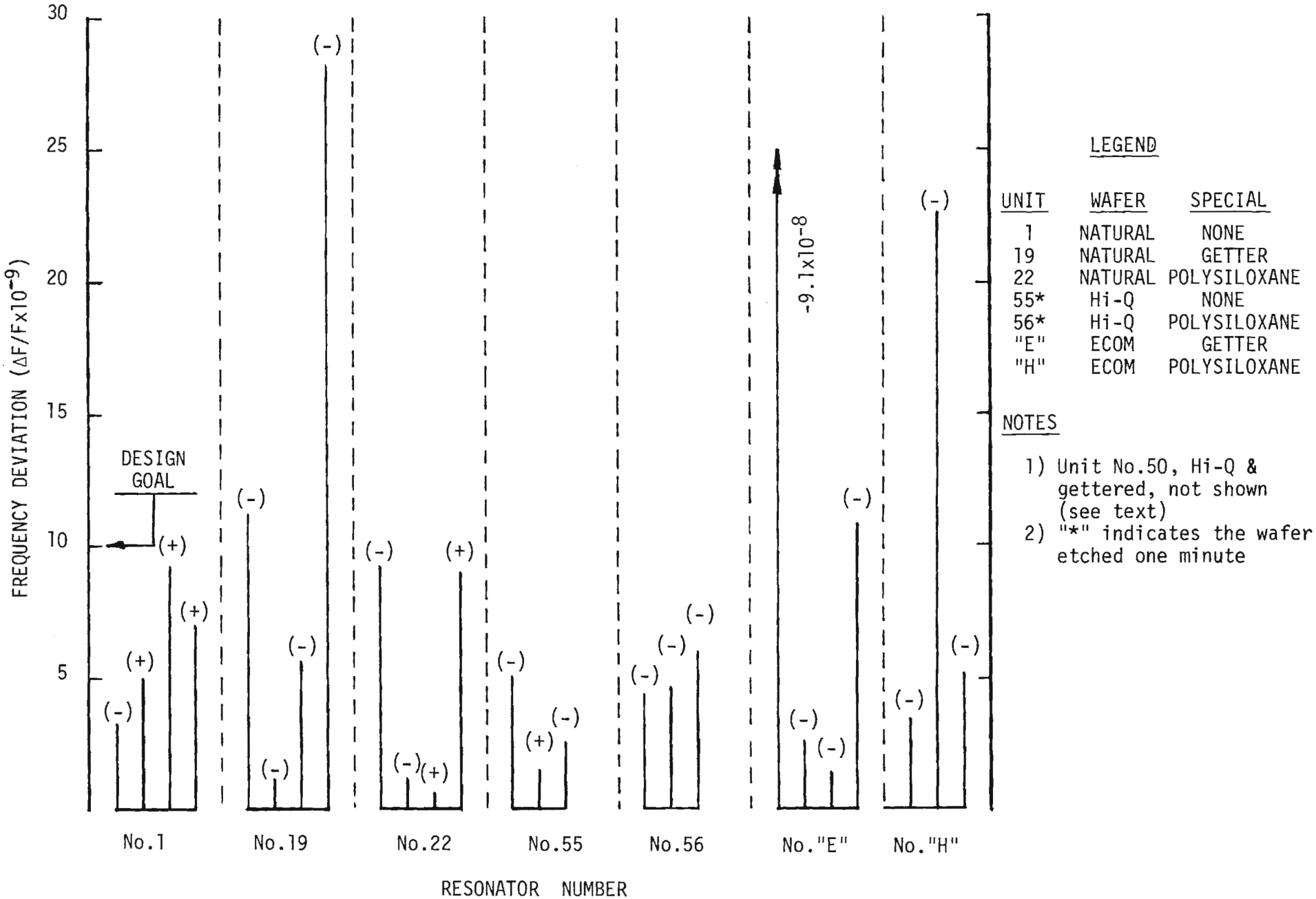

Fig. 16. Thermal frequency deviation for variuos resonators. Temperature was cycled from -55°C to +90°C at about one week intervals.

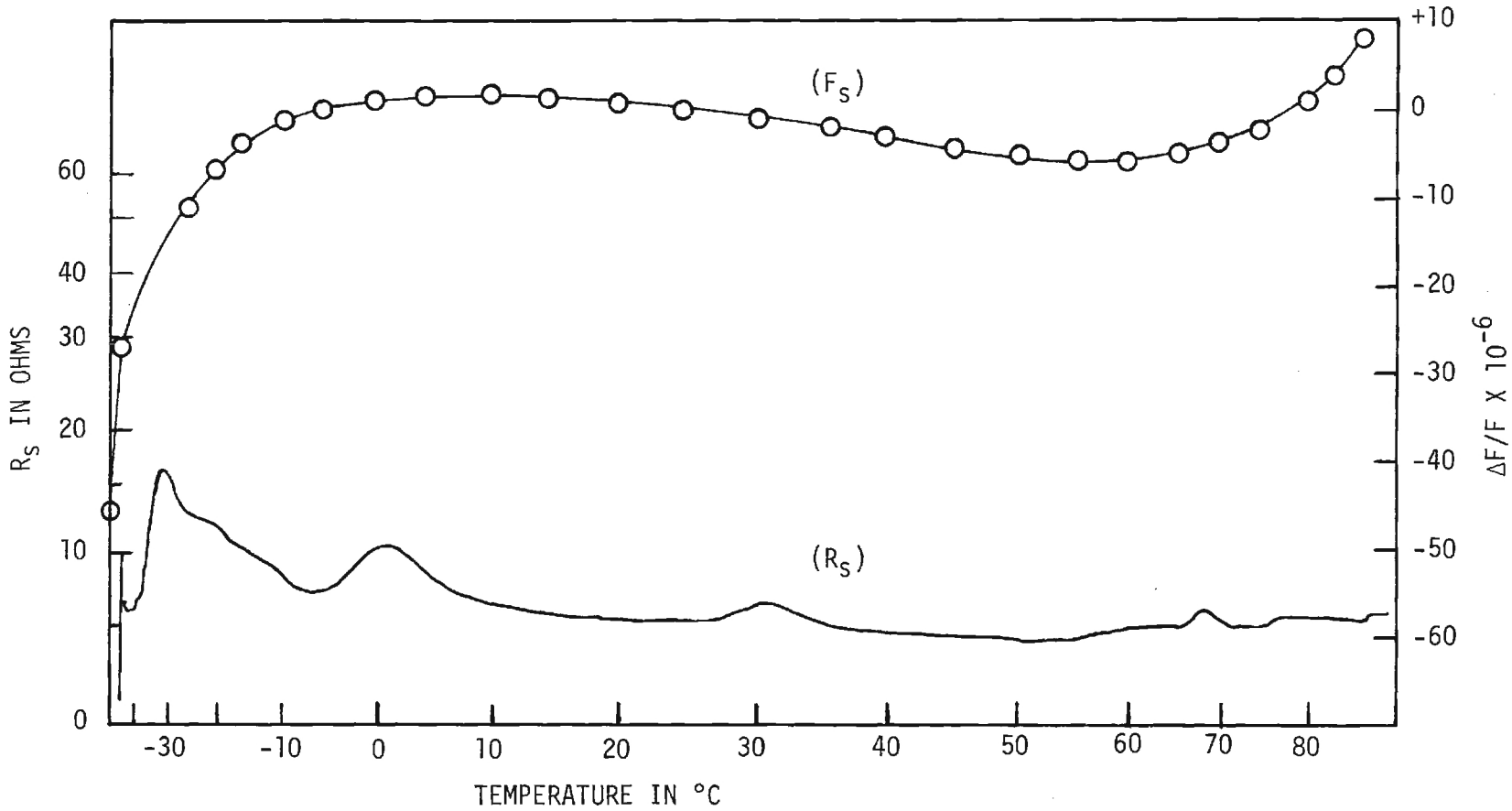

Fig. 17. Frequency and resistance vs temperature data for natural quartz unit No. 9.

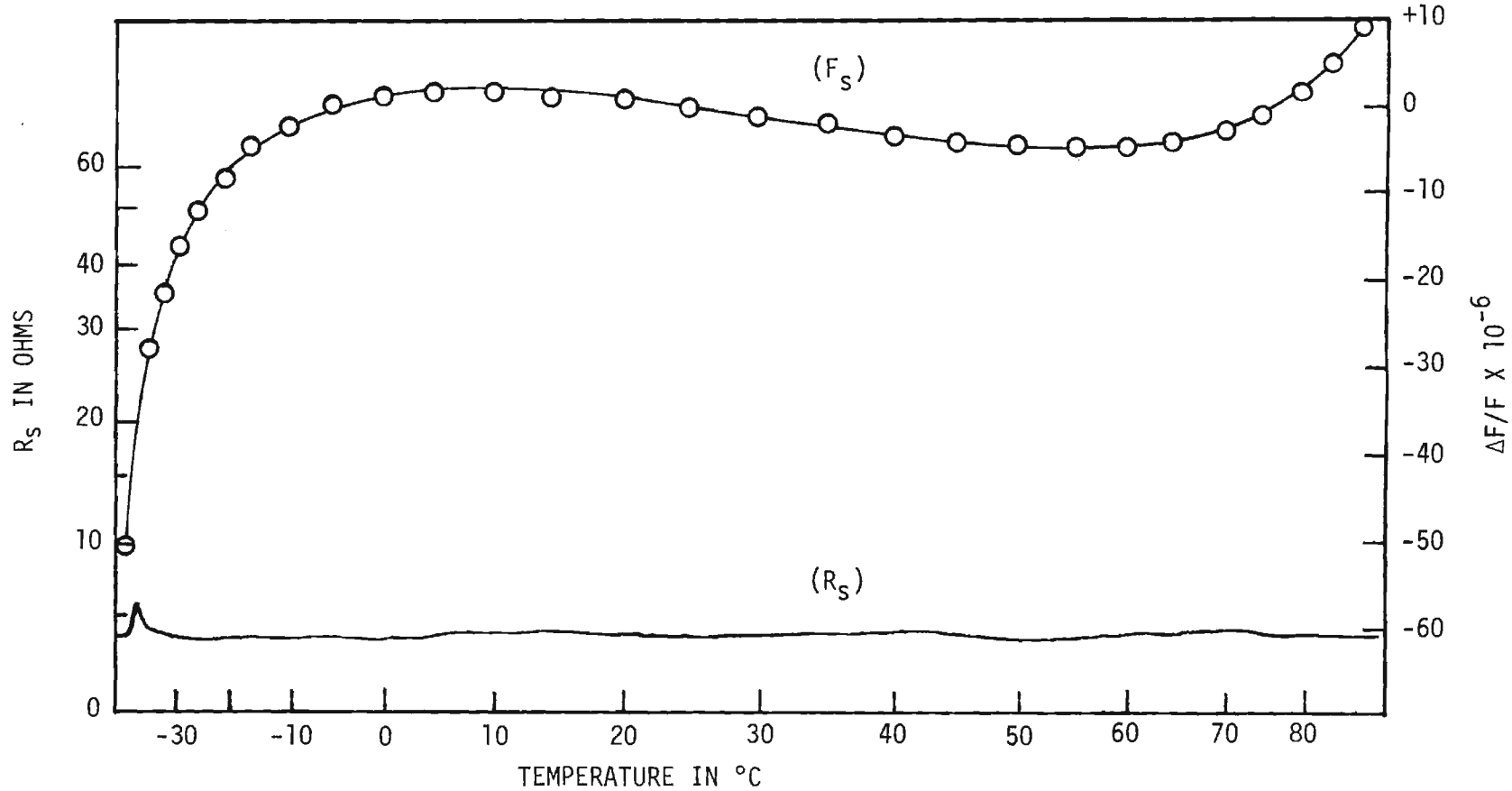

Fig. 18. Frequency and resistance vs temperature data for natural quartz unit No. 5.

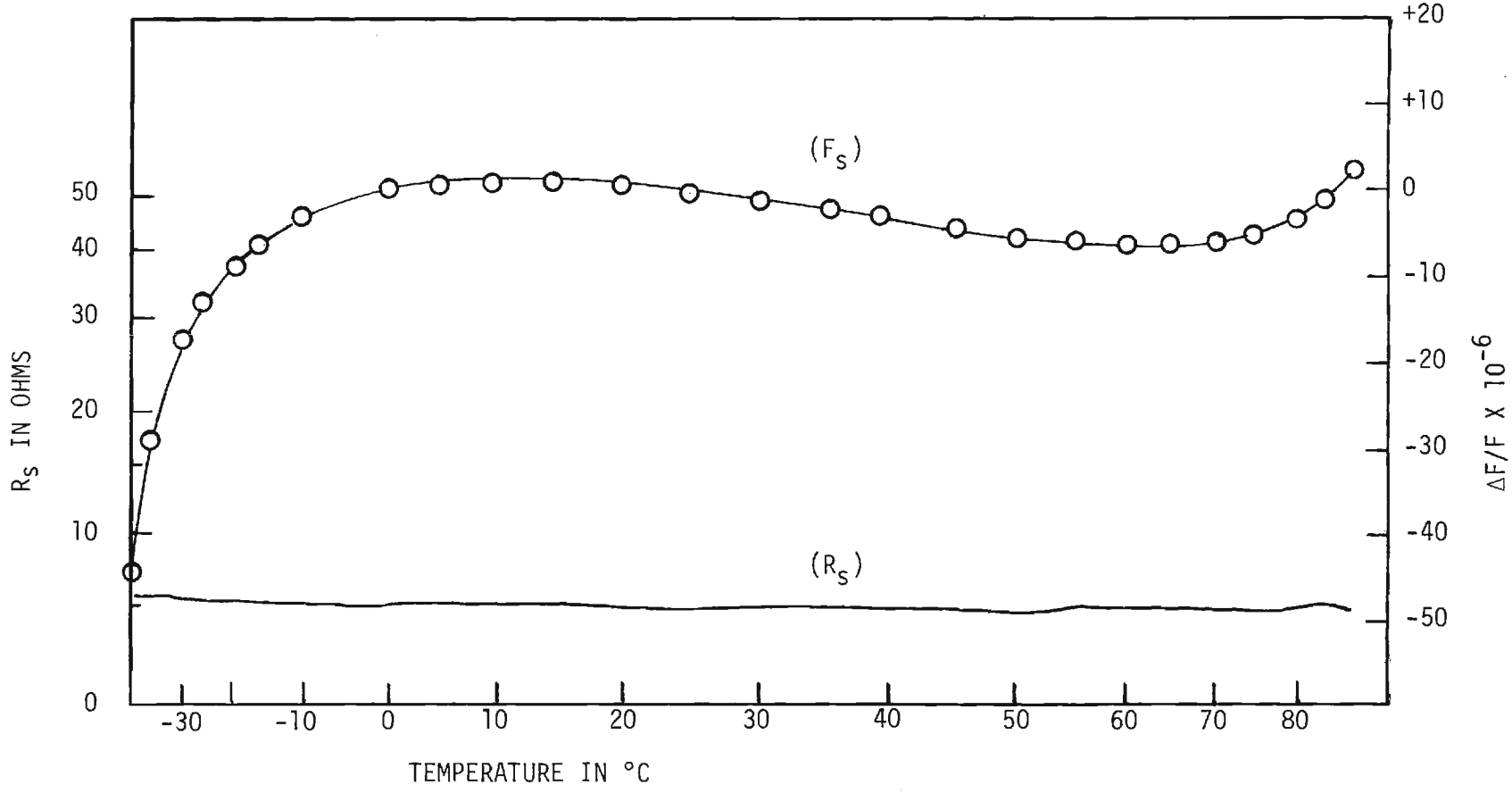

Fig. 19. Frequency and resistance vs temperature data for Hi-Q quartz unit No. 50.

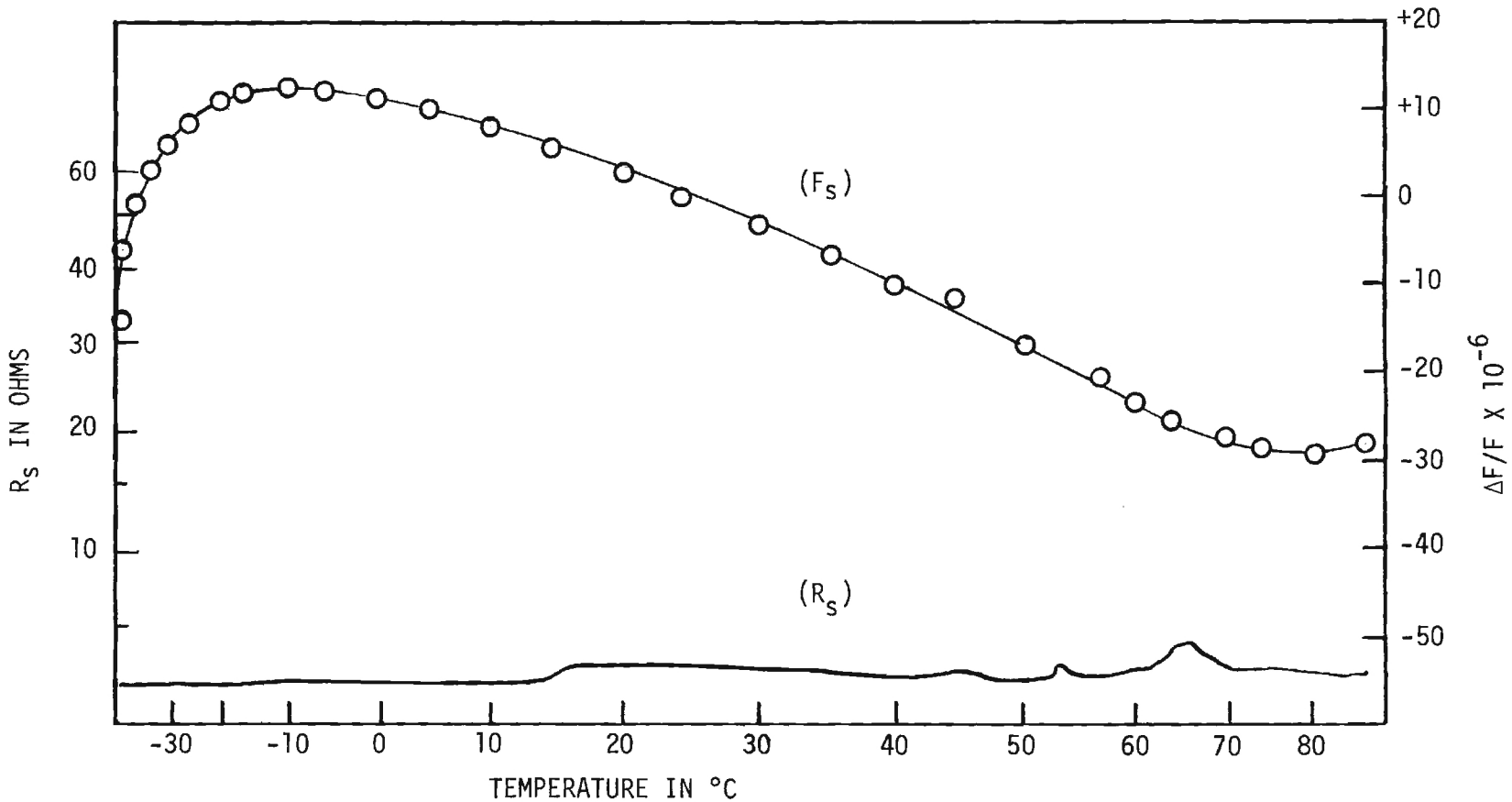

Fig. 20. Frequency and resistance vs temperature data for ECOM-furnished-quartz unit "F".

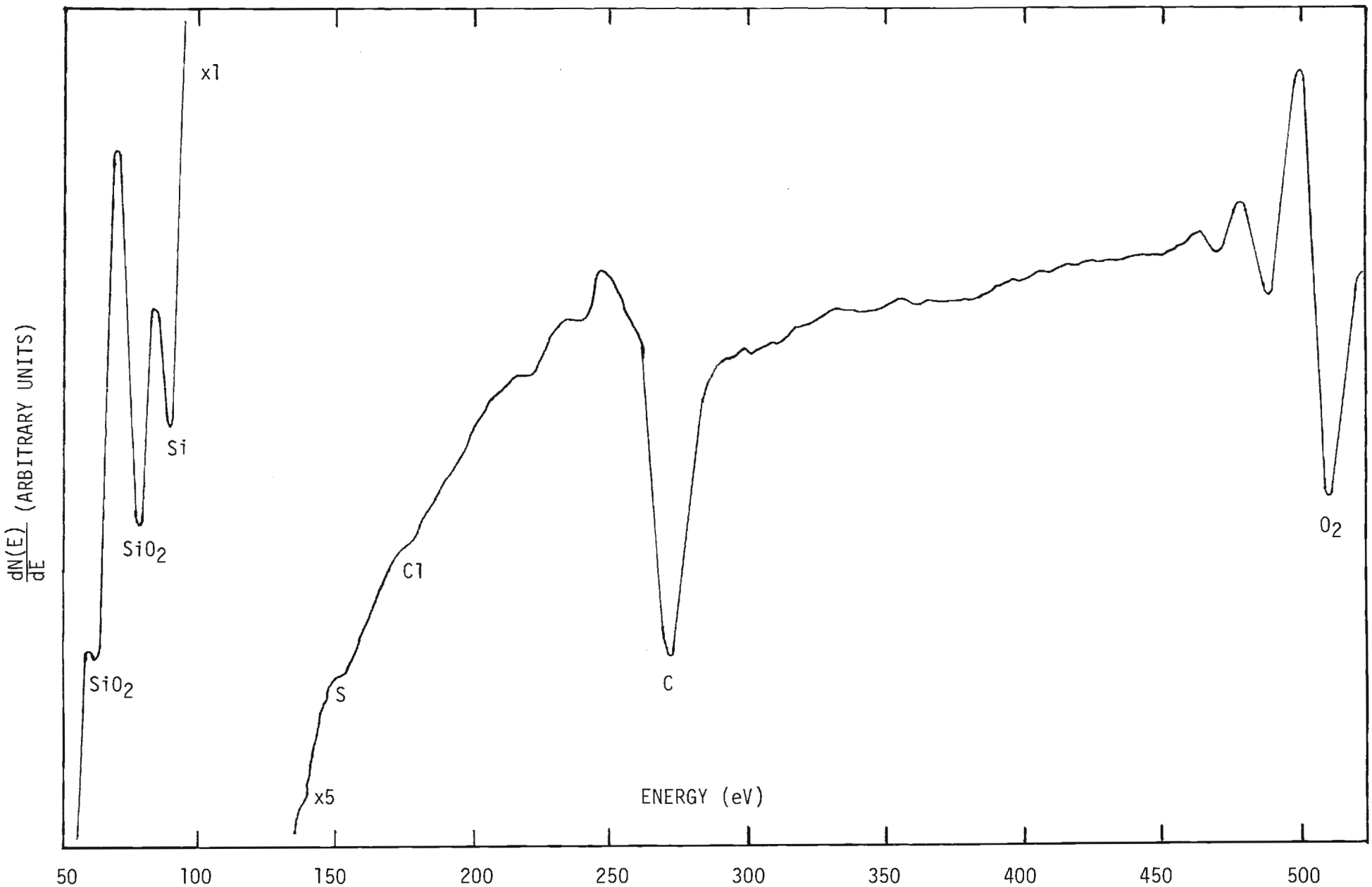

Fig. 21. Auger electron spectrum from the surface of a quartz wafer in the as-received condition.

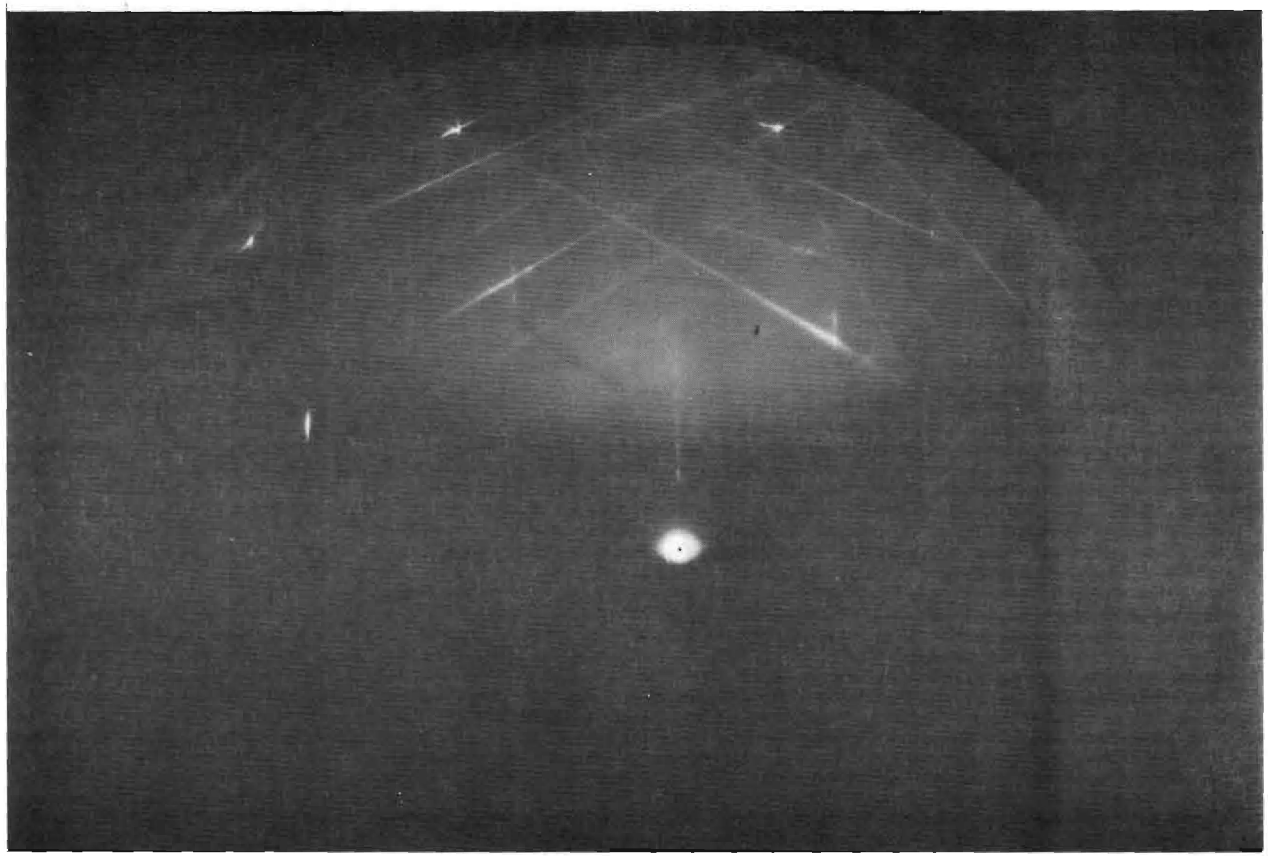

Fig. 22. Kikuchi-line diffraction pattern obtained from a freshly cleaned Hi-Q cultured quartz wafer. The cleaning agent was chrome-sulfuric acid.

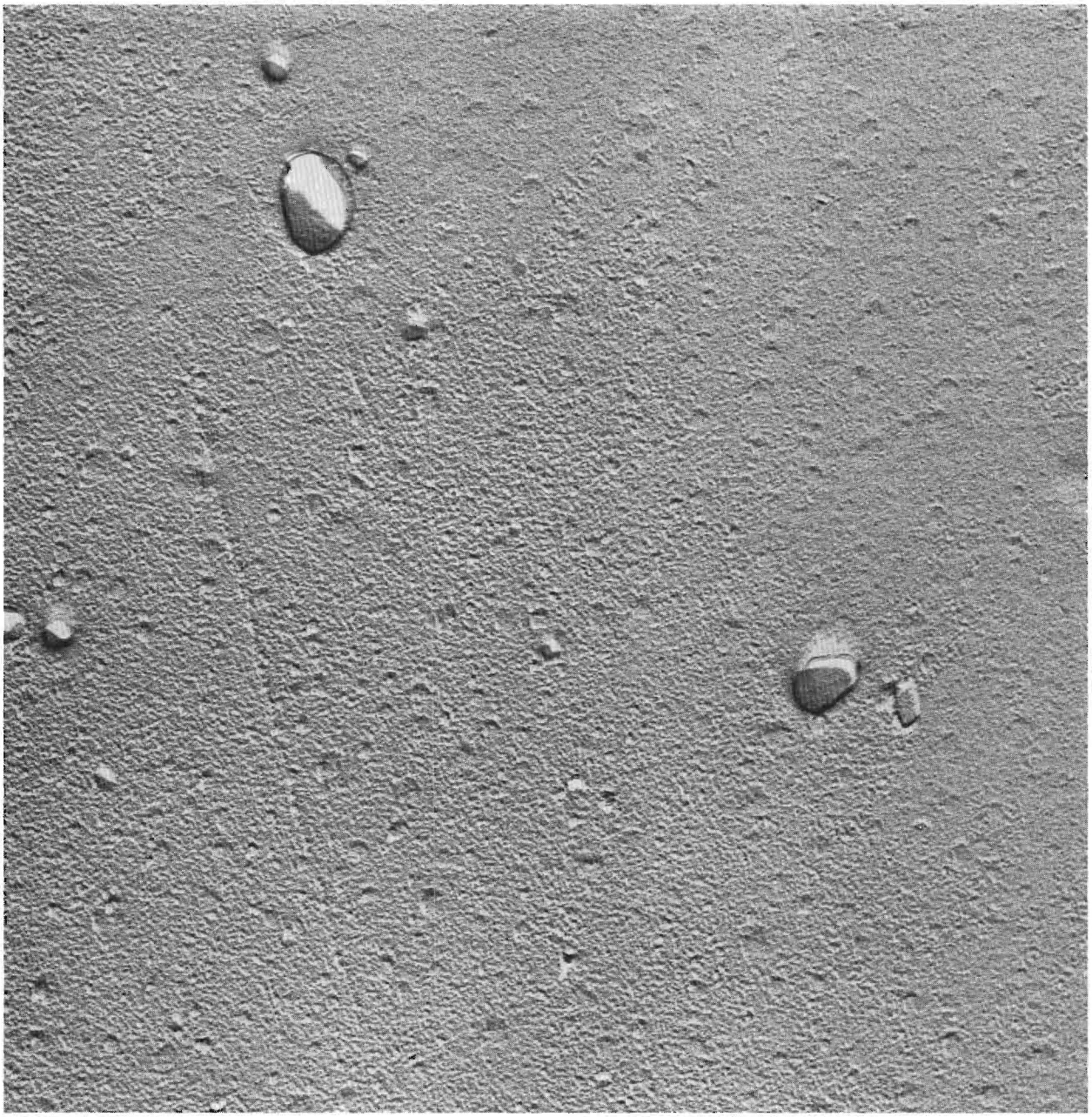

(x46,700)

Fig. 23. Surface replica of an as-received Hi-Q cultured quartz wafer.

(x30,700)

Fig. 24. Surface replica of an as-received natural quartz wafer, prepared by ECOM.

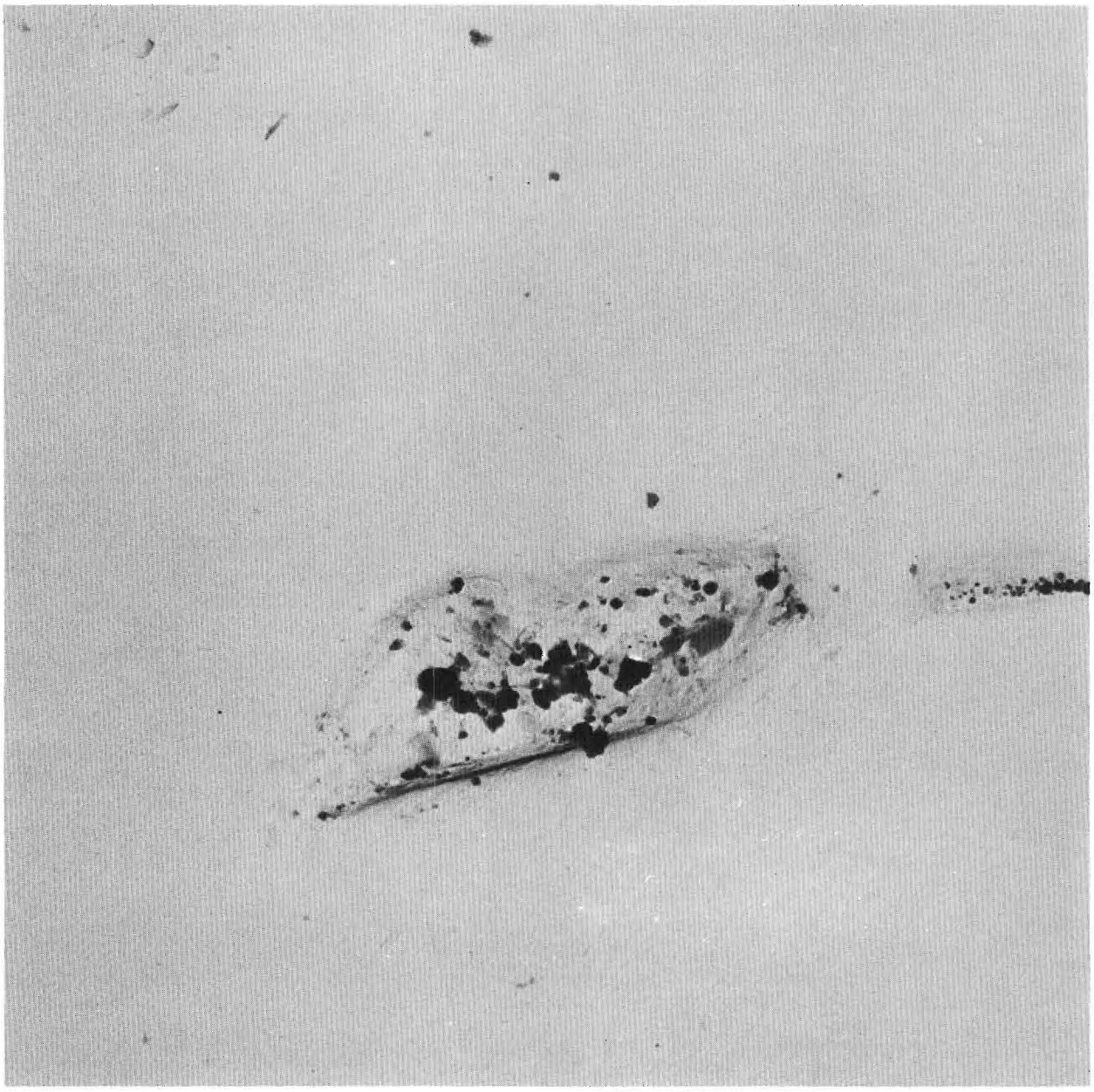

(x16,000)

Fig. 25. Platinum preshadowed carbon extraction replica of a cleaned Hi-Q cultured quartz surface showing extracted particles.

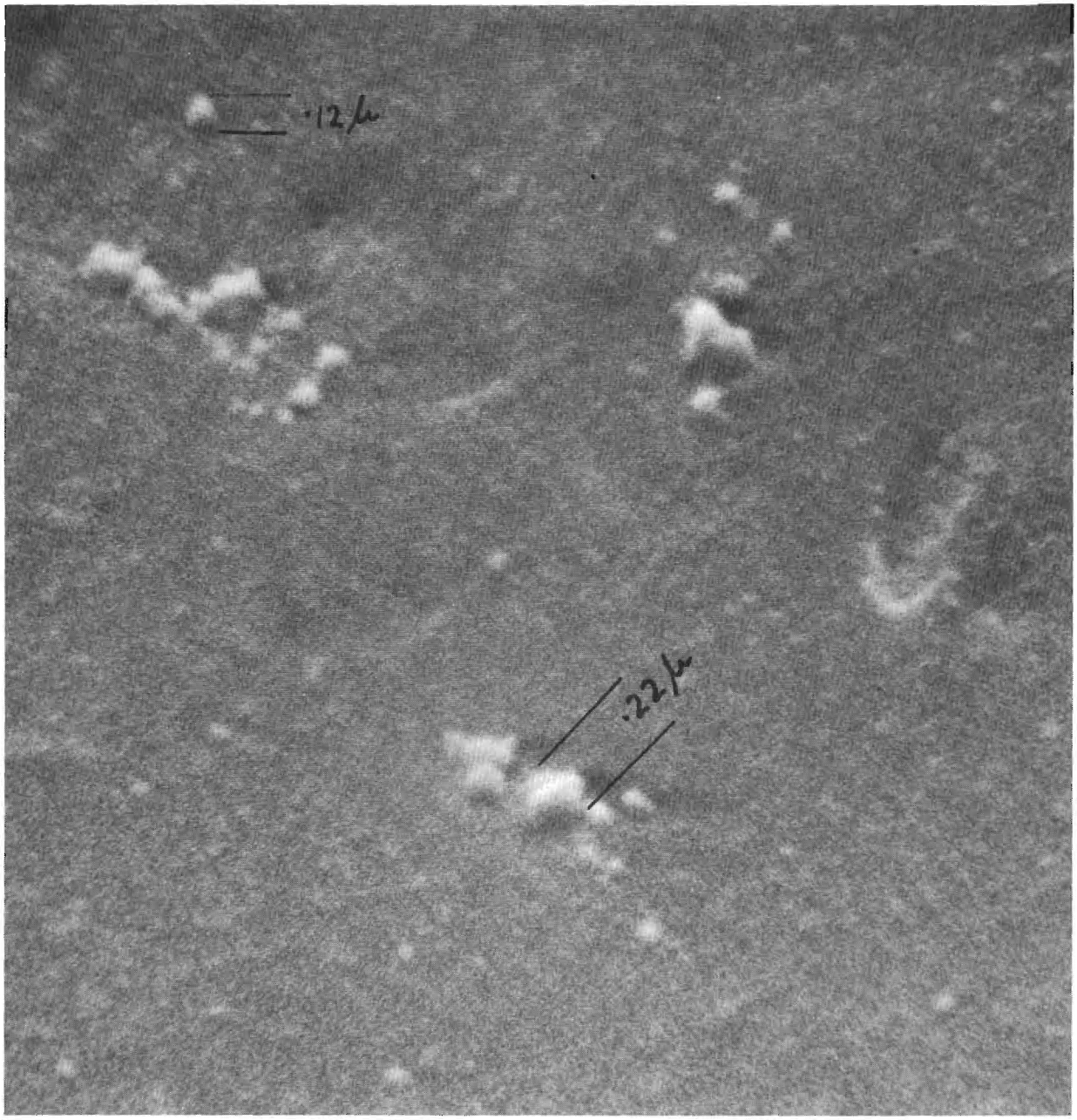

(x40,300)

Fig. 26. Scanning electron micrograph of a natural quartz wafer surface which had been etch-polished for 40 min.

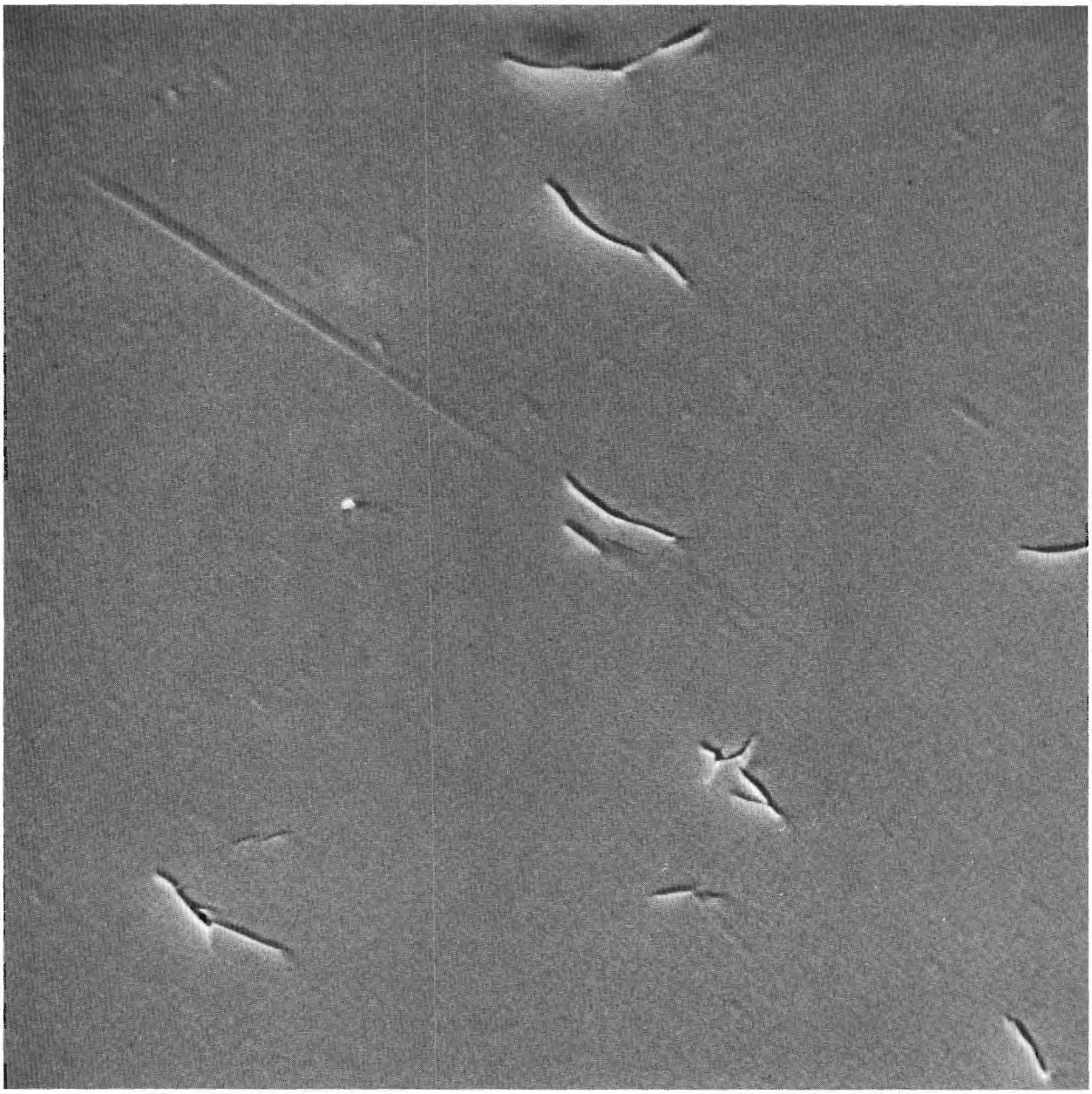

(x3540)

Fig. 27. Scanning electron micrograph of a natural quartz wafer surface which had been etched 10 min in saturated $NH_4F.HF$.

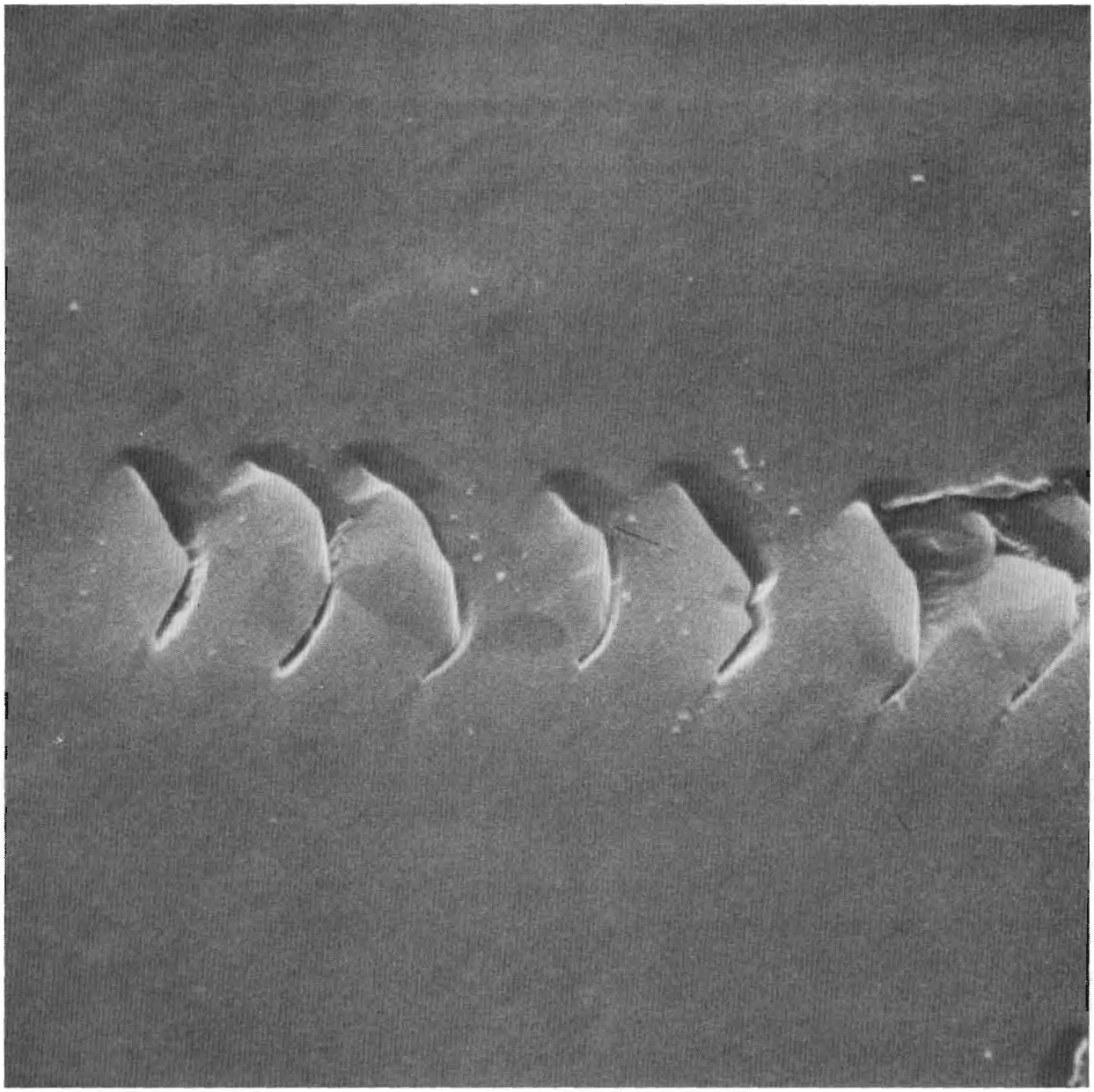

(x8500)

Fig. 28. Scanning electron micrograph of an etched (15min) Hi-Q cultured quartz wafer, showing aligned surface features.

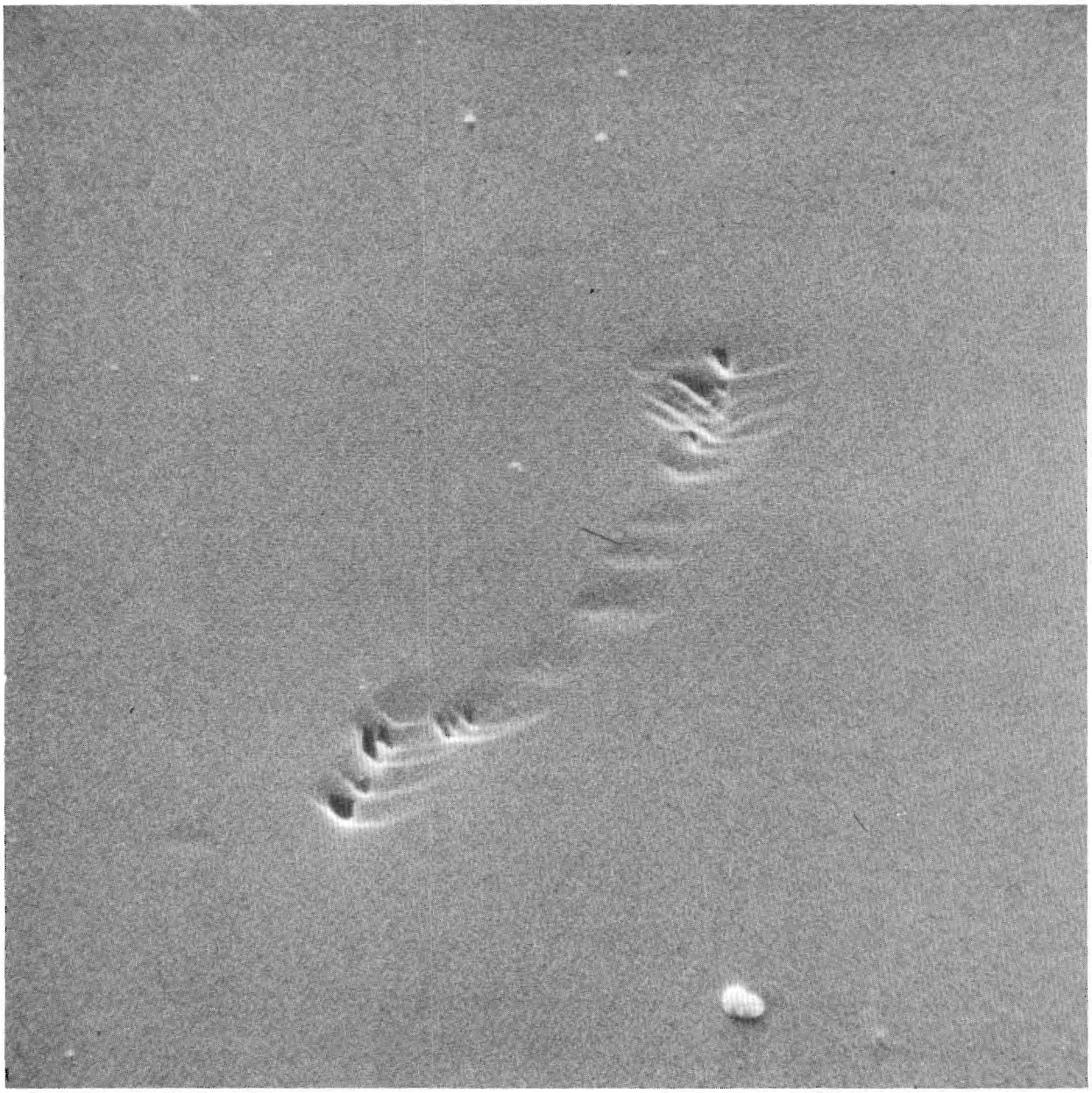

(x8840)

Fig. 29. Scanning electron micrograph of an etched (15min) natural quartz wafer which had been prepared by ECOM.

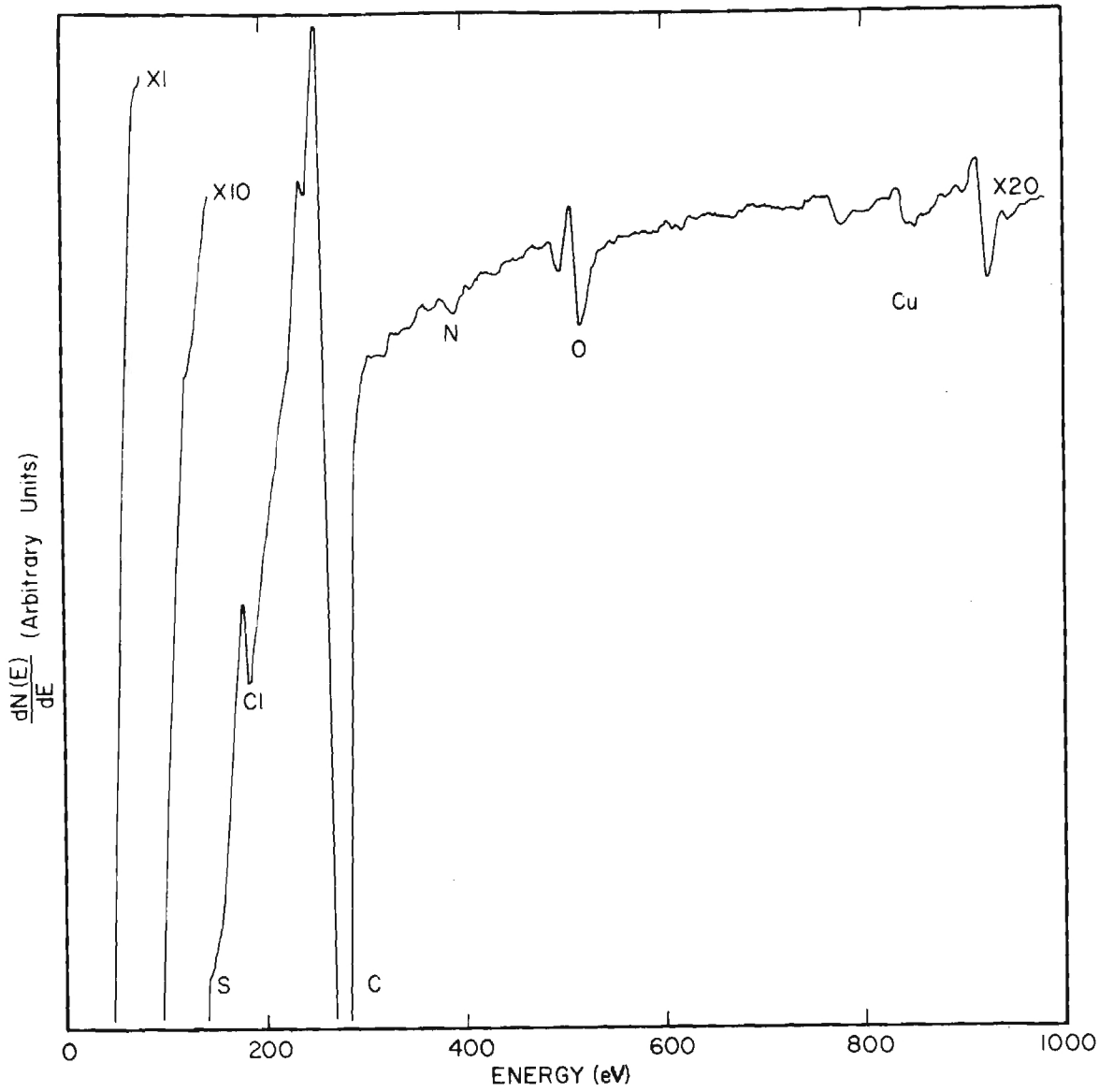

Fig. 30. Auger electron spectrum from a copper electrode surface immediately following 25°C deposition at 10^{-9} torr.

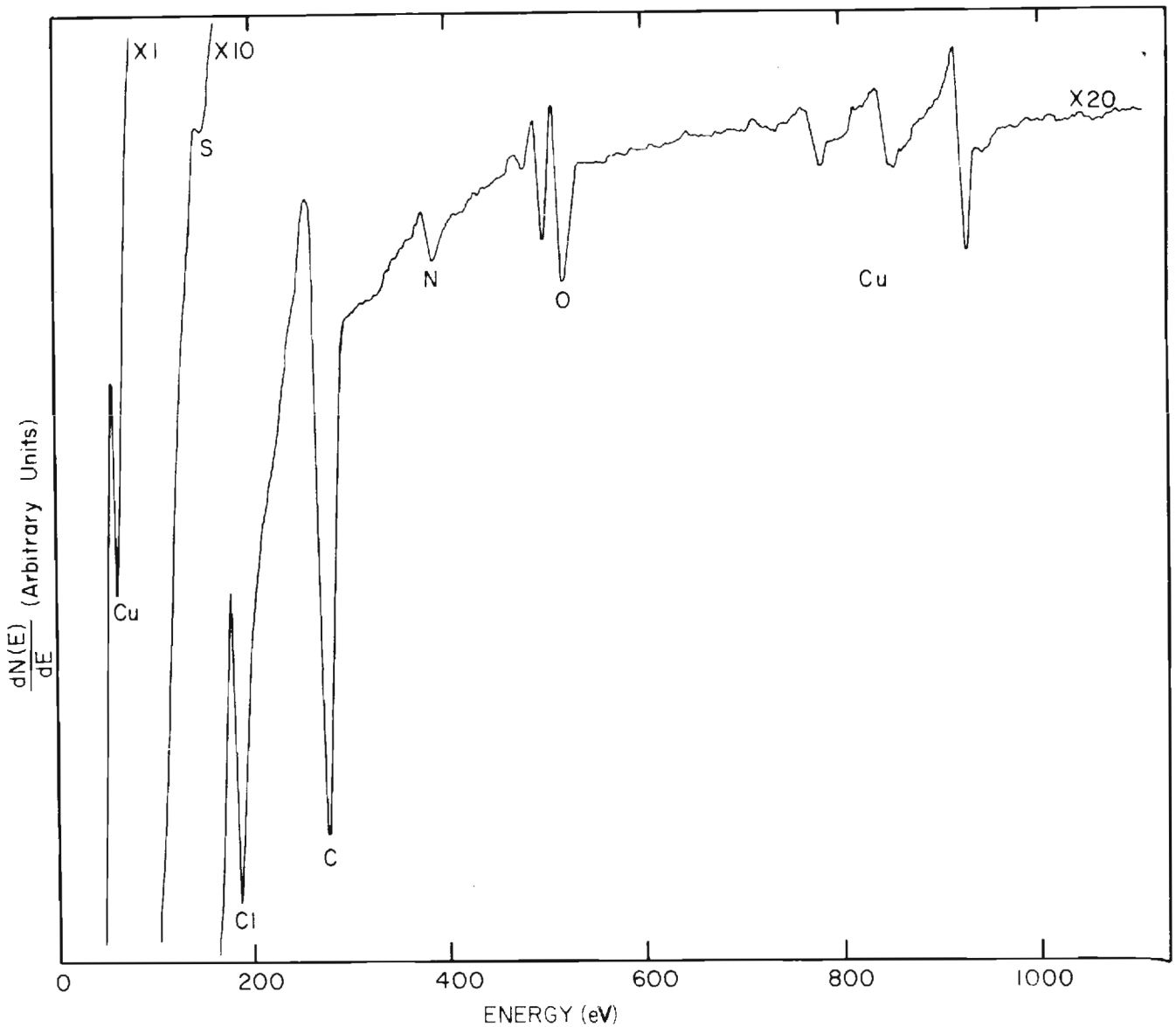

Fig. 31. Auger electron spectrum from a copper electrode surface 25°C deposition and a 20hr bakeout in vacuum at 200°C.

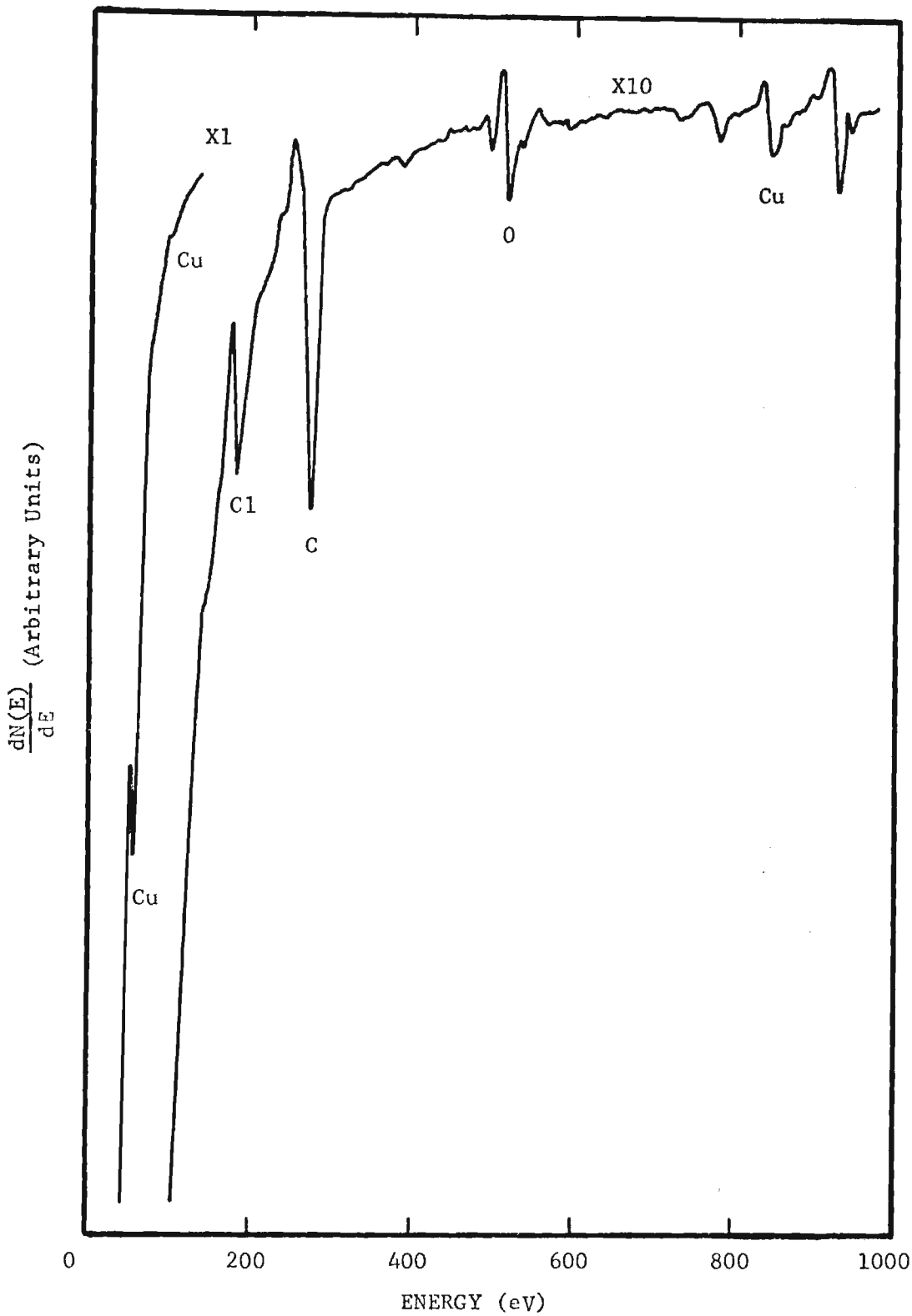

Fig. 32. Auger electron spectrum from a copper-plated quartz wafer after it was vapor degreased with trichloroethylene.

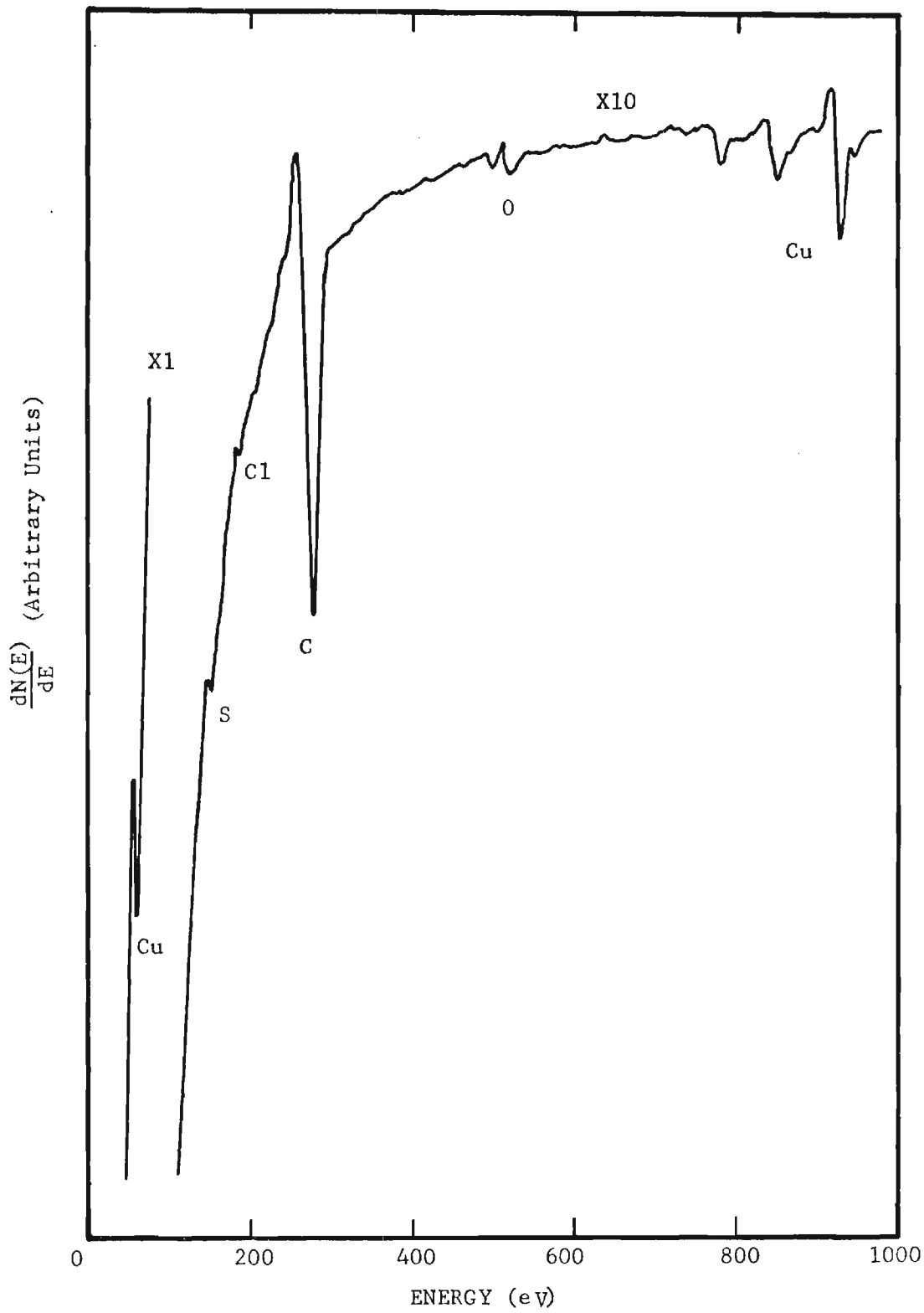

Fig. 33. Auger electron spectrum from a copper-plated quartz specimen after cleaning it with MICRO® and then rinsing in distilled water.

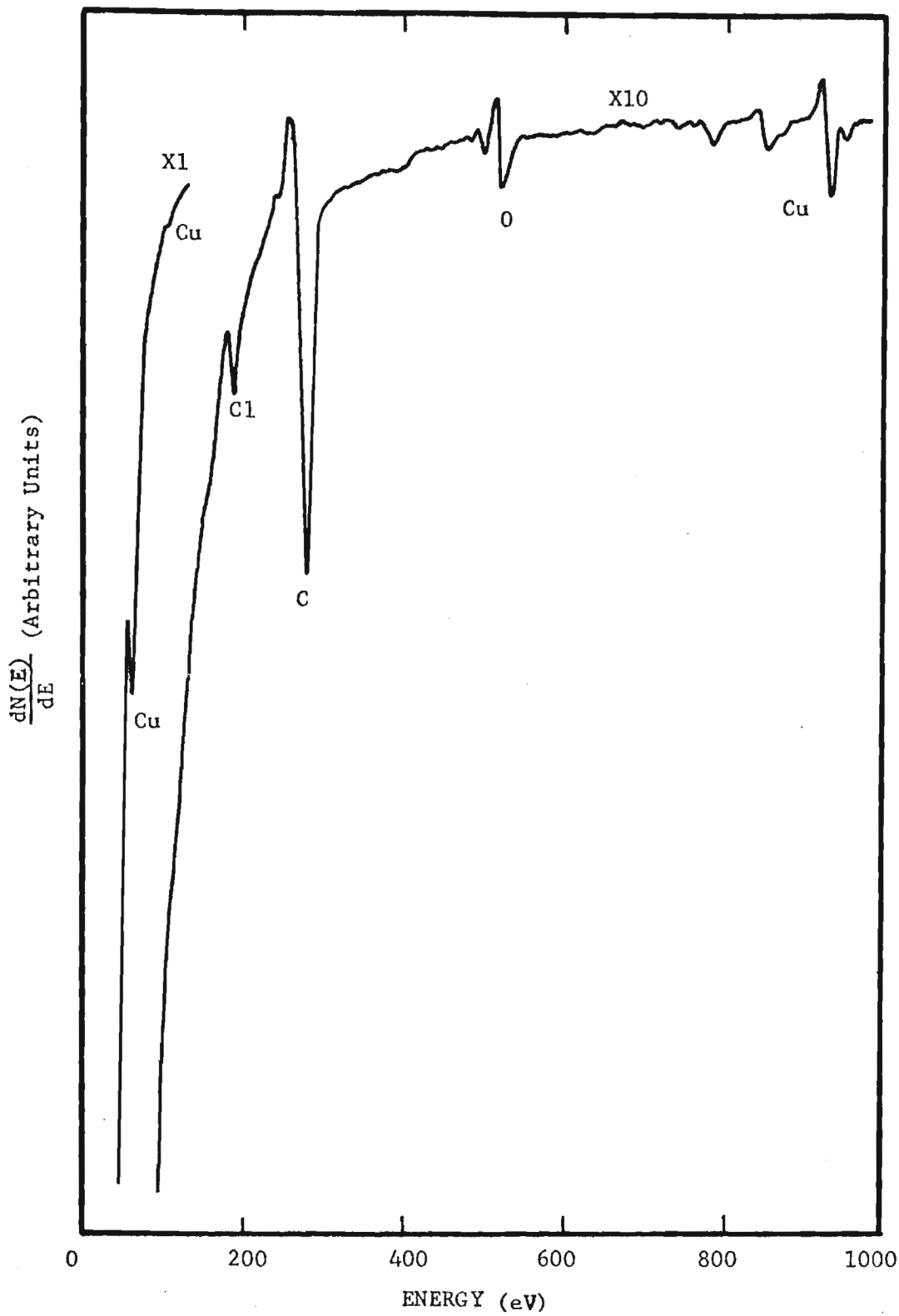

Fig. 34. Auger electron spectrum from a copper-plated quartz wafer after it was rinsed in methanol.

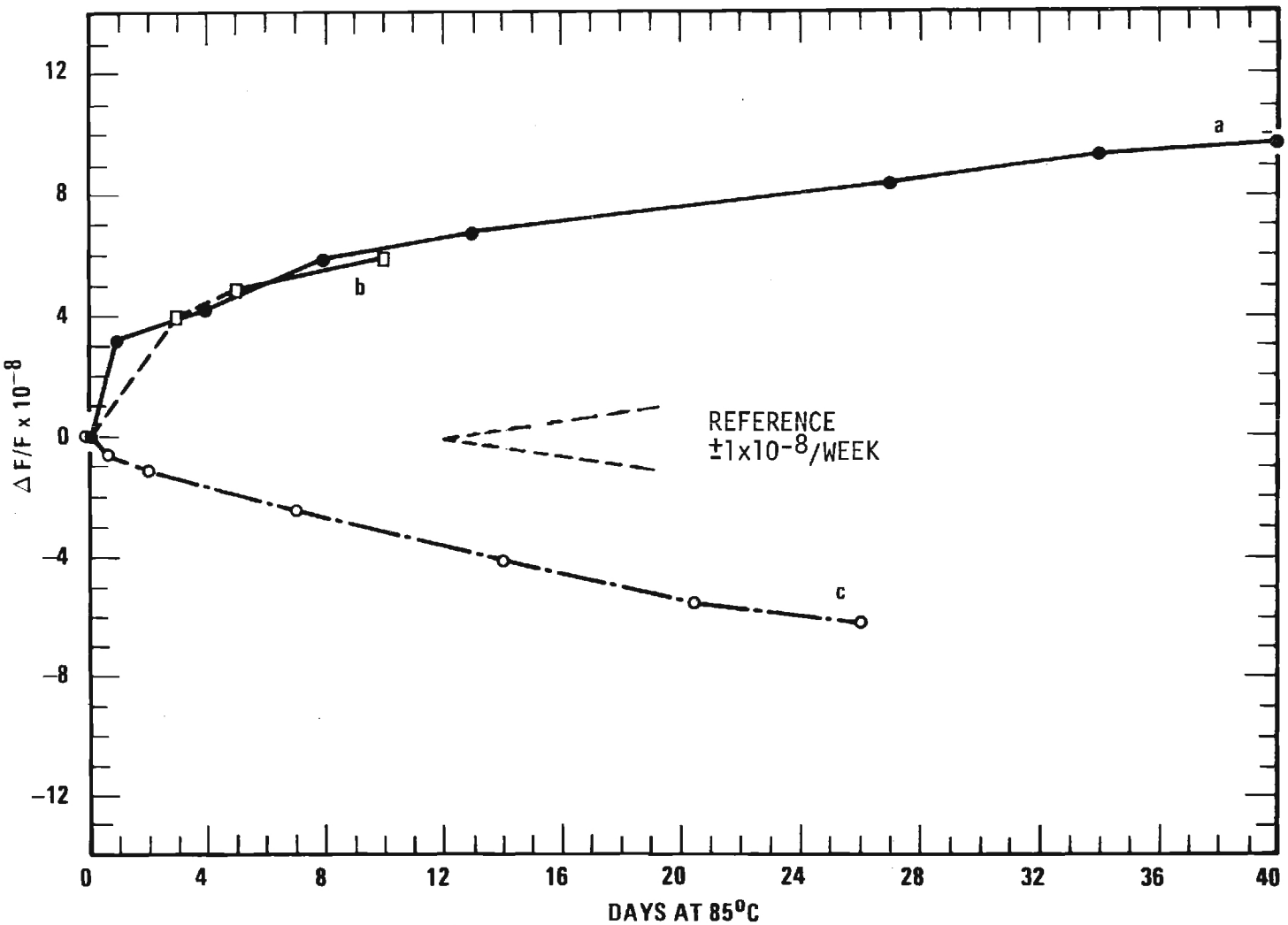

Fig. 35. Aging data for quartz resonators initially heated in vacuum to 200°C with copper electrodes deposited a) at 25°C followed by a 200°C bakeout, b) 200°C followed by a 200°C bakeout, and c) 25°C followed by a 300°C bakeout.

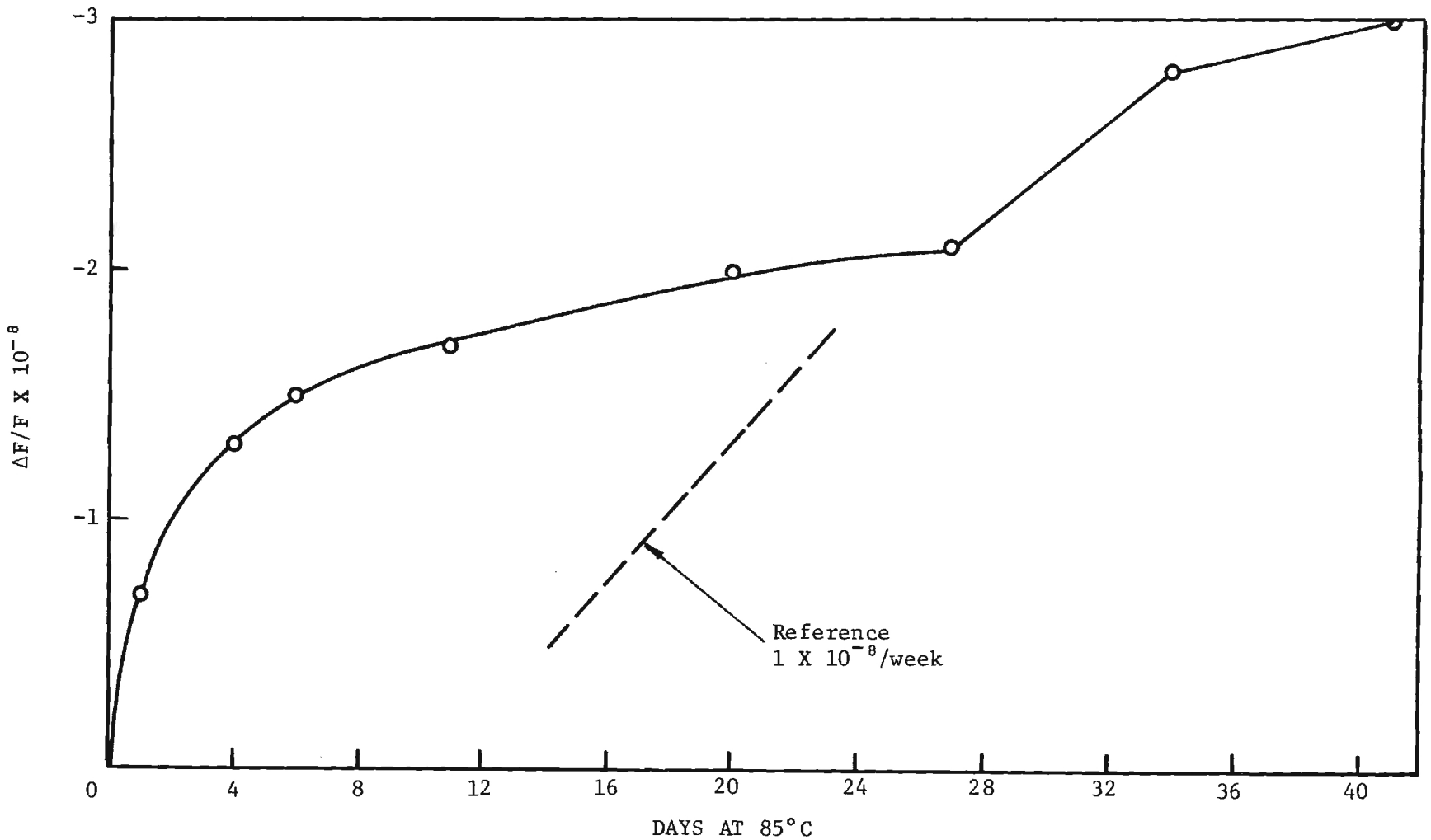

Fig. 36. The 85°C aging data for a copper-plated quartz resonator which was finally cleaned with MICRO® rather than by vapor degreasing in trichloroethylene. The subsequent bakeout in vacuum was 20hr at 200°C, followed by coldweld sealing at low pressure. Note negative aging.

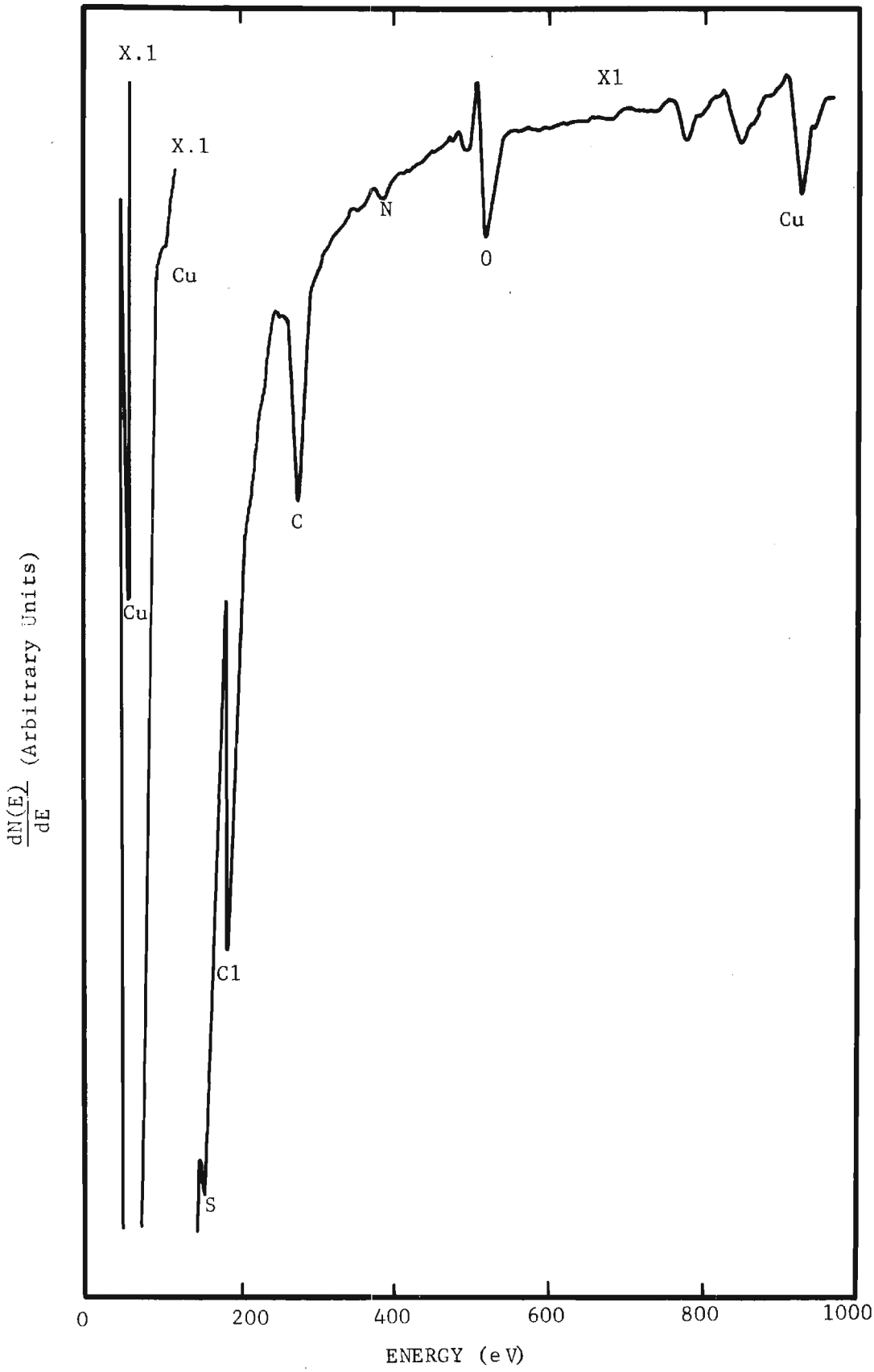

Fig. 37. Auger electron spectrum from a copper foil specimen after it was given a light etch in nitric acid and rinsed in tap water.

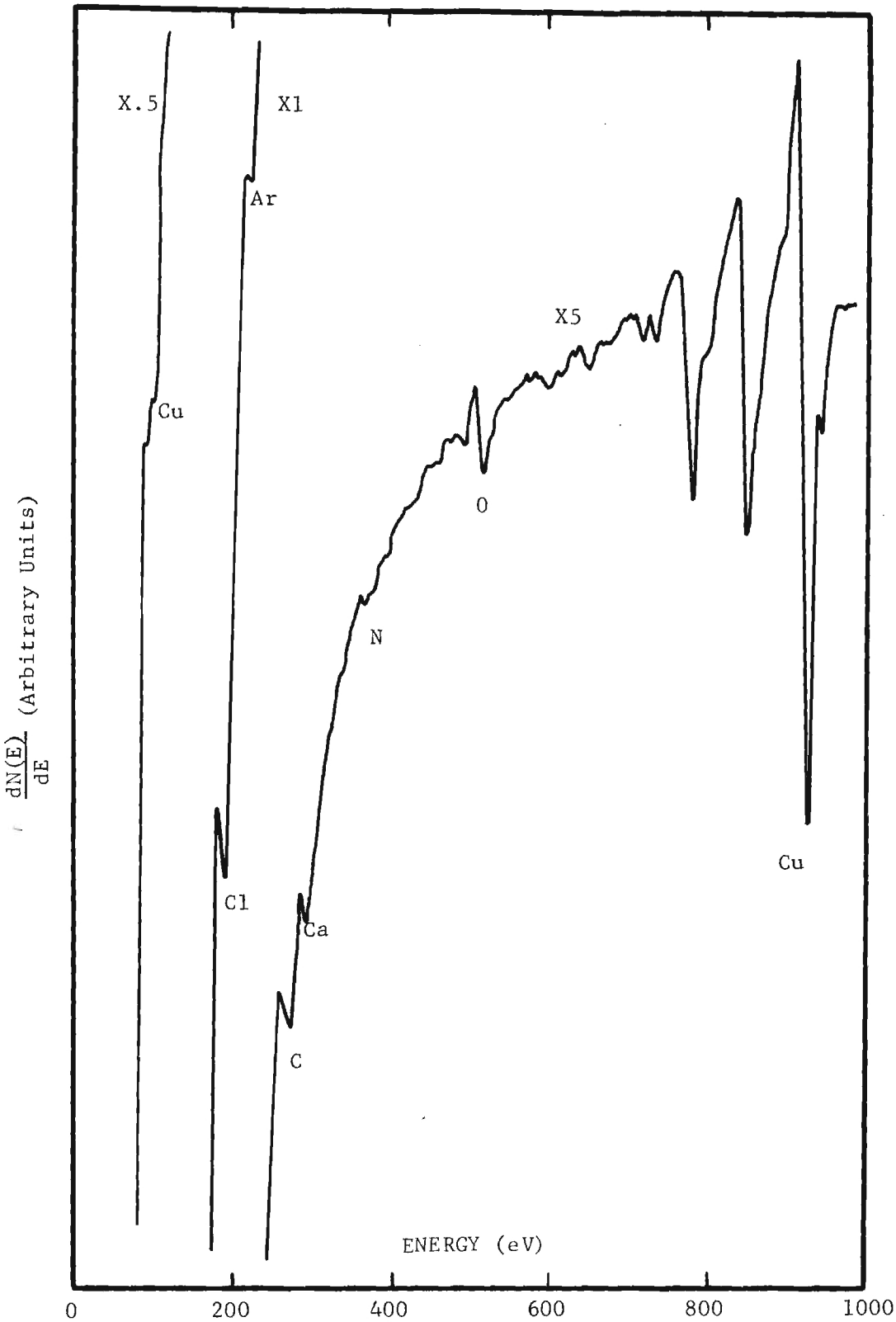

Fig. 38. Auger electron spectrum from the same specimen used to obtain the data of Fig.37, after heating for 2min at 600°C in the spectrometer vacuum.

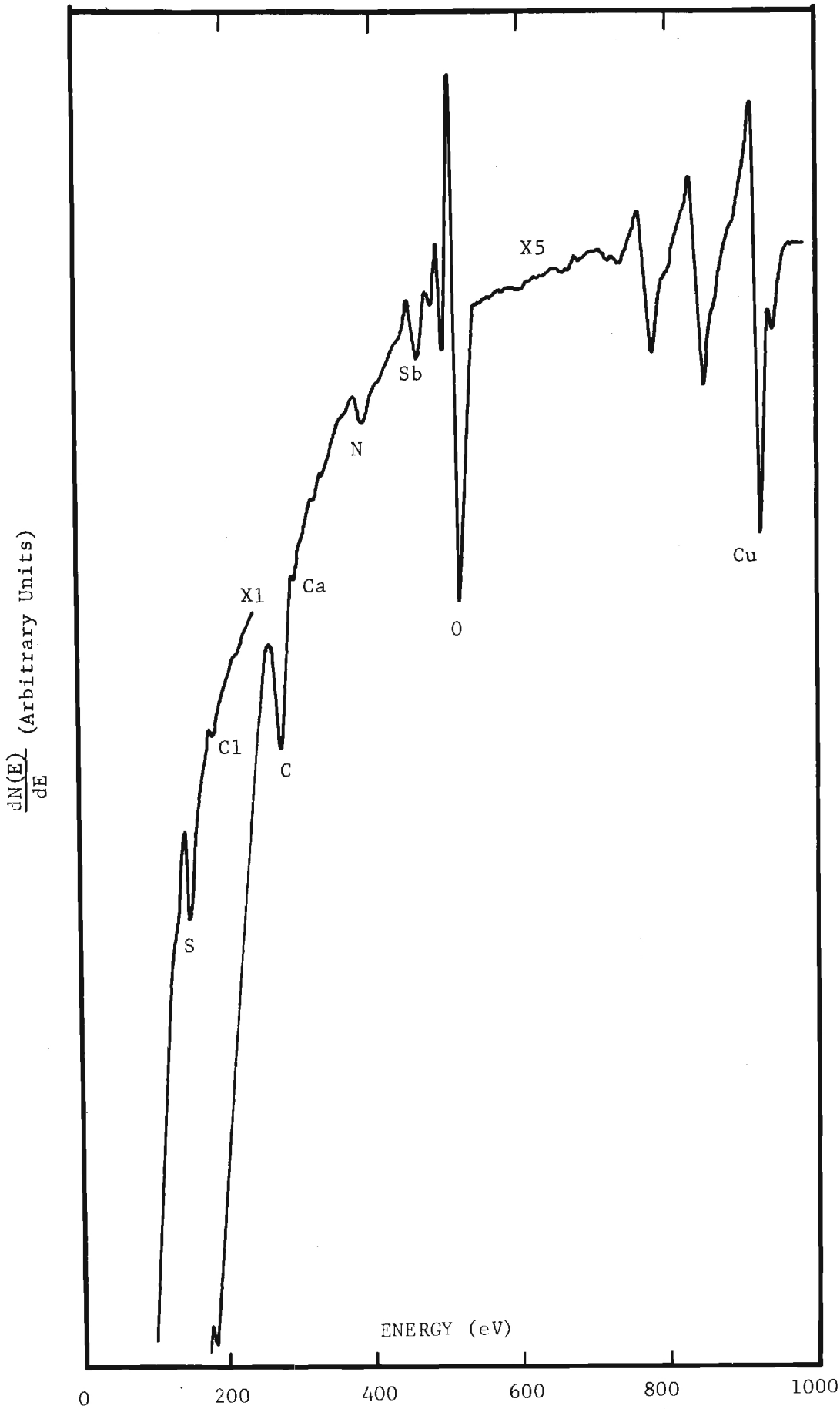

Fig. 39. Auger electron spectrum from the copper foil specimen after cycling the AES system to atmosphere of air and then reevacuating to about 10^{-10} torr.

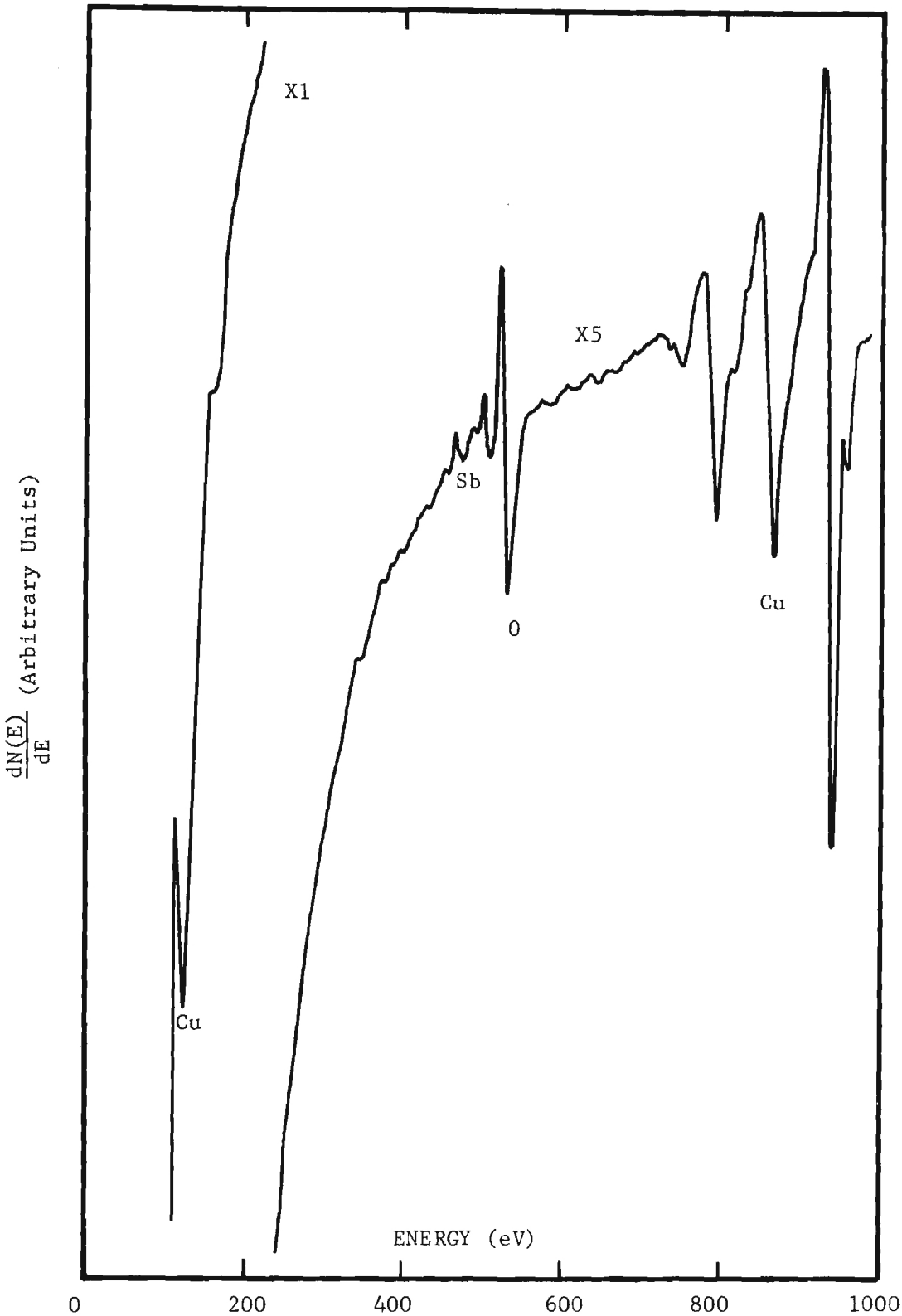

Fig. 40. Auger electron spectrum from the copper foil specimen after heating 1min at 300°C in the AES system following exposure to one atmosphere of air and reevacuating.

DISTRIBUTION LIST

Department of Defense

101 Defense Documentation Center
Attn: DDC-TCA
Cameron Station (Bldg 5)
*012 Alexandria, Virginia 22314

102 Dir.of Defense Research & Engineering
Attn: Technical Library
RM 3E-1039, The Pentagon
001 Washington, D. C. 20301

107 Director
National Security Agency
Attn: TDL
001 Fort George G. Meade
Maryland 20755

108 Director, Defense Nuclear Agency
Attn: Technical Library
001 Washington, D. C. 20305

Department of the Navy

200 Office of Naval Research
Code 427
001 Arlington, Va. 22217

203 Naval Ship Engineering Center
Attn: Code 61798
Prince Georges Center Bldg.
001 Hyattsville, Md. 20782

205 Director
Naval Research Laboratory
Code 2627
001 Washington, D. C. 20390

206 Commander
Naval Electronics Laboratory Cen.
Attn: Library
001 San Diego, California 92152

207 Commander
U. S. Naval Ordnance Laboratory
Attn: Technical Library
001 White Oak, Silver Spring
Maryland 20910

210 Commandant, Marine Corps
HQ, U. S. Marine Corps
Attn: Code AO4C
001 Washington, D. C. 20380

212 Communications-Electronics Division
Development Center
Marine Corps Development & Educ. Comd.
001 Quantico, Virginia 22134

217 Naval Air Systems Command
Code: AIR-5336
Main Navy Building
001 Washington, D. C. 20325

Department of the Air Force

301 Rome Air Development Center
Attn: Documents Library (TDLD)
001 Griffiss AFB, New York 13440

307 HQ ESD(TRI)
L. G. Hanscom Field
001 Bedford, Massachusetts 01730

308 Air Force Avionics Laboratory
Attn: AFAL/WR
001 Wright-Patterson AFB, Ohio 45433

309 Air Force Avionics Laboratory
Attn: AFAL/DOT, STINFO
002 Wright-Patterson AFB, Ohio 45433

310 RECON CENTRAL/RSA
AF Avionics Laboratory
001 Wright-Patterson AFB, Ohio 45433

*Decrease to 2 copies if report is not releasable to public. See ECOMR 70-31 for types of reports not to be sent to DDC.

314 HQ, Air Force Systems Command
Attn: DLTE
Andrews AFB
001 Washington, D. C. 20331

315 Director
Air University Library
Attn: AUL/LSE-64-285
001 Maxwell AFB, Alabama 36112

319 Air Force Weapons Laboratory
Attn: WLTL
001 Kirtland AFB, New Mexico 87117

Department of the Army

400 HQDA (DAMI-ZA)
002 Wash. DC 20310

401 HQDA (DAFD-ZAA)
002 Wash. DC 20310

405 OFC, Asst. Sec. of the Army(R&D)
Attn: Asst. for Research
Room 3-E-379, The Pentagon
001 Washington, D. C. 20310

408 HQDA (DARD-ARP/Dr. R. B. Watson)
001 Wash. DC 20310

409 Commanding General
U. S. Army Materiel Command
Attn: AMCMA-EE
001 Washington, D. C. 20315

415 Commanding General
U. S. Army Materiel Command
Attn: AMCRD-H
001 Washington, D. C. 20315

419 Commanding General
U. S. Army Missile Command
Attn: AMSMI-RR, Dr. J. P. Hallowes
001 Redstone Arsenal, Alabama 35809

421 CG, U. S. Army Missile Command
Redstone Scientific Info Center
Attn: Chief, Document Section
002 Redstone Arsenal, Alabama 35809

423 Commanding General
U.S. Army Weapons Command
Attn: AMSWE-REF
001 Rock Island, Illinois 61201

427 Commanding Officer
USACDC Combat Support Group
002 Fort Belvoir, Va. 22060

430 Commanding Officer
USACDC CBR Agency
001 Fort McClellan, Ala. 36201

431 Commanding Officer
USACDC Intelligence Agency
001 Fort Huachuca, Arizona 85613

432 Commanding Officer
USACDC FAA
001 Fort Sill, Oklahoma 73503

433 HQ, U.S. Army Aviation Systems Command
Attn: AMSAV-C-AD
P. O. Box 209
001 St. Louis, Missouri 63166

442 Commanding Officer
Harry Diamond Laboratories
Attn: Library
001 Washington, D. C. 20438

443 C.O., USA Foreign Science & Tech. Center
Attn: AMXST-IS1
220 Seventh St., N. E.
002 Charlottesville, Virginia 22901

444 C.O., USA Foreign Science Div.
Attn: AMXST CE Division
220 7th St., N. E.
001 Charlottesville, Va. 22901

448 Commanding Officer
Picatinny Arsenal
Attn: SMUPA-TVI
001 Dover, New Jersey 07801

449 Commanding Officer
Picatinny Arsenal
Attn: SMUPA-RT-S, Bldg. 59
002 Dover, N. J. 07801

451 Commanding Officer
Frankford Arsenal
Attn: W1000-65-1
(Mr. Helfrich)
001 Philadelphia, Penna. 19137

462 Commanding Officer
U. S. Army Materials and Mech. Rsch. Center
Attn: AMXMR-Atl. Tech Library Branch
001 Watertown, Massachusetts 02172

463 President
U. S. Army Artillery Board
001 Fort Sill, Oklahoma 73503

464 Commanding Officer
Aberdeen Proving Ground
Attn: Technical Library, Bldg. 313
002 Aberdeen Proving Ground
Maryland 21005

465 Commanding Officer
Aberdeen Proving Ground
Attn: STEAP-TL
001 Aberdeen Proving Ground
Maryland 21005

478 Chief, USAECOM Field Engr Office
U. S. Army Electronic Proving Ground
Attn: STEEP-LN-F (Mr. H. A. Ide)
001 Fort Huachuca, Arizona 85613

480 Commanding Officer
USASA Test and Evaluation Cen.
001 Fort Huachuca, Arizona 85613

483 U. S. Army Research Office-Durham
Attn: CRDARD-IP
Box CM, Duke Station
001 Durham, N. C. 27706

484 U. S. Army Research Office-Durham
Attn: Dr. Robert J. Lontz
Box CM, Duke Station
001 Durham, North Carolina 27706

486 Commanding Officer
USA Mobility Eqpt. R&D Cen.
Attn: Technical Document Cen. Bldg. 315
002 Fort Belvoir, Virginia 22060

488 USA Security Agcy. Combat DFV ACTV
Attn: IACDA-EW
Arlington Hall Station, Bldg.420
001 Arlington, Virginia 22212

489 Commanding General
U. S. Army Tank-Automotive Command
Attn: AMSTA-RH-FL
001 Warren, Michigan 48090

492 Commandant
U.S. Army Air Defense School
Attn: C&S Dept. MSL Sci. Div.
001 Fort Bliss, Texas 79916

493 Director
U.S.A. Engr. Waterways Exper. Station
Attn: Research Center Library
002 Vicksburg, Mississippi 39180

495 CG, Deseret Test Center
Attn: STEPD-TT-ME(S) Met. Div.
Bldg. 103, Soldiers Circle
001 Fort Douglas, Utah 84113

500 Commanding Officer
YUMA Proving Ground
Attn: STEYP-AD(Tech Library)
001 Yuma, Arizona 85364

501 Commanding Officer
U. S. Army Arctic Test Center
002 APO, Seattle 98733

502 CO, U. S. Army Tropic Test Center
Attn: STETC-AD-TL
002 APO, New York 09827

503 Director
U. S. Army Advanced Matl. Concepts AG
Attn: AMXAM
001 Washington, D. C. 20315

504 Commanding General
U. S. Army Materiel Command
Attn: AMCRD-R (H. Cohen)
001 Washington, D. C. 20315

506 U. S. Army Security Agency
Combat Developments Activity
Attn: Support Division
003 Arlington Hall Station, Va. 22212

508 Commanding Officer
USACDC Infantry Agency
Attn: Central Files
001 Fort Benning, Georgia 31905

509 Commanding Officer
USACDC Maintenance Agency
Attn: CDCMA-D
001 Aberdeen Proving Ground
Maryland 21005

512 Commanding Officer
USACDC Armor Agency
001 Fort Knox, Kentucky 40121

515 Commanding Officer
USACDC Inst. of Systems Analysis
Attn: CDISA-SSCI & CDISA-STANO
001 Fort Belvoir, Va. 22060

516 Commandant
U. S. Army Field Artillery School
Attn: Target Acquisition Dept.
002 Fort Sill, Oklahoma 73503

517 Commanding General
U. S. Army Missile Command
Attn: AMSMI-RFG (Mr. N. Bell)
001 Redstone Arsenal, Alabama 35809

518 Commanding Officer
Harry Diamond Laboratories
Attn: AMXDO-RCB (Mr. J. Nemarich)
001 Washington, D. C. 20438

596 Commanding Officer
U. S. Army Combat Developments Command
Communications-Electronics Agency
001 Fort Monmouth, New Jersey 07703

598 Commanding Officer
U. S. Army Satellite Communications Agency
Attn: AMCPM-SC-3
001 Fort Monmouth, New Jersey 07703

599 TRI-TAC Office
Attn: CSS (Dr. Pritchard)
001 Fort Monmouth, N. J. 07703

U. S. Army Electronics Command

*604 U. S. Army Liaison Office
MIT, Bldg. 26, Rm. 131
77 Massachusetts Avenue
001 Cambridge, Mass. 02139

605 U. S. Army Liaison Office
MIT-Lincoln Laboratory
Room A-210
P. O. Box 73
001 Lexington, Mass. 02173

607 Commanding General
U. S. Army Tank-Automotive Command
Attn: AMSTA-Z, Dr. J. Parks
001 Warren, Michigan 48090

610 Director
Night Vision Laboratory (USAECOM)
Attn: AMSEL-NV-OR (Mr. S. Segal)
001 Fort Belvoir, Virginia 22060

614 Chief
Missile Electronic Warfare Tech. Area
EW Lab, USA Electronics Command
001 White Sands Missile Range
New Mexico 88002

616 CG, U. S. Army Electronics Command
ATTN: AMSEL-PP/P-IED, Mr. C. Mogavero
225 South 18th Street
001 Philadelphia, Penna. 19103

617 Chief, Intelligence Materiel Dev. Office
Electronic Warfare Lab., USAECOM
001 Fort Holabird, Maryland 21219

*Unclassified, unlimited reports only.

680 Commanding General
U. S. Army Electronics Command
000 Fort Monmouth, N. J. 07703

1 AMSEL-NV-D
1 AMSEL-NL-D
1 AMSEL-WL-D
1 AMSEL-VL-D
3 AMSEL-CT-D
1 AMSEL-BL-D
1 AMSEL-TL-DT
** 3 AMSEL-TL-SF (Dr. John Vig)
1 AMSEL-TL-SF (Ofc of Record)
1 AMSEL-TE
1 AMSEL-MA-MP
2 AMSEL-MS-TI
1 AMSEL-GG-TD
1 AMSEL-TL-ST
25 Originating Office

Other Recipients

701 Sylvania Electronic Systems-Western Div.
Attn: Technical Reports Library
P. O. Box 205
001 Mountain View, Calif. 94040

703 NASA Scientific & Tech. Info. Facility
Attn: Acquisitions Branch (S-AK/DL)
P. O. Box 33
002 College Park, Maryland 20740

705 Advisory Group on Electron Devices
201 Varick St. 9th Floor
002 New York, New York 10014

706 Advisory Group on Electron Devices
Attn: Secy., SP GR on Optical Masers
201 Varick St.
002 New York, New York 10014

708 Ballistic Missile Radiation Anal. Cen.
Univ. of Michigan, Willow Run Lab
Institute of Science and Technology
001 P. O. Box 618, Ann Arbor, Michigan 48107

710 Metals and Ceramics Information Ctr. (MCIC)
Battelle Columbus Laboratories
505 King Avenue
001 Columbus, Ohio 43201

712 Electronic Properties Information Center
Hughes Aircraft Company
Centinela and Teale Streets
001 Culver City, California 90230

715 Plastics Tech Eval. Center
Picatinny Arsenal, Bldg. 3401
001 Dover, N. J. 07801

717 Reliability Analysis Center
Rome Air Development Center
Attn: J. M. Schramp/RCRM
001 Griffiss AFB, New York 13440

718 Remote Area Conflict Info. Center
Battelle Memorial Institute
505 King Avenue
001 Columbus, Ohio 43201

719 Shock and Vibration Info. Center
Naval Research Laboratory (Code 6020)
001 Washington, D. C. 20390

720 Thermophysical Properties Res. Center
Purdue University, Research Park
2595 Yeager Road
001 Lafayette, Indiana 47906

721 Vela Seismic Info. Center
University of Michigan
Box 618
003 Ann Arbor, Michigan 48107

** Or number specified in contract. Add COTR's mail symbol.

Unclassified
Security Classification

DOCUMENT CONTROL DATA - R & D

(Security classification of title, body of abstract and indexing annotation must be entered when the overall report is classified)

1. ORIGINATING ACTIVITY *(Corporate author)*
Georgia Institute of Technology
Engineering Experiment Station
Atlanta, Georgia 30332

2a. REPORT SECURITY CLASSIFICATION
Unclassified

2b. GROUP

3. REPORT TITLE

Precision Single Sideband Crystal Units

4. DESCRIPTIVE NOTES *(Type of report and inclusive dates)*
Final Report, 15 December 1971 to 31 January 1973

5. AUTHOR(S) *(First name, middle initial, last name)*

Raymond K. Hart
Walter H. Hicklin

6. REPORT DATE
May 1973

7a. TOTAL NO OF PAGES
75

7b. NO. OF REFS
16

8a. CONTRACT OR GRANT NO
DAAB07-72-C-0087

b. PROJECT NO
DAAB07-72-Q-0060

c.
Task-04

d.

9a. ORIGINATOR'S REPORT NUMBER(S)
A-1388-F

9b OTHER REPORT NO(S) *(Any other numbers that may be assigned this report)*
ECOM-0087-F

10. DISTRIBUTION STATEMENT

Approved for public release; distribution unlimited.

11. SUPPLEMENTARY NOTES

12 SPONSORING MILITARY ACTIVITY
United States Army Electronics Command
Fort Monmouth, New Jersey 07703
(AMSEL-TL-SF)

13. ABSTRACT

The purpose of this work was to develop single sideband (SSB) quartz crystal units which exhibit long-term aging of $< \pm 2\times10^{-10}$/week whenmeasured at the upper turning point (UTP) of 62°C, and after a stabilization period of four weeks. In addition to the low aging requirement, the frequency hysteresis that often occurs under conditions of varying temperatures was investigated. Two concurrent work programs were employed to a) fabricate resonators under precisely controlled conditions and b) investigate their characteristics. All wafers used in resonator construction were preterminated by electro-bonding in HC-6 holders, plated with copper electrodes, and then hermetically sealed in containers by the cold-weld precess. The plating and sealing operations were carried out in an ultrahigh vacuum chamber without venting to air between operations. Both the cleaned surfaces of quartz wafers and of deposited electrode material were chemically and physically characterized by sophisticated electron-optical-spectrometric instrumentation. The results of these investigations were related to the various processes used in resonator preparation. The best aging performance was from wafers a) etched 1 min, b) polysiloxane coated before electrode deposition, and c) final fabrication of mounted wafers in same low pressure environment. The frequency deviation requirement of $< \pm 1\times10^{-8}$ during temperature cycling (-55 to +90°C) was met in 84% of cases tested. The results of this work indicate that performance of quartz resonators can be improved by fabricating them in systems and from materials that enable precise control of variables to be exercised. Monitoring of these variables by suitably sensitive instrumentation is essential.

DD FORM 1 NOV 65 1473

Unclassified
Security Classification

15

14. KEY WORDS	LINK A ROLE	LINK A WT	LINK B ROLE	LINK B WT	LINK C ROLE	LINK C WT
Aging						
Auger Electron Spectroscopy						
High Energy Electron Diffraction						
Quartz Resonators						
Reliability						
Scanning Electron Microscopy						
Temperature Compensated Crystal Oscillators						
Upper Turning Point						